

## Report on the First ESO-CERN Symposium on “Large Scale Structure of the Universe, Cosmology and Fundamental Physics”

G. Setti, ESO

The first ESO-CERN Symposium was held at CERN, Geneva, from 21st to 25th November 1983 and was attended by approximately 200 participants. The discussions concentrated on the general field of Cosmology, where the progress made in the past twenty years, both in elementary particles and astronomy, has shown that these two fields of basic research are merging toward a new and fundamental understanding of the laws that govern our Universe. A detailed account is contained in the Proceedings of the Symposium which will be available in a few months.

The meeting was started with an introductory lecture by D. W. Sciama (Oxford and Trieste) who highlighted the numerous and fundamental problems the understanding of which appears to require a joint effort of particle physicists, astrophysicists and cosmologists.

As discussed by L. Woltjer (ESO), the astronomical observations have shown that the Universe is not only expanding, but also strongly evolving in the sense that the physical properties of the galaxies have changed with time. For instance, it has been discovered that certain classes of objects, such as radio galaxies and quasars, were more numerous and probably more powerful in the past than they are now. This, together with the discovery of the properties of the so-called universal background radiation, has led to the conclusion that the Universe can be described by the most simple homogeneous and isotropic models of General Relativity, whereby it has evolved from a very condensed and very hot phase about 20 billion years ago—the “hot big-bang”. This interpretation has an additional attraction: it can explain in a very natural way the abundances of certain elements, which would be extremely difficult to account for by the nuclear processes taking place in stars. Accordingly, the bulk of elements, such as helium and

deuterium, were produced when the age of the Universe was only about 100 seconds, the temperature about one billion degrees and the density of the order of the density of water, in a phase that lasted about 8 minutes. At that moment the Universe was essentially a gaseous mixture composed of protons, neutrons, electrons, positrons, neutrinos and anti-neutrinos (and perhaps some other exotic particles, such as photinos) immersed in a heat bath of photons. The equilibrium between these components is maintained by the weak interaction, one of the four fundamental forces which are believed to govern all natural phenomena.\* The weak force together with the “hot big-bang” model allows definite predictions about the abundances of primordial elements. As pointed out by J. Audouze (Paris), this astrophysics model limits the number of neutrino types to no more than 4, which is already significantly better than the upper limit of about twenty obtained in particle physics experiments (data on  $Z^0$  decay obtained at CERN). Another important constraint that stems from primordial element abundances is that the present

\* The four fundamental forces are: the *electromagnetic force*, which acts among electrically charged particles and is transmitted by the photon (it governs the structure of the atom); the *weak force*, which acts on leptons and hadrons and is transmitted by the bosons  $W^+$ ,  $W^-$ ,  $Z^0$  (it is responsible for the beta decay of radioactive elements); the *strong force*, which acts on hadrons and is transmitted by particles called pions and kaons (it is responsible for the nuclear forces that keep together the protons and neutrons in the atomic nuclei; the strong interaction among the quarks, which are supposed to be the constituents of the protons and neutrons, is due to particles called gluons); and the *gravitational force*, which acts on everything and is transmitted by a particle called graviton.

[The leptons include the electron, the muon and the tau particles and the three corresponding types of neutrinos. The hadrons include the baryons (which ultimately decay into protons) and the mesons.]

density of baryonic matter in the Universe cannot be more than about 10% of the "closure" density, that is to say, the density which divides the model universes derived from general relativity into "open" and "closed". If the density is less than the closure density then the Universe is "open" and will expand forever to infinity or, vice-versa, it will reach a maximum size at some time in the future and will then recollapse under the action of its own gravity. In principle, it should be possible, by means of astronomical observations, to find out in what kind of universe we live. In practice, however, this entails the use of a class of astronomical objects (such as galaxies of a certain type) which should be bright enough to permit a mapping of the Universe in depth and whose intrinsic properties do not change with the cosmic time. As discussed by A. Sandage (Pasadena), despite great efforts it has not yet been possible to separate the evolutionary effects from those due to the geometry of the Universe. The solution to this fundamental problem has probably to await the advent of both the Space Telescope and the large telescopes of the future, such as the VLT.

That most of the matter in the Universe may indeed be in non-luminous form has been convincingly argued by S. Faber (Lick Observatory) on the basis of observations of different types of galaxies, groups and clusters of galaxies. It appears as though in these different types of astronomical conditions ordinary visible matter makes up only about 10% of the total mass involved. The nature of this "dark" matter has been the subject of many speculations and everything, from certain types of elementary particles, to mini black-holes, up to very

massive stars with a mass of about one million times the mass of the Sun, has been proposed. To illustrate how unsatisfactory the situation is, it suffices to remark that the masses involved in these different proposals extend over a range of at least *seventy* orders of magnitude!

A very important theoretical development has taken place in the past few years with the application of the concepts of grand unified theories of physics (GUTs) to cosmology. To highlight this let us first briefly summarize some of the basic problems facing the cosmologists.

Strangely enough, the first problem comes about because the Universe looks so isotropic. Observations of galaxies and extragalactic radio sources (radio galaxies and quasars) show that the distribution of condensed matter in space, aside from local irregularities, is isotropic to better than one part in a hundred. But a much stricter limit is derived from the observations of the 3°K universal radiation which, as reported by D. T. Wilkinson (Princeton), appears to be intrinsically isotropic on all angular scales to better than one part in ten thousand. However, in the framework of the standard "hot big-bang" model it can be shown that two hypothetical observers placed, say, 180° apart in the sky at a distance corresponding to the last moment in which the universal radiation interacted with ordinary matter, could not have communicated with each other. Technically speaking, this is equivalent to saying that the "horizons" of the two observers, whose radii increase with the speed of light (the maximum possible speed), were still well separated. Now the isotropy problem arises because it is difficult to see how regions of space which had no time from



*The ESO guesthouse in Santiago where the visiting astronomers are happy to rest for one day after more than 20 hours in a plane.*

the moment of the original explosion to come into physical interaction can look so similar, as indicated by the isotropy measurements mentioned above.

The second problem, which in technical terms is known as the "flatness" problem, is directly related to the density of matter in the Universe. It arises from the simple observation that any deviation of the matter density from the "closure" density increases with cosmic time. Thus, if the present density of the Universe is only about 10% of the closure density—as indicated by observations of the content of baryonic matter—at the time when the Universe was only about 100 seconds old (or when the compression factor was  $\sim 10$  billion), the density of matter deviated from the closure density only by one part in one hundred thousand. Most researchers consider this fine-tuning very unnatural and, consequently, believe that the matter density must have always been very close to the "closure" density.

The third problem is concerned with the apparent asymmetry in the matter/anti-matter content of the Universe, that is to say, with the evidence that the Universe is essentially composed of baryons. In the simple standard "hot big-bang" model, there is no reason to think that initially at least the Universe was not highly symmetric, with equal numbers of baryons and anti-baryons in equilibrium with the radiation field: baryons and anti-baryons annihilate into photons and, vice-versa, photons materialize into baryon/anti-baryon pairs. Because of the cooling due to the expansion of the Universe, eventually all baryon/anti-baryon pairs annihilated giving rise to a corresponding number of photons that constitute the universal radiation field now observed at a temperature of 3°K, but somehow a small amount of baryons was left over. That the deviation from a perfect baryon/anti-baryon symmetry should have been small is shown by the fact that presently there are about 100 million photons per baryon (the universal radiation has cooled down to its present temperature of about 3°K because of the expansion of the Universe, but the number of photons has been conserved). If the Universe was baryon symmetric to start with, the above picture of course implies that the baryon number has not been strictly conserved (it should be remembered that a baryon and an anti-baryon add exactly in the opposite way, giving a total baryon number identically equal to zero).

Recent developments in elementary particle physics and fundamental theory, when applied to cosmology, may in fact indicate an elegant way out of these problems. After the successful confirmation of the Glashow, Salam and Weinberg theory on the unification of electromagnetic and weak forces recently obtained at CERN with the discovery of the  $W^+$  and  $Z^0$  bosons, as discussed by P. Darrilat (CERN), there is now an increased confidence in the theoretical approach to the unification of all fundamental forces. It should be noted that almost a century has elapsed since Maxwell made the first fundamental step of incorporating electric and magnetic forces into one unified scheme—the theory of electromagnetism. As reviewed by P. Fayet (Paris), there are a number of theoretical models which have been proposed to unify the electro-weak and strong interactions, generally known as Grand Unified Theories (GUTs). At this moment, it still appears difficult to work out definite quantitative predictions, but one quantity which seems to be fairly well estimated is the energy of the particles above which the models should become exact, that is to say, the unification energy at which the forces lose their individuality. This energy turns out to be about  $10^{14}$  GeV, which corresponds to a mass which is about  $10^{12}$  times the mass of the  $W^+$  and  $Z^0$  bosons. This means, of course, that a direct verification of the GUTs via the production of the particles which mediate the unified force is unthinkable, except in the too distant future. However, in the "hot big-bang"

## Tentative Time-table of Council Sessions and Committee Meetings in 1984

April 13	Scientific Technical Committee
May 22	Users Committee
May 23	Finance Committee
June 4–5	Observing Programmes Committee
June 6	Committee of Council, Geneva
June 7	Council, Geneva
October 8	Scientific Technical Committee, Chile
November 13–14	Finance Committee
November 27–28	Observing Programmes Committee
November 28	Committee of Council
November 29–30	Council

All meetings will take place at ESO in Garching unless stated otherwise.

picture, these extremely high energies are reached naturally at the very beginning of the life history of the Universe, when its age was less than about  $10^{-35}$  seconds. After this time, the cooling due to the expansion of the Universe brings the average energy of the particles below  $10^{14}$  GeV.

One of the predictions of GUTs is that the proton should decay with a half-life in the range  $10^{31}$ – $10^{33}$  years, very much greater than the age of the Universe ( $\sim 2 \times 10^{10}$  years). This possibility arises because in the GUTs the quarks, which are the constituents of the baryons, and the leptons are parts of the same picture. As a consequence, the baryonic number need not be conserved any more, as had been assumed in the classical models of elementary particle theory. The results of a number of experiments set up to measure the proton half-life were reviewed by E. Fiorini (Milan). The most stringent result is now being obtained from the Ohio Morton Salt mine experiment which sets a lower limit to the proton half-life of  $1.5 \times 10^{32}$  years. This result already enables one to rule out the simplest of the GUT models which predicts that the proton half-life would be at most  $10^{31}$  years.

Because of the non-conservation of the baryonic number, one can work out a scheme which leads in the first  $10^{-35}$  seconds to a baryon asymmetric universe, even if one had started from conditions of perfect symmetry between particles and anti-particles, in this way explaining one of the basic cosmological problems outlined before. Unfortunately, it is not yet possible, within the framework of GUTs, to make a quantitatively precise estimate of the excess of matter over anti-matter.

In a related context, G. Giacomelli (Bologna) reviewed the present status of the search for monopoles, the magnetic counterparts of the electric charge, whose existence is predicted by the GUT's schemes. Since their mass is enormous ( $\sim 10^{15}$  GeV), they cannot be produced in the laboratory, but of course might have been produced in the very early phases of the "hot big-bang" and now pervade the Universe. In fact, the production might have been so copious that one has to invoke "suppression" schemes to avoid conflict with the upper limit on their present space density.

Another important feature of the more elaborate GUTs is the expectation that neutrinos have non-zero rest mass. Obviously, this immediately raises the possibility that "dark" matter, which may pervade the Universe as previously discussed, is provided by the neutrino sea. In the standard "hot big-bang" model one can compute, in a fairly accurate way, the number density of neutrinos which turns out to be of the same order as the photon density in the 3°K universal radiation field, that is

to say, about 100 million, or so, per cubic metre. With this kind of density a very small mass of neutrinos, corresponding to a rest-mass energy of a few tens of an electron volt, is already sufficient to provide the "closure" density of the Universe. However, there appear to be difficulties with this kind of picture. Calculations which simulate the non-linear growth of structures in the expanding Universe can be compared with the observed distribution of galaxies which, as discussed in detail by J. H. Oort, appear to cluster on the large scale in configurations (superclusters) whose sizes are typically 150 million light-years. In a universe dominated by massive neutrinos, the characteristic scale on which matter condensations can form and collapse is clearly controlled by the maximum distance neutrinos can travel before they are cooled down, due to the expansion of the universe. As pointed out by J. Silk (Berkeley), this distance is too large and apparently leads to a typical size which by far exceeds the observed clustering scale of galaxies. Consequently, if the standard cosmological parameters hold, one would have to conclude that neutrinos cannot provide the missing mass in the Universe. Clearly, the solution to all these problems depends, in the end, on a direct measurement of the neutrino mass. According to R. L. Mössbauer (Munich), who reviewed the experimental situation for the measurements of the masses of the various kinds of neutrinos, the most recent result of an experiment carried out in the Soviet Union indicates that the rest-mass energy of the electron neutrino should be at least 20 eV. This result is clearly of crucial importance and one hopes that other experiments will soon allow to verify its validity.

An important development in theoretical cosmology, which would in fact provide a solution to the isotropy and flatness problems discussed earlier, has recently been proposed by Guth in the framework of GUTs. After the first  $10^{-35}$  seconds, the cooling due to the expansion of the Universe would bring the thermal energy below the grand unification energy of  $10^{14}$  GeV, the electro-weak and the strong forces would again acquire their identity and one would expect something to happen at the transition time (more technically one expects a decrease in the symmetry properties of the fields). Guth's basic idea is that essentially nothing happens for a while: the Universe expands and cools down by many factors of ten, while certain properties of the system remain, so to say, "frozen". The system lives for a while in an "excited" state which would drive the expansion in such a way as to enable an effective exchange of information through the Universe. Essentially, a very small piece of the Universe, which is causally connected in the initial phase of this expansion where, roughly speaking, the expansion velocity is less than the velocity of light, is then stretched by a very large factor (of the order of  $10^{44}$ ), and from this piece our entire Universe is made. At the same time, this would lead to a model universe in which the density is *almost exactly* the closure density. When the system makes the transition to its "normal" state, the energy which had been "frozen" in the fields is suddenly released and the Universe is reheated to a thermal energy of approximately  $10^{14}$  GeV, and the considerations we outlined before apply again. It is as if the Universe was born anew. These types of theoretical schemes are known as inflationary models. As discussed by D. Nanopoulos (CERN), however, there are still a number of difficulties concerned with a fuller understanding of the basic physics at work and, in particular, the most recent investigations lead to models that are affected by inhomogeneities which appear to be so large that their presence would contradict what can be allowed in the real Universe. However, the basic idea of "inflation" is extremely appealing and one other possibility is that it can be applied to even earlier times, when the Universe was only  $10^{-43}$  seconds old. This time, known as the Planck time, corresponds to a

thermal energy of approximately  $10^{19}$  GeV above which all four fundamental forces of nature are unified, including gravity. The basic physics prevailing at that moment may be correctly described by the so-called supersymmetric theories, such as "supergravity". The most remarkable property of these theories, as reviewed by Fayet, is that they correlate particles with adjacent spins, such as particles with spin 1 and spin  $\frac{1}{2}$ , and therefore bring together bosons (such as the photon) and fermions (such as the electron and the proton). The existence of a number of new particles is then predicted. Thus, in "supergravity", which originates from supersymmetry by assuming that its properties are locally invariant, one recovers not only the graviton, which is the spin 2 particle which mediates the gravitational field in general relativity, but also a spin  $3/2$  particle called the gravitino. Thus, the partner of the photon would be a new spin  $1/2$  particle called photino. These new particles, the "...ino"s, could play an important role in cosmology and, if massive, they could provide the missing mass needed to close the Universe, avoiding some of the problems associated with neutrinos as previously illustrated.

Clearly, supersymmetric theories are still highly speculative and there is, as yet, no experimental verification of their validity. However, it is interesting to note that astronomical observations could shed some light on the existence of the new particles that are predicted. For instance, Sciama has pointed out that the annihilation of photinos and anti-photinos, if they are indeed massive enough, could produce a large background flux of radiation detectable by far ultraviolet and soft X-ray measurements.

Thus the Universe appears to provide the "natural" laboratory where one can hope to test fundamental theories of physics, while, at the same time, any progress in experimental particle physics may increase our confidence that these theories can be applied to an understanding of the basic

## SECOND ANNOUNCEMENT OF AN ESO WORKSHOP ON THE VIRGO CLUSTER OF GALAXIES

Since the first announcement of this workshop was issued in the previous Messenger (No. 34, December 1983) the date has been fixed and a preliminary programme made. The workshop will be held in **Garching**, from **September 4-7, 1984**.

The programme covers the following topics: Redshifts, observations in the radio continuum and in HI, infrared observations (with special emphasis on IRAS results), optical spectroscopy, spiral pattern analysis, galactic content and structure, the population of dwarf galaxies, UV and X-ray observation, the cluster dynamics, and the interaction with the environment.

Among the invited speakers are: W. Forman, W.K. Huchtmeier, J. Huchra, R.C. Kennicutt, C. Kotanyi, A. Sandage, G.A. Tammann and R.B. Tully.

Those interested in participating in this workshop and/or presenting contributed papers (probably mostly in the form of poster papers) should write to:

O.-G. Richter	B. Binggelli
M. Tarengi	Astronomisches Institut
European Southern Observatory	Venusstr. 7
Karl-Schwarzschild-Straße 2	CH-4102 Binningen
D-8046 Garching bei München	Switzerland
Federal Republic of Germany	

cosmological problems. Admittedly, we are still at the beginning of the road, but the interplay between particle physics and cosmology may indeed lead us to a deeper understanding of the fundamental laws of nature.

A most remarkable paper was presented by S.W. Hawking (Cambridge) who showed that, under certain plausible assumptions, the Universe may be described by a wave function obeying a simple Schrödinger equation such that the

most probable state would correspond to an oscillating model universe, singularity free, which is initially inflating and where the entropy does not change with time.

The Symposium ended with two concluding lectures by M.J. Rees (Cambridge) and J. Ellis (CERN) respectively, who summarized beautifully the main items discussed during the meeting and set the perspective for future work from the astrophysicist's and particle physicist's standpoint.

## Chromospheric Emission, Rotation and X-ray Coronae of Late-type Stars

*R. Pallavicini, Arcetri Astrophysical Observatory, Florence, Italy*

In a short note which appeared in 1913 in the *Astrophysical Journal*, G. Eberhard and K. Schwarzschild reported on the observation of emission reversals at the centre of K line of Ca II in some bright late-type stars (Arcturus, Aldebaran,  $\alpha$  Gem). They also noticed that the same phenomenon is usually observed in active regions on the Sun. To my knowledge, this was the first time that chromospheric emission was reported from stars other than the Sun. Since those early days our knowledge of stellar chromospheres has enormously increased, mainly through systematic surveys in the H and K lines of Ca II. More recently, observations at UV and X-ray wavelengths from space have provided ample evidence that chromospheres, transition regions and coronae are common to stars throughout the HR diagram. What is more significant is that these observations have demonstrated that magnetic fields play a fundamental role in the heating of outer stellar atmospheres and that the observed emission levels are in strong qualitative and quantitative disagreement with the predictions of the standard theory of coronal formation via the generation and dissipation of acoustic waves. The emphasis at present is on heating mechanisms which are based on the stressing and dissipation of magnetic fields generated by dynamo action in subphotospheric convection zones. As a result of this, stellar rotation has come to play a central role in the heating problem, as a controlling factor of the efficiency of the dynamo process. It can be anticipated that in the near future new accurate determinations of stellar rotation rates, as well as new measurements of transition regions and coronal emission from space will substantially increase our understanding of the process of coronal magnetic heating in late-type stars.

### Chromospheric and Coronal Heating

In the solar atmosphere, the temperature, after decreasing outwards to a minimum value of  $\approx 4,500$  K in the upper photosphere, starts to rise again, reaching  $10^4$  K in the chromosphere and more than one million degrees in the corona. Since heat cannot flow from lower to higher temperature regions (second law of thermodynamics) the observed temperature rise requires a non-thermal energy flux to be added to the thermal flux generated by thermonuclear reactions in the core of the Sun and flowing outwards under the form of radiation and convection. For stars of spectral type later than early F—stars which are known on theoretical grounds to possess outer convection zones—the required energy flux has been traditionally ascribed to the generation of acoustic waves by turbulent motions in the convection zone.

These waves, propagating in an atmosphere of rapidly decreasing density, steepen into shocks and dissipate their kinetic energy into thermal energy, thus producing the observed temperature rise.

In its simplest formulation this theory, first suggested by L. Biermann and M. Schwarzschild in the late forties and since then universally accepted, neglects the presence of magnetic fields which are considered as an unnecessary, easily avoidable, complication. Consequently, generation of acoustic waves and heating of outer stellar atmospheres are supposed to be spatially homogeneous and temporally constant, at variance with spatially resolved observations of the Sun, which show the chromosphere and corona to be both highly structured and time variable. For example, Fig. 1 shows a spectroheliogram of the Sun obtained in the K line of Ca II. Enhanced chromospheric emission is observed from magnetically disturbed active regions ("plages"), as well as from the

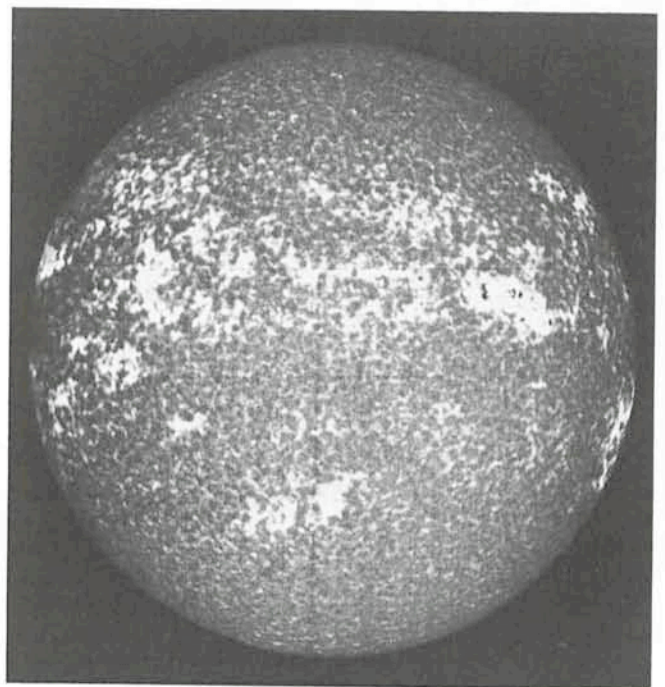


Fig. 1: Spectroheliogram of the Sun in the K line of Ca II obtained at the Solar Tower of the Arcetri Observatory. Notice the enhanced emission from the chromospheric network and from magnetically disturbed active regions.

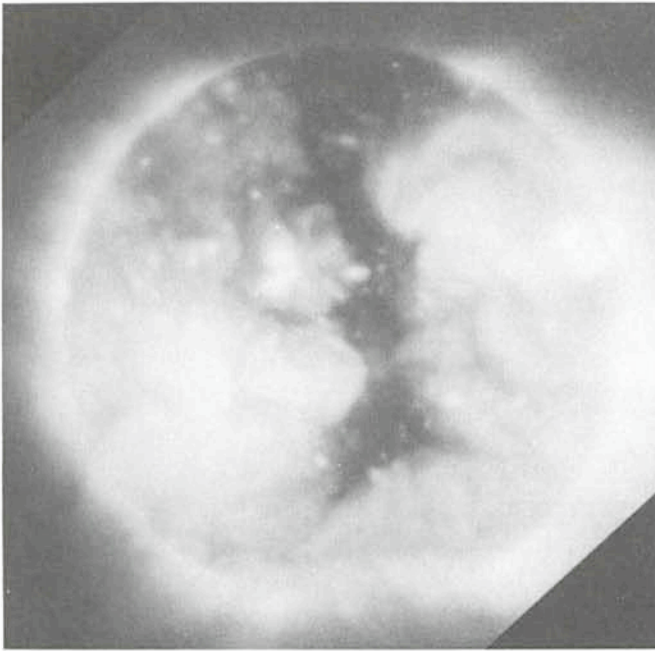


Fig. 2: X-ray photograph of the Sun obtained in 1973 from the SKYLAB spacecraft. Most of the X-ray emission comes from loop-like structures tracing magnetic field lines. The dark elongated feature is a coronal hole (courtesy American Science and Engineering).

boundaries of large convective cells where magnetic field lines are compressed by the fluid motions.

To give another example, Fig. 2 shows a photograph of the Sun obtained at X-ray wavelengths from onboard SKYLAB. Again, is apparent the highly structured nature of the corona which is formed by closed arch-shaped structures which apparently trace magnetic field lines. Only regions of low magnetic field intensity, where the lines of force are open to the interplanetary space, are devoid of dense coronal material and appear as dark features on X-ray photographs. Such regions, called for obvious reasons "coronal holes", are now known to be the source of high velocity wind streams flowing through the interplanetary space.

Further constraints on the heating mechanism have been provided by observations of wave motions in the solar transition region, as well as by stellar observations from the International Ultraviolet Explorer and the EINSTEIN Observatory. Solar observations of line broadenings and shifts from OSO-8 and the Solar Maximum Mission have shown evidence of the presence of acoustic waves in the transition region between the chromosphere and the corona. Unfortunately, the energy flux associated with the detected motions, although probably sufficient to heat the solar chromosphere, is too short by several orders of magnitude to heat the transition region and the corona.

At the same time stellar observations from IUE and the EINSTEIN Observatory have demonstrated the existence of transition regions and coronae for late-type stars of virtually all spectral types and luminosity classes (the only exceptions are late-type giants and supergiants with strong winds and large mass loss rates). This is in gross discrepancy with the acoustic theory which predicts that only stars of spectral type F and G should possess high temperature coronae. Early-type stars would be excluded by the absence of an appreciable outer convection zone, while coronal emission from K and M stars would be drastically reduced by the decrease of the convective velocity towards later spectral types and by the strong

dependence (to the eighth power) of the acoustic energy flux on the convective velocity.

More significantly, X-ray and UV observations, as well as previous ground-based observations in the Ca II lines, have shown that a very broad range of chromospheric and coronal emission levels exist for stars of the same spectral type and luminosity class. This observational result indicates that other parameters in addition to effective temperature and gravity are relevant for the heating of stellar chromospheres and coronae. As discussed below, a fundamental parameter may be rotation, owing to the key role played by rotation in determining the degree of dynamo-generated magnetic activity at the star surface.

How can magnetic fields help to solve some of these difficulties? The simplest way is to add a magnetic field to the treatment of wave generation, propagation and dissipation in a star with a subphotospheric convection zone. For instance, magnetoacoustic slow-mode waves, which are generated much more efficiently in magnetic regions than simple acoustic waves, might be very good candidates for heating stellar chromospheres, as suggested by R. Stein and P. Ulmschneider. Slow-mode waves can explain the observed spatial inhomogeneity and temporal variability of the solar chromosphere, as well as different levels of chromospheric activity in stars with the same effective temperature and gravity. Different activity levels, in fact, may result from different fractions of the stellar surface covered by magnetic fields.

Magnetoacoustic slow-mode waves are essentially acoustic waves channelled by the magnetic field. Their inclusion, therefore, does not solve the problem of the low energy fluxes associated with the wave motions measured by OSO-8 and SMM. In the corona, it is necessary to invoke other types of waves, for instance Alfvén waves, which have much longer damping lengths, or to attribute coronal heating to the dissipation of electric currents flowing in non-potential magnetic field configurations. Both Alfvén waves and current dissipation require the presence in the corona of magnetic flux tubes, such as those observed in X-ray photographs of the Sun (Fig. 2), as well as the presence of a certain degree of surface turbulence at the loop footpoints to shake or twist the lines of force. If the fluid motions are fast enough, Alfvén waves are generated; if on the contrary the flux tubes are twisted slowly a DC current is produced. The dissipation of Alfvén waves and of electric currents in the corona is a complex problem, a detailed treatment of which is far beyond the limits of this paper. Research in this exciting field is being pursued quite actively by several groups of plasma and solar physicists.

## The Role of Rotation

That rotation may be important in determining the degree of activity in late-type stars is not a novel concept. This suggestion was made early in the sixties as a result of extensive observations of Ca II emission and rotation carried out mainly by O. C. Wilson and R. Kraft. By observing a number of star clusters of different ages (Hyades, Pleiades, Coma) and by comparison with observations of field stars, a statistical relationship was discovered between stellar rotation, chromospheric Ca II K emission and age, in the sense that both stellar rotation and Ca II K emission decline with age in main-sequence stars. At the same time, it was pointed out that the "average" rotational velocity of stars drops precipitously at about the same spectral type (middle F) at which subphotospheric convection zones and chromospheric emission become prominent.

A quite convincing scenario was immediately put forward to explain these observations. Late-type stars which possess outer convection zones are able to develop chromospheres

and coronae, by some mechanism related to the presence of convective motions (e.g. generation of acoustic or magnetoacoustic waves). Analogously with the Sun, these stars will also be subject to coronal expansion under the form of a stellar wind. The mass loss associated with the wind (of the order of  $10^{-14}$  solar masses per year for the Sun) is far too small to have any appreciable effect on the evolution of the star. However, it may be an important source of angular momentum loss, because of the braking action of magnetic field lines carried along by the wind. Calculations for the Sun show that the characteristic time for angular momentum loss due to the outflowing of matter in the presence of magnetic fields is comparable to the life-time of a solar-type star on the main-sequence. This explains the rapid drop of the average rotational velocities of main-sequence stars at about spectral type F5, as well as the observed decline of rotation rate with age at each spectral type.

More difficult to understand is why Ca II emission should decrease with age. A possible clue is given once more by the solar analogy. We know that the intensity of Ca II emission in the Sun is proportional to the average intensity of the surface magnetic field. If this is true for stars in general, we should ask ourselves why stellar fields decline with age. The simplest explanation is that the magnetic field of a star is a remnant of the interstellar field which remained trapped in the star at the time of its formation. As the star gets older, magnetic energy may be gradually converted into thermal and mechanical energy which is eventually radiated away. It seems unlikely, however, that primordial magnetic fields may have survived resistive decay in the relatively long-lived stars of spectral type later than F. More likely, and the generally accepted view, is that magnetic fields in late-type stars are continually regenerated by an internal dynamo involving rotation and convection. This is the mechanism which is thought to be responsible for the cyclic emergence of sunspots at the surface of the Sun.

The interaction of rotation and convection in the Sun produces differential rotation, with equatorial zones moving faster than high latitude zones. The shear action of differential rotation on a "seed" poloidal magnetic field produces field amplification by the so-called  $\omega$ -effect, and gives rise to a toroidal component which eventually emerges at the star surface by magnetic buoyancy. Cyclonic turbulence will in turn regenerate a poloidal field from the toroidal one (the  $\alpha$ -effect) and the process will repeat itself in a cyclic pattern. Since both the  $\omega$ - and  $\alpha$ -effect depend linearly on the angular velocity of rotation, the efficiency of the process is higher for more rapidly rotating stars, and this may explain the observed higher level of chromospheric emission in young, more rapidly rotating stars.

There are a number of empirical facts which support this interpretation. First, there is the case of RS CVn stars which are detached binary systems with an extremely high degree of chromospheric and coronal activity. Of the two component stars, the more active one is usually a K subgiant, that is an evolved star. As the star gets older and moves out of the main sequence, its radius increases and its angular velocity decreases, owing to conservation of angular momentum. We would therefore expect a very low efficiency of dynamo action in these evolved stars. On the contrary, we observe a very high degree of activity. The explanation is that tidal interaction of the two components produces synchronism of orbital and rotational periods, thus strongly increasing the rotation rate of the two stars. The equatorial rotation rate of the K IV component in RS CVn systems is in fact of the order of several tens of kilometres per second, on average.

Another, possibly related, line of evidence is provided by the so-called BY Dra syndrome in certain dMe stars. As shown by B. Bopp and collaborators, the high degree of activity of these

systems is probably due to rapid rotation. In most cases BY Dra stars are young: in a few cases, however, the same phenomenon appears to occur in old stars which are members of binary systems and in which rapid rotation is enforced by tidal interaction. To summarize, there are a number of observational facts and theoretical considerations which all indicate rotation to be important in determining the level of chromospheric and coronal activity in late-type stars, via the generation of magnetic fields by dynamo action and their subsequent stressing and dissipation of turbulent motions.

With the advent of space observations, particularly after the launch of IUE and the EINSTEIN Observatory, a number of studies have been carried out with the purpose of determining in a quantitative way the law of dependence of chromospheric and coronal emission on rotation. The aim was to use this information to obtain a better understanding of dynamo action and coronal magnetic heating in late-type stars. The results of one such study are shown in Fig. 3, which is a correlation diagram of X-ray luminosity (as observed by the EINSTEIN Observatory) and rotational velocity for stars of spectral type later than middle F. The plot shows a clear dependence of X-ray coronal emission on rotation, which in first approximation can be expressed by a quadratic law. The plot, however, shows also the presence of a large scatter around the average relationship, which makes it difficult to determine the exact functional form of the dependence as well as to ascertain the relevance of other parameters (for instance, spectral type or, equivalently, depth of the convection zone).

One of the difficulties encountered in making correlation diagrams such as the one shown in Fig. 3 is the lack of accurate determinations of rotation velocities for the vast majority of stars of spectral type G and K which rotate at rates less—often much less—than  $10 \text{ km s}^{-1}$ . Only recently high resolution spectroscopic determinations of very low rotational velocities have become possible, but the results are still scanty and virtually absent for southern stars. For this reason, M. Pakull of the Technische Universität in Berlin and myself started in 1982 a programme of high resolution observations of cool stars using the Coudé Echelle Spectrometer (CES) at ESO, with the purpose of measuring rotational velocities and

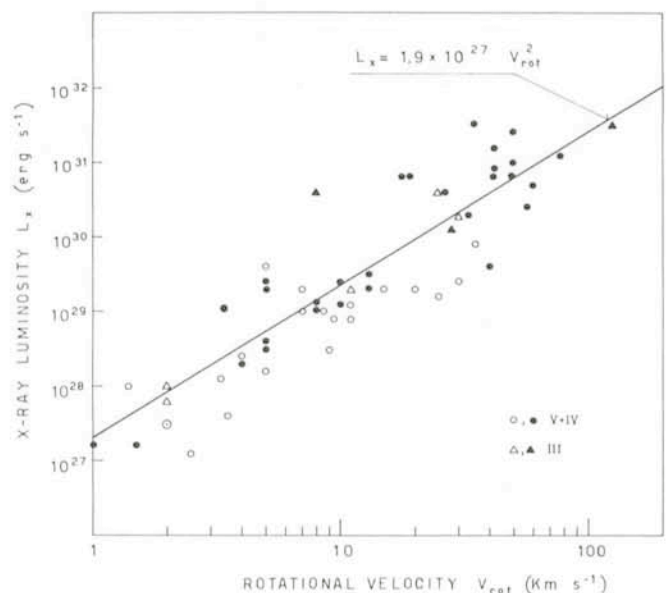


Fig. 3: Correlation diagram of X-ray luminosity vs. stellar rotation for late-type stars as determined by the author on the basis of X-ray observations from the EINSTEIN satellite and available data on stellar rotation rates. Filled symbols refer to rotation rates inferred from photometric or orbital periods.

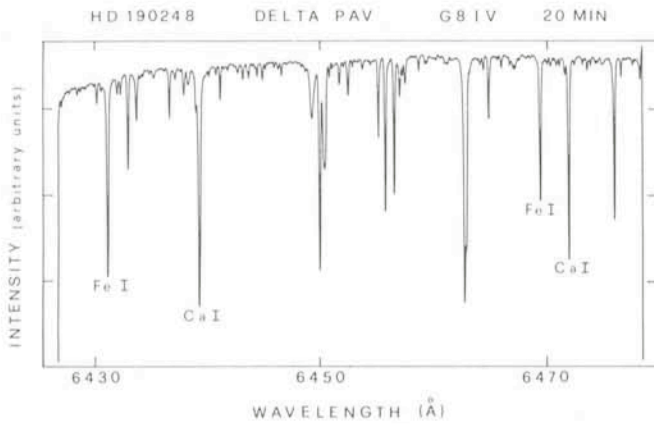


Fig. 4: Quick-look spectrum of the G8IV star  $\delta$  Pav at a central wavelength of 6450 Å obtained at La Silla on 18 July 1983 using the CES. Lines to be used for deriving rotational velocities with the technique referred to in the text are indicated.

chromospheric Ca II K emission for a number of southern stars previously detected at X-ray wavelengths by the EINSTEIN Observatory. The preliminary results of this programme are summarized in the next two sections.

### Measuring Rotational Velocities with the CES

The classical method of measuring stellar rotation is based on the broadening of photospheric absorption lines by the Doppler shift of the radiation emanating from the approaching and receding areas of the star. Application of this technique to stars of spectral type G or later, which rotate quite slowly, becomes increasingly difficult. Not only very high spectral resolutions are required, but what is more important is that other broadening mechanisms, such as micro- and macroturbulence, become comparable to, and even larger than, rotation. An effective method for discriminating between different broadening mechanisms is mandatory. In practice, it is not convenient to use standard techniques for stars rotating at velocities lower than 10–15 km s<sup>-1</sup> (we recall that the equatorial rotational rate of the Sun is only 2 km s<sup>-1</sup>).

A suitable technique which has been suggested for measuring very low rotational velocities is the Fourier analysis of line profiles, which can be applied whenever the data are of sufficiently high quality. The basic principles of the method have been described by D. Gray in his standard monograph "Theory and Observation of Normal Stellar Photospheres", as well as in a number of subsequent papers scattered in the specialized literature. In practice, the observed profile is compared with a grid of computed profiles obtained by broadening a narrow absorption line profile derived from stellar model calculations. The broadened profiles are obtained taking into account the effects of rotation, microturbulence and macroturbulence. In order to discriminate between competing broadening mechanisms, the comparison is made in the Fourier domain, taking advantage of the fact that profiles broadened by different mechanisms have distinctly different Fourier transforms. Rotational rates of late-type stars obtained by this technique have recently been published by D. Gray, M. Smith, D. Soderblom and others.

An instrument which appears particularly suitable for this type of measurement is the Coudé Echelle Spectrometer (CES) recently installed at La Silla. We used this instrument fed from the 1.4 m Coudé Auxiliary Telescope (CAT) in two runs (3–9 December 1982, observer: M. Pakull; and 18–30 July 1983, observer: R. Pallavicini). The instrument was operated in

the multi-channel mode with a 1,872 element Reticon detector. The high resolving power attainable, the very pure instrumental profile and the virtually absent scattered light are among the advantages offered by this instrument for the measurement of extremely low rotation rates of bright stars.

The observations were carried out in the red part of the spectrum at central wavelengths of 6020, 6250 and 6450 Å. In all cases the entrance slit was 200 micron corresponding to a resolving power  $\lambda/\Delta\lambda$  of the order of  $1.2 \times 10^5$ . The spectral range covered at the above wavelengths was about 50 Å. The signal-to-noise ratio was in all cases greater than 100. We have observed more than 50 southern bright stars of spectral types F5 to K5 and luminosity classes III, IV and V.

Fig. 4 shows an example of the quick look data obtained at a central wavelength of 6450 Å for the subgiant star  $\delta$  Pav ( $V = 3.6$ ). The seeing was good and the integration time was 20 min. Fig. 5 shows the reduced normalized spectrum of 26 Aql ( $V = 5.01$ ) at a central wavelength of 6250 Å. Typically, we have found that in average seeing conditions good spectra could be obtained in less than 1 hour integration time for stars brighter than  $V = 6.0$ .

The spectral regions chosen by us contain a number of unblended, intermediate-strength lines which are suitable for deriving projected rotational velocities  $v \sin i$  using Fourier techniques. Some of the lines to be modelled are indicated in Fig. 4. We are analysing these data in collaboration with D. Soderblom of the Harvard-Smithsonian Center for Astrophysics for main-sequence stars, and in collaboration with D. Gray of the University of Western Ontario for giants. Preliminary inspection of the data shows that most stars in our sample have extremely narrow lines indicating rotational velocities not substantially different from that of the Sun. Slow rotators, therefore, appear to dominate our sample of nearby stars, in spite of the fact that the latter was chosen mainly on the basis of X-ray observations. A few stars, however, have broadened lines which imply rotational velocities a factor 4 or 5 higher than for the Sun. When completely reduced, these data will be used in conjunction with previously determined X-ray fluxes to improve the correlation diagram of X-ray luminosity vs rotation shown in Fig. 3.

### Measuring Ca II K Emission with the CES

During our observing runs at La Silla we have used the Coudé Echelle Spectrometer also for measuring Ca II K emission at 3933.7 Å, for the same stars observed in the red for rotation.

Observations in the violet with the CES + Reticon are much more difficult than in the red. The efficiency of the Reticon, which is about 70% at 6000 Å, drops to 30% at the K line. In addition, in our programme, we were observing late-type stars which are intrinsically fainter in the U band than in the V band,

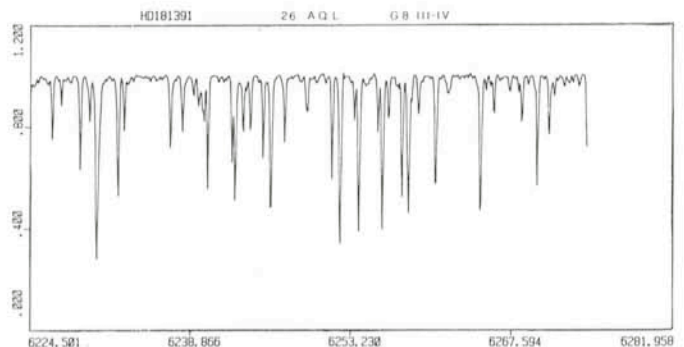


Fig. 5: Reduced normalized spectrum of the G8III-IV star 26 Aql at a central wavelength of 6250 Å obtained on 19 July 1983 using the CES.

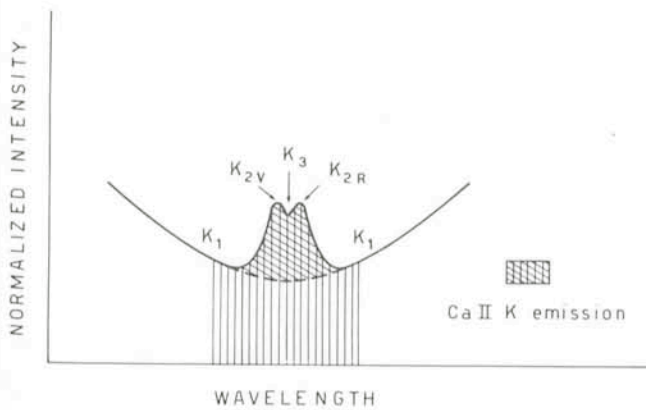


Fig. 6: Schematic diagram of the central reversal in the K line of Ca II for active late-type stars.

and, more importantly, we were interested in the—normally small—emission component at the bottom of a very deep absorption line. For all these reasons, observations in the violet turned out to be practical only for quite bright objects, and even so at the expenses of rather long integration times (usually of the order of a few hours).

The main motivation for our observations in the violet was to obtain accurate values of chromospheric Ca II emission fluxes calibrated in absolute units. It should be recalled that most observations made in the past were on a relative scale, which is not particularly suitable for discussing problems of energy balance and dissipation in stellar chromospheres. This is particularly true for southern stars, for which this information is virtually absent. Observations with the CES allow the simultaneous recording of a  $\approx 30 \text{ \AA}$  band at the K line, which may be centred in such a way as to contain the emission reversal as well as the nearby pseudo-continuum at  $3950 \text{ \AA}$ . From these observations, we can derive absolute fluxes in the emission component by using for instance the photoelectric calibration of the continuum spectrum at  $3950 \text{ \AA}$  obtained a few years ago by S. Catalano of the Catania Astrophysical Observatory.

Another correction must be made to the derived equivalent width of the central emission component. Fig. 6 shows a schematic diagram of the central part of the K line in a late-type star. The central emission reversal K is superimposed on an underlying photospheric contribution which is indicated in Fig. 6 by the dashed line obtained by extrapolating the inner

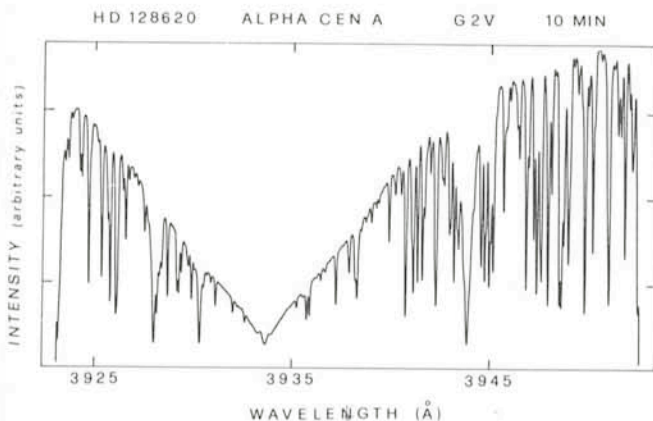


Fig. 7: Quick-look spectrum of the G2V star  $\alpha$  Cen A in the K line of Ca II obtained on 28 July 1983 using the CES. A quite similar spectrum is obtained when observing solar radiation reflected from the Moon.

absorption wings to the line centre. In order to obtain a correct estimate of chromospheric energy losses in the K line it is necessary to subtract the photospheric contribution, either empirically by extrapolating the inner wings to the line centre, or better still by subtracting a photospheric contribution computed on the basis of radiative equilibrium model atmospheres. This correction may be quite strong for stars of spectral type F and early G and may be an important source of error in deriving chromospheric radiative losses for these stars.

We have observed about 40 stars in the K line of Ca II. For very bright objects such as  $\alpha$  Cen A and  $\alpha$  Cen B we have been able to obtain high resolution spectra ( $\lambda/\Delta\lambda \approx 10^5$ ) using reasonably short exposure times. For all the other stars, we have used a somewhat reduced resolving power, ranging from  $3 \times 10^4$  to  $6 \times 10^4$ , and typical exposure times from 1 to 4 hours. Even in the worst case, however, the spectral resolution is  $\approx 120 \text{ m\AA}$ , more than adequate to resolve structures in the central emission component.

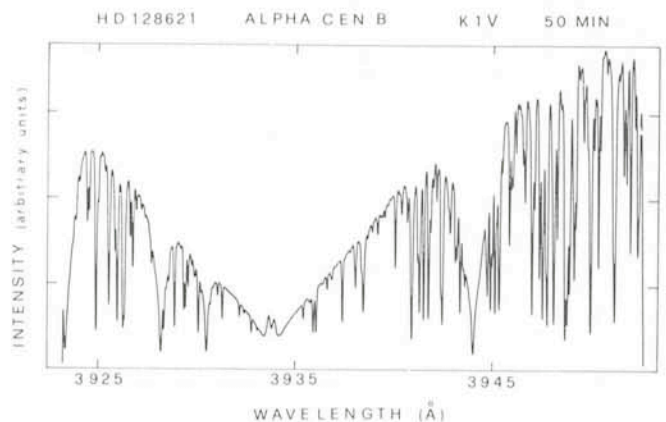


Fig. 8: Quick-look spectrum of the K1V star  $\alpha$  Cen B in the K line of Ca II obtained on 28 July 1983 at La Silla.

Figs. 7 and 8 show high resolution quick look spectra of  $\alpha$  Cen A and B. The G2V star  $\alpha$  Cen A shows a barely visible emission component, similar to that appearing in integrated spectra of the Sun (obtained by looking at the reflected light from the Moon). The spectrum of the K1V star  $\alpha$  Cen B, on the contrary, shows quite clearly the central reversal. It is interesting to note, however, that the energy flux in the K line is approximately equal for the two stars, stressing the importance of obtaining spectra calibrated in absolute units. The fact that the central reversal is much more easily seen in  $\alpha$  Cen B is simply due to the fact that the underlying photospheric background is much reduced, thus allowing the chromosphere to shine out more clearly by contrast.

Fig. 9 shows the reduced spectrum of the central part of the K line in the K5V star  $\epsilon$  Ind ( $V = 4.7$ ). Notice the very strong central reversal, which indicates a degree of chromospheric activity higher than the one typical of stars of the same spectral type. Fig. 10 shows the combined spectrum of the visual binary system 53 Aqr A + B obtained in a 4-hour exposure. Since the two component stars are quite faint for observations with the CES in the violet ( $V = 6.3$  and  $V = 6.6$ , respectively) we have used a rather wide slit ( $1,000 \text{ m\AA}$ ) collecting light from both stars simultaneously. We know from an old photographic spectrum published in 1965 by G. Herbig that the intensity of the central reversal is approximately the same for the two components. Although their spectral types (G1V and G2V) are about the same as for the Sun and  $\alpha$  Cen A, their chromo-

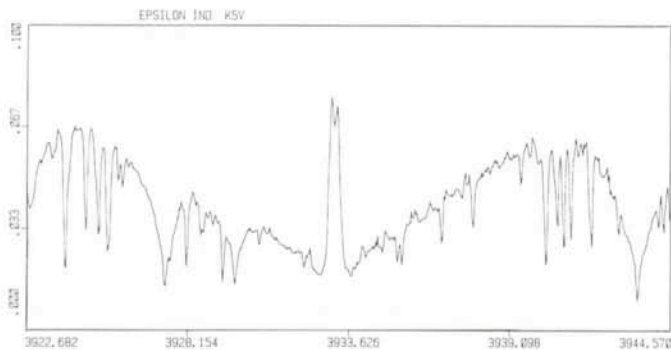


Fig. 9: Reduced spectrum of the K5V star  $\epsilon$  Ind in the K line of Ca II obtained on 27 July 1983 using the CES. Notice the strong central reversal.

spheric emission is strongly enhanced with respect to the average Sun or  $\alpha$  Cen A. In fact, it is more similar to that emitted by plage regions on the Sun. This is in agreement with the relatively high rotation rate of the two stars, which is a factor 4 higher than for the Sun. This system was not pointed at by the EINSTEIN Observatory. Observations at X-ray and UV wavelengths from IUE and EXOSAT are planned for 1984 as part of the authors's Guest Investigator programmes on these satellites.

I would like to conclude by emphasizing the importance of obtaining, preferably simultaneously, accurate values of chromospheric and coronal radiative losses for stars of different spectral types and degree of activity. It is not clear at present, even in the case of the Sun, whether the same mechanism is responsible for heating chromospheres as well as coronae. Although magnetic fields appear to be fundamental in both cases, their role in the heating problem may be different at different levels in a stellar atmosphere. It is quite conceivable, on the basis of the available evidence, that magnetoacoustic slow-mode waves may be the main process of non-thermal energy deposition at chromospheric levels,

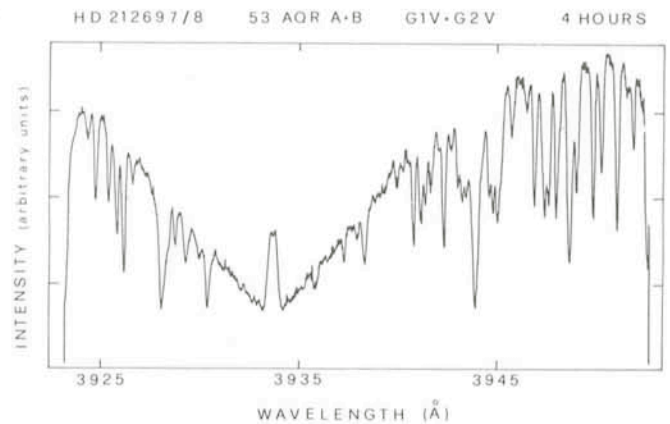


Fig. 10: Combined spectrum of the visual binary system 53 Aqr A+B in the K line of Ca II obtained on 29 July 1983 using the CES. The chromospheric emission reversal from these young rapidly rotating G1V+G2V stars is much higher than for  $\alpha$  Cen A or the Sun.

while Alfvén waves and possibly current dissipation are probably needed at coronal heights. A correlation diagram of coronal X-ray fluxes vs chromospheric Ca II K fluxes may provide insights into the problem of chromospheric and coronal heating, provided one has some additional information on the ratio of Ca II K losses to total chromospheric radiative losses for stars of different spectral types. Observations made with the CES at La Silla, although somewhat limited by the present difficulty of observing faint objects at short wavelengths, may be instrumental in providing the necessary data basis for such studies.

### Acknowledgements

It is a pleasure to acknowledge the cooperation of M. Pakull in the acquisition, analysis and interpretation of the ESO observations, as well as for enlightening discussions related to the subject of this paper.

## List of Preprints Published at ESO Scientific Group

### December 1983—February 1984

299. F. Caputo, V. Castellani and M. L. Quarta: A Self-consistent Approach to the Age of Globular Cluster M15. *Astronomy and Astrophysics*. December 1983.
300. C. Cacciari, V. Caloi, V. Castellani and F. Fusi Pecci: IUE Observations of UV Bright Stars in Globular Clusters M15 and wCen. *Astronomy and Astrophysics*. December 1983.
301. V. Caloi, V. Castellani, D. Galluccio and W. Wamsteker: Far Ultraviolet Spectra of the Nuclei of Globular Clusters M30, M54, M70. *Astronomy and Astrophysics*. December 1983.
302. F. Caputo, V. Castellani, R. di Gregorio and A. Tornambé: Theoretical RR Lyrae Pulsators from Synthetic Horizontal Branches. *Astronomy and Astrophysics*. December 1983.
303. S. Cristiani, M.-P. Véron and P. Véron: On the Completeness of the Braccisi Deep Quasar Survey. *Astronomy and Astrophysics*. December 1983.
304. M. Rosa, M. Joubert and P. Benvenuti: IUE Spectra of Extragalactic H II Regions. I. The Catalogue and the Atlas. *Astronomy and Astrophysics*. December 1983.
305. J. Krautter, B. Reipurth and W. Eichendorf: Spectrophotometry of Southern Herbig-Haro and Related Objects. *Astronomy and Astrophysics*. January 1984.
306. M. Iye: Oscillations of Rotating Polytopic Gas Disks. *Monthly Notices of the Royal Astronomical Society*. January 1984.
307. D. Baade and R. Ferlet: Discovery of a Possibly Rotation-induced Resonant Coupling of two Nonradial Pulsation Modes in  $\gamma$  Arae (Bllb). *Astronomy and Astrophysics*. January 1984.
308. M.-H. Ulrich and D. L. Meier: 5 GHz Observations of Cores in Extended Radio Galaxies. *Astronomical Journal*. January 1984.
309. M. Mayor et al.: Studies of Dynamical Properties of Globular Clusters. I. Kinematic Parameters and Binary Frequency in 47 Tucanae. *Astronomy and Astrophysics*. January 1984.
310. T. Ueda, M. Noguchi, M. Iye and S. Aoki: Global Modal Analysis of Disk Galaxies: Application to an SO Galaxy NGC 3115. *Astrophysical Journal*. January 1984.
311. D. Gillet and J.-P. J. Lafon: On Radiative Shocks in Atomic and Molecular Stellar Atmospheres. II. The Precursor Structure. *Astronomy and Astrophysics*. February 1984.
312. O.-G. Richter: Redshifts in Klemola 27. *Astronomy and Astrophysics, Supplement Series*. February 1984.
313. D. R. Jiang, C. Perrier and P. Léna: NGC 2024 # 2: Infrared Speckle Interferometry and Nature of the Source. *Astronomy and Astrophysics*. February 1984.
314. W. K. Huchtmeier and O.-G. Richter: HI Observations of Isolated Spiral Galaxies. *Astronomy and Astrophysics*. February 1984.

# Spectroscopic Study of a Sample of Visual Double Stars

Y. Chmielewski and M. Jousson, *Observatoire de Genève*

## Basic Parameters of a Stellar Atmosphere

We learn what we know about stars from the photons that originate in their atmospheres and eventually reach our telescopes. Therefore, if we want to account for the spectral distribution of the radiation received from a star we must know the physical properties in its atmosphere. One of the great achievements of the last twenty years in the theory of the stellar atmospheres has been the calculation of detailed models of their average physical properties. This theory teaches us that the atmosphere of a well-behaved star can be characterized by a small number of parameters. Once they are specified, the computation of the model stellar atmosphere follows in a unique way, within the assumed approximations. The most important of these parameters are the effective temperature, the surface gravity and the chemical composition. For the sake of completeness, two more parameters have to be mentioned: the mixing length and the microturbulence. They pertain to very crude approximations behind which is hidden our poor understanding of such phenomena as convection or turbulence in the atmospheres of the stars. In general, the microturbulence and the mixing length are adjusted in a more or less empirical way. In fact, there are indications that they might not be fully independent from the other parameters.

The effective temperature,  $T_{\text{eff}}$ , is by definition the temperature of an ideal blackbody radiating the same total flux  $F$  as the star considered. If  $R$  is the radius of the star, its total luminosity is given by  $L = 4\pi R^2 F = 4\pi R^2 \sigma T_{\text{eff}}^4$ . The value of  $T_{\text{eff}}$  is typical of the temperatures found in the layers of the atmosphere where the continuum radiation is formed. The surface gravity of the star,  $g$ , is given by the relation  $g = GM/R^2$  where  $M$  is the mass of the star and  $G$  is the universal gravitation constant. In hydrostatic equilibrium the pressure supports the weight of the atmospheric gas and, hence, is directly correlated to  $g$ . In principle the specification of the chemical composition of the atmospheric gas requires the knowledge of the individual abundances of about five to twenty elements that play a role in the determination of the state of the atmosphere and of its absorption coefficient. Fortunately, it turns out that the abundances of the important elements heavier than helium vary in lockstep, so that the specification of the chemical composition is reduced to two parameters: the abundance of helium and a general "metallicity" parameter, often referred to as  $[Fe/H]$ , or  $[M/H]$ . There is however a restriction for the elements C, N and O which have recently been shown to follow a different pattern, in particular in giant stars, due to evolutionary effects.

## The Determination of the Stellar Atmospheric Parameters

The direct determination of the effective temperature of a star requires the measurement of the angular radius of the star and the determination of the absolute flux received from it at the earth, integrated over the entire electromagnetic spectrum (ultraviolet + visible + infrared). For the determination of surface gravities, masses and absolute radii are needed. In some cases, the distance (i.e. the parallax) needs to be measured with good accuracy to convert angular diameters into absolute diameters. Thus, direct determinations of effective temperatures and gravities require measurements that are difficult and are feasible only for a restricted number of stars submitted to strong selection effects. For other stars,  $T_{\text{eff}}$  and  $g$

can be determined only by indirect methods which all make use of results derived from model stellar atmospheres.

The chemical composition cannot be measured independently of some temperature and pressure parameters. The strengths of the absorption lines in a stellar spectrum are the observable quantities which are the most sensitive to the chemical composition. However, they are also strongly dependent on the excitation and ionization conditions which prevail in the atmosphere and which are controlled by the values of  $T_{\text{eff}}$  and  $g$ . Thus, we have a highly coupled problem and we must derive a global solution from the analysis of the stellar spectrum.

Spectrophotometric and photometric techniques, which measure the distribution of the continuum radiation, as affected by the line blocking and by interstellar reddening, may provide good indicators for  $T_{\text{eff}}$ ,  $g$  and  $[M/H]$ . They often lose sensitivity for the cooler stars where the coupling between the effects is harder to disentangle. A very detailed discussion of the problem and of its solution may be found in a paper by Grenon (1978, *Publ. Observ. Genève*, sér. b, fasc. 5).

## Spectroscopic Methods

In any case the photometric metallicity indicators have to be calibrated upon results from high resolution spectroscopy of stellar line spectra. It is therefore important to have safe and accurate methods available for the analysis of stellar line spectra in view of the determination of the chemical composition. Since the effects of temperature, gravity and chemical composition on the line spectrum of a star are strongly coupled, it appears advisable, for the sake of internal consistency, to derive  $T_{\text{eff}}$  and  $g$  as well as the chemical composition from the analysis of the line spectrum itself.

The usual spectroscopic temperature indicator is provided by the relative strengths of lines of different excitations of a given ion of a given element. Interpreted with the help of the Boltzmann equation, they give an excitation temperature which is related to the effective temperature by means of a model stellar atmosphere. The relative numbers of atoms of a given element in the different possible states of ionization depend on the temperature and on the electron pressure, as expressed by the Saha equation. The "classical" spectroscopic method for the determination of  $g$  makes use of this property: the temperature being supposed known, an electronic pressure is chosen in such a way that the abundances deduced from the lines of two different ions of a given element are equal. However, the electronic pressure depends not only on  $g$  but also on the chemical composition in an intricate way. Usually the final solution is obtained at the end of an iterative procedure. Other spectroscopic indicators are sometimes used for the determination of the gravity. The strength of molecular lines depends on the dissociation equilibrium which is function of the pressure and of the abundances. Basically the method does not differ much from the ionization equilibrium. A third approach makes use of the fact that the broadening of the strong metal lines in the spectrum depends directly on the gas pressure (see Fig. 1). In this method, which requires observations of rather high resolution, the effects of pressure and chemical composition are more easily disentangled than in the previous ones. Its drawback resides in our insufficient understanding of the collisional broadening mechanisms at the atomic scale; it is compensated for by empirical fits to the

solar spectrum, provided that the transition probability is known with sufficient accuracy.

## The Arcturus Disillusion

Arcturus is a star that is very friendly to the astronomers. Since it is very beautiful and very bright, it has been measured many times and in very great detail. It has the best measured parallax for a giant star and several measurements of its diameter have been published. The high resolution Atlas of the optical spectrum of Arcturus published in 1968 by Griffin has been a landmark in the history of stellar spectroscopy. Several authors have used this Atlas for a detailed spectroscopic analysis. But, disappointingly, they obtain very discordant results. Estimates for its effective temperature range between 4,200 and 4,500 K. Even worse, the derived values for  $\log g$  go from 0.9 to 2.1, i. e.  $g$  values differing by a factor of 16. With all the data available for Arcturus, a value of the mass can be derived from the values obtained for  $T_{\text{eff}}$  and  $\log g$ . The resulting estimates of the mass given by the different authors vary between 0.2 and 1.2  $M_{\odot}$ . Amazingly the iron abundances derived show little scatter, everybody agreeing on a value around  $[\text{Fe}/\text{H}] = -0.7 \pm 0.2$ . The situation for Arcturus just exemplifies the general inadequacy and the lack of sensitivity of many of the standard spectroscopic techniques for the determination of  $T_{\text{eff}}$  and  $g$ . It has been so disturbing that it instigated the convention of a workshop in Cambridge in March 1981 where the problem was discussed in detail. The proceedings of this meeting are quite enlightening in that respect. (It is shown in particular how some basic inaccuracies in the measurement of the observable quantities translate into fundamental uncertainties in the basic parameters.)

## Visual Double Stars

The problem at stake is to try and find spectroscopic indicators that are more sensitive to the basic parameters of a stellar atmosphere than the usual standard techniques. The main difficulty is the highly coupled nature of the problem of the interpretation of the absorption lines. In such a case the best solution is to bring additional constraints into the problem in order to disentangle the effects of the different parameters on an observable feature. Such constraints may be found in the study of each component of a visual binary system. If their separation is wide enough, so that their individual magnitudes can be accurately measured, we know the ratio of their luminosities since they are located at the same distance from us. We can further assume that the two components have the same initial chemical composition. Binary systems are indeed usually thought to be coeval and, when their separation is so large that the tidal effects are negligible, the two components behave and evolve separately, just like single stars. These constraints are quite powerful and should prove extremely useful for a critical evaluation of the sensitivity of the different spectroscopic estimators to the variations of the different atmospheric parameters.

A sample of visual binary systems has been selected for that purpose. The systems were first chosen such that both components had spectral types going from late F to K. The brightest secondaries in systems of that kind have magnitudes fainter than 6 or 7. Since we want to make a systematic evaluation of the possible spectroscopic estimators of the stellar parameters, we must have as broad a wavelength coverage as possible with a resolution typical of most spectroscopic abundance studies. Until now, the ECHELEC spectrograph at the 1.5 m telescope has been the only one at ESO satisfying these observational requirements. The broad

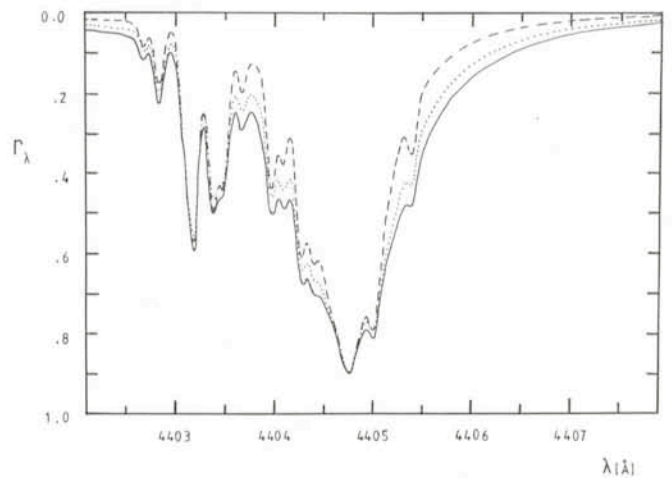


Fig. 1: Relative flux ( $\Gamma_{\lambda}$ ) of the synthetic spectrum with the Fe I 4404.8 Å line profile as computed for three different model atmospheres with a metallicity  $[\text{Fe}/\text{H}] = +0.15$ . The solid line corresponds to a model with  $T_{\text{eff}} = 5450$  and  $\log g = 4.5$ , the dotted line to  $T_{\text{eff}} = 5550$ ,  $\log g = 4.5$  and the dashed line to  $T_{\text{eff}} = 5450$ ,  $\log g = 3.75$ . The profile is insensitive to the adopted microturbulence ( $\xi = 1.0$  km/s). It has been further broadened by a Gaussian macroturbulence of 2 km/s, a rotation velocity  $v \sin i = 2$  km/s and a Gaussian instrumental profile of 2.5 km/s. The model atmospheres are very carefully scaled from the solar empirical model of Holweger and Müller (1974, Solar Physics 39, 19), with corrections interpolated in the theoretical grid of Bell et al. (1976, Astronomy and Astrophysics, Suppl. 23, 37). The blue wing includes contributions from blended atomic and molecular lines, whilst the far wing has been left on purpose free from blending.

wavelength coverage is made possible by the use of the Echelle grating with the cross-disperser. Given the speed of the spectrograph, it was decided to select visual binaries with secondaries brighter than the 9th magnitude. The sample contains systems with pairs of unevolved stars as well as systems where one, or both, components are giant stars. A few systems are so near that they have good parallaxes and that it has been possible to determine their orbit. This will add further constraints on mass and luminosity, even though in some cases their angular separation is small and their individual magnitudes are less well measured. A number of pairs of this sample which are located in the northern hemisphere are observed from the Observatoire de Haute-Provence where a twin of the ESO instrumentation is available. Altogether spectra for 24 pairs have already been obtained. Other observations for these pairs will be secured in the next periods until 3 spectra are available for each component of each pair.

The stars of the sample will be submitted to a complete classical differential analysis. Unevolved stars will be analysed relative to the Sun and giants relative to  $\epsilon$  Vir. Whenever the spectral types of the two components of a double star will not be too different, the secondary will also be analysed differentially relative to the primary. A search will be made for features (or ratios) most sensitive to a given parameter, but still sufficiently decoupled from the others. We intend to use the sample in a way similar to that used by Grenon (1978) for the calibration of the Geneva photometry for cool stars. For a given estimator, each binary pair provides a locus of variation at constant metallicity. Playing with the relative luminosities and stages of evolution of the components will allow to separate effects from  $T_{\text{eff}}$  and  $g$ . This method will first be used for components belonging to the interval of spectral types where classical spectroscopic analysis is generally considered to be valid (i. e. about F8 to K4). A few binaries in our

sample have secondaries later than K5. It will then be interesting to see if, and how, some of our estimators can be extrapolated in their direction.

Finally, this study may yield several important by-products, such as detailed abundance differences between the components of a system containing a dwarf and a giant, or age determination and tests of evolutionary sequences in the HR diagram.

A number of our spectra have now been digitized and reduced, and we have begun the analysis for some of the "simple" cases, such as 16 Cyg A and B. We are specially

investigating some interesting indicators. It seems that ratios formed with Fe I lines around  $\lambda 4872$ ,  $\lambda 4889$  and  $\lambda 4891$  would provide sensitive temperature indicators. Another example is the line of Fe I at  $\lambda 4404.8$  which seems much more sensitive to changes in gravity than in effective temperature, as illustrated in Fig. 1. Combined with another fainter Fe I line of about the same excitation, in order to cancel the effects of chemical composition, it should give a good gravity estimator.

This programme will be rewarding only if it is carried through with the greatest care. But we think the questions at stake certainly deserve the effort.

## Quasar Surface Densities

*S. Cristiani, ESO*

The story of the discovery of quasars has been told many times (see e.g. the 24th Liège International Astrophysical Colloquium 1983), nevertheless, it is always exciting to recall the first uncertain steps taken around 1960, when very little was known about this major component of the universe. In that period the identification of several radio sources, listed in the 3C catalogue, with more or less distant galaxies had been performed, but for many of them the optical counterpart was still unknown. In 1960 Matthews et al. (1) investigated with the 200" telescope of Mt. Palomar the fields corresponding to the sources 3C48, 3C196 and 3C286. They could not find any trace of galaxies, the radio position indicating on the contrary three objects of stellar appearance. At that time no radio star was actually known besides the Sun, thus the discovery raised some questions, which became even more puzzling when spectroscopic observations revealed that each of these "stars" emitted a lot of ultraviolet and blue light with a few emission lines, different from case to case, which could not be plausibly identified with any known element. Many theoretical possibilities were opened, but, before any thorough examination could be performed, the nature of the problem was completely changed with the identification of the radio source 3C273, carried out by Hazard, MacKey and Shimmins in 1962 (2) with the 210 ft Parkes radio telescope. By means of several lunar occultations, the position of the source was measured with an uncertainty less than 1" and its structure was shown to consist of two components separated by 19.5 arcsec. The relative accuracy of these measurements allowed an indisputable optical identification with a stellar object of about 13th V magnitude with an associated jet extending as far as 19.3 arcsec. Schmidt (3) took a spectrum of this object, which showed six broad emission lines which could be interpreted as being due to known elements assuming an unexpectedly large redshift of 0.158. It was possible to apply the same interpretation to 3C48, 3C196, and 3C286, when their spectra were reexamined, adopting respectively redshifts of 0.37, 0.87 and 0.85. At that time the radio galaxy 3C295 ( $z = 0.46$ ) was already known, nevertheless the discovery was upsetting: if the redshift of 3C273 is cosmological, then its absolute magnitude is  $-27$  (assuming a Hubble constant of 50 km/s/Mpc), that is about 40 times brighter than the brightest galaxies.

Since then many other amazing properties of these objects have been recognized: the ultraviolet excess, used as an aid for the identification of radio sources, led to the discovery of a few objects with similar colours far from any known radio source (the "interlopers" (4)), and finally a special survey for ultraviolet excess objects showed that radio quiet quasi stellar

objects are not rare (5); variability, X-ray and gamma emission, the presence of absorption lines provided further information on the nature of these objects as well as new puzzling questions on the physical processes involved. The importance of complete surveys was soon felt, as stressed by Ryle and Sandage in the conclusion of their 1964 paper (at that time less than 10 QSOs were known): "The initial success of this survey suggests that many more objects of this type remain to be found. When a representative sample of these objects is available for study, such questions as the occurrence or non-occurrence of the objects in clusters of galaxies, the spatial distribution and the distribution over the plane of the sky, the presence or absence of light variations, the connection of the optical to the radio spectrum, the absolute luminosities and the dispersion about a mean, and the form of the redshift-apparent magnitude relation can be studied." Since then, in fact, a great effort has been made in order to establish complete samples of quasars down to fainter and fainter limiting magnitudes, up to higher and higher redshifts. In this subtle game astronomers have always had to face the presence of hidden selection effects, trying to disentangle the intrinsic properties of QSOs from instrumental biases. One of the most powerful tools available is the early-day UV excess method, which has now been refined in multicolour techniques.

A. Braccisi intended to take advantage of the quasar infrared excess and used an I plate, in addition to the same two-colour plate used in 1965 by Sandage and Véron, to construct a complete catalogue of candidates to a limiting magnitude of  $B = 19.4$ . The infrared excess was not entirely helpful at that stage due to the relatively large measurement errors; however the investigation was successful and led to the discovery of a number of new quasars (6), since most of the faint UV excess objects at high galactic latitude, as those selected in this survey, turn out to be quasars (of low redshift). This line of research was pursued and resulted in a sample of 175 UV excess objects down to  $B = 19.4$  in the same field (7) and a sample of very faint ultraviolet objects down to  $B = 20.1$  in a restricted 1.72 sq. deg. area of this field (8). These surveys constituted for many years the only ones with "sufficient size, completeness, and purity for proper analysis" (9) and are still, together with other samples selected by various authors (especially noteworthy is the survey of Schmidt and Green on 10,714 square degrees above galactic latitude  $30^\circ$  which is expected to be complete to  $B = 16$ ), of extreme importance for the study of the change of the surface density of quasars with limiting magnitudes. Such observations are fundamental to

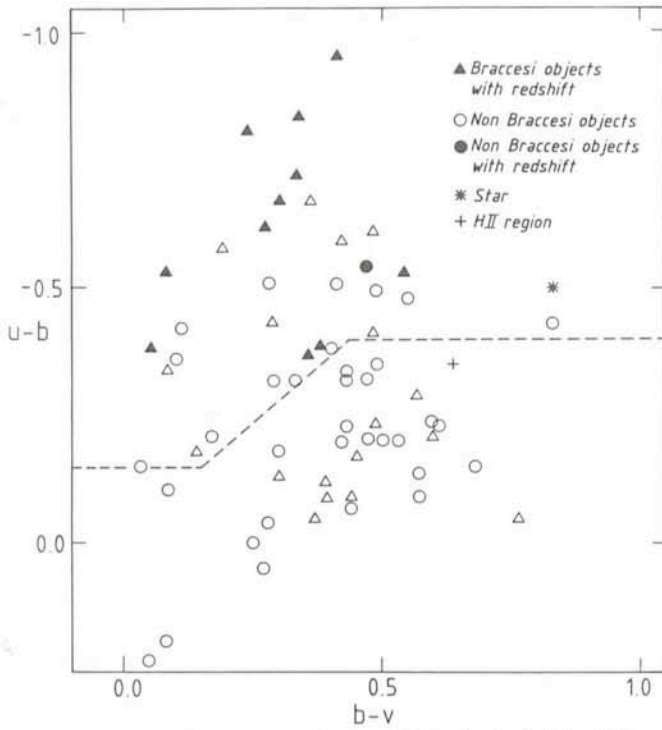


Fig. 1: The two-colour diagram for the objects in the Cristiani, Véron and Véron survey.

determine the quasar luminosity function at the various cosmic epochs, their evolutionary history as well as the physical conditions of the early universe.

To achieve this goal, detailed analyses are required and the completeness of the surveys on which the analyses rely must be carefully examined. Embarrassing large discrepancies in the quasar surface densities have been quoted by the various authors, revealing instrumental artifacts previously unsuspected. Even small effects can mask or alternatively simulate the evolutionary behaviour of quasars, heavily affecting any conclusion. As an example, the decrease of the quasar surface density beyond  $z = 2.2$ , claimed some years ago, was purely a selection effect, later recognized by means of new search techniques. The best way to get rid of such effects is to reobserve the same fields using other methods.

On account of these considerations several direct and gresns plates were taken at the prime focus of the CFH 3.6 m telescope in Hawaii of a 0.46 sq. deg. area included in the Braccesi 1.72 sq. deg. field (10). The best IIIa-J gresns plate has been searched for emission line and UV excess objects. The final selection was carried out by examining PDS tracings of these objects on IIIa-J and IIIa-F gresns plates and provided a list of 185 objects whose U, B, and V magnitudes were measured on the original 48" Palomar Schmidt plates used by Formigini et al. by means of PDS digitization and the standard IHAP reduction package. The low resolution slitless methods are known to be dependent on a number of parameters (such as seeing, resolution, etc.) which make it difficult to estimate the completeness. However, all the candidates found by Formigini et al. in the field are also in our list which we believe to be complete down to  $B = 20.2$ . For the 75 objects contained in the unvignetted 0.46 sq. deg. part of the field and brighter than  $B = 20.1$  the two-colour diagram (Fig. 1) allows the selection of 36 quasar candidates. The objects above the broken line, corresponding to an empirical but effective criterion stated by Braccesi et al. (11), are with all probability quasars with redshift lower than 2.3. Furthermore, it is

expected that all the quasars with redshift lower than 2.3 are included in this group; it is easy to check that none should lie outside the above-mentioned region by drawing the two-colour diagram for all the quasars known in the literature with photoelectric measurements. As a result of this survey, the completeness of the Braccesi deep quasar survey is confirmed but only down to a B magnitude of about 19.8, with the incompleteness rising abruptly from this point (Fig. 2). Of the

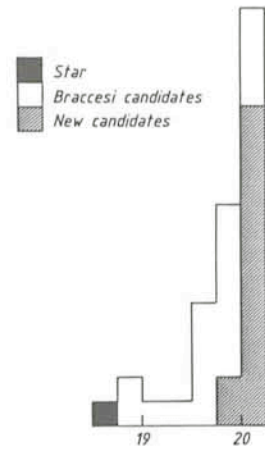


Fig. 2: Histogram showing the magnitude distribution of the candidates in the Cristiani, Véron and Véron survey.

36 quasar candidates one is known to be a star; if all the others turn out to be quasars, the surface density at  $B = 20.1$  would be 76 QSO/sq. deg. However, this number cannot be directly compared with the values derived from other surveys which are usually restricted to quasars brighter than  $M_B = -24$  and with redshift lower than 2.3. Spectroscopic follow-up is therefore greatly needed. Among the objects selected which lie under the broken line in Fig. 1, we believe to have found a few high redshift quasars (the IIIa-J emulsion is particularly effective to detect the Ly $\alpha$  emission for redshifts between 2

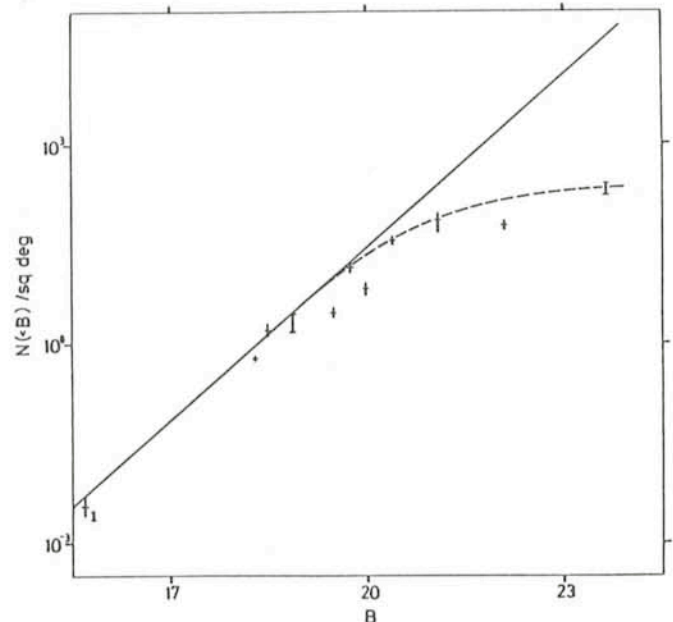


Fig. 3: The number-magnitude diagram of quasars from Véron and Véron, 1982, *Astronomy and Astrophysics* 105, 405.

and 3.5). Higher dispersion spectroscopy of these objects and a detailed colorimetric study could provide a starting point for an investigation of the surface density of high redshift quasars, the present knowledge of which is greatly unsatisfactory. There is evidence of a decrease of the quasar space density beyond  $z = 3.5$ , but a detailed unbiased analysis is still lacking. This subject is of course of fundamental importance since it brings direct inferences on the evolutionary history of these objects and of the Universe itself.

Other independent methods can be applied to test and improve the completeness of the sample, and at present an automatic search for faint variable objects in the  $6.5 \times 6.5$  sq. deg. field investigated by Braccisi et al. in 1970 is under way by Hawkins, M. R. S., Cristiani, S., Véron-Cetty, M. P., Véron, P., and Braccisi, A. This technique provides a powerful independent method of selecting quasar candidates which is particularly valuable in this case, since the completeness of the sample is checked and, at the same time, a statistically significant analysis of the quasar variability can be carried out, with remarkable consequences for the understanding of the physical processes involved in the quasar phenomenon.

Fig. 3 summarizes the present knowledge of the quasar surface density which is for astronomers a cause of dissatisfaction, for many questions are unanswered and a quantity of

work still remains to be done, and at the same time a reason for pride, since properties of objects as far as several billion light-years have been determined.

### References

1. Matthews, T. A., Bolton, J. G., Greenstein, J. L., Münch, G., and Sandage, A. R., 1961, Am. Astr. Soc. Meeting, N. Y., *Sky and Telescope* **21**, 148.
2. Hazard, C., Mackey, M. B., and Shimmins, A. T., 1963, *Nature* **197**, 1037.
3. Schmidt, M., 1963, *Nature* **197**, 1040.
4. Ryle, M., and Sandage, A. R., 1964, *Astrophysical Journal* **139**, 419.
5. Sandage, A. R., and Véron, P., 1965, *Astrophysical Journal* **142**, 412.
6. Braccisi, A., Lynds, R., and Sandage, A. R., 1968, *Astrophysical Journal* **152**, L105.
7. Braccisi, A., Formigini, L., and Gandolfi, E., 1970, *Astronomy and Astrophysics* **5**, 264.
8. Formigini, L., Zitelli, V., Bonoli, F., and Braccisi, A., 1980, *Astronomy and Astrophysics Supplement Series* **39**, 129.
9. Setti, G., and Woltjer, L., 1973, *Annals N. Y. Acad. Sciences* **224** 8.
10. Cristiani, S., Véron-Cetty, M. P., and Véron, P., 1983, ESO Preprint 303.
11. Braccisi et al. 1980, *Astronomy and Astrophysics* **85**, 80.

## The Story of the Eclipsing, Double-lined Binary HD 224113

R. Haefner, Universitäts-Sternwarte München

For an observing astronomer it is always very exciting to record an unexpected event, even if this is "only" the detection of the optical variability of a spectroscopic binary. This happened to me in July 1978 when I performed a photometric programme at the ESO 50 cm telescope. Since the allotted observing time was a bit too late to follow my programme stars until the end of the night, I had prepared a list of about 20 radial velocity variables to check their photometric behaviour during the remaining hours. The first object I selected was HD 224113, a B6V star with a magnitude of  $V \sim 6.1$ . Suddenly, after some minutes of observation the brightness dropped off and faded away continuously until the rising sun prevented further measurements. The nature and range of the variation ( $\Delta V \sim 0.2$ ) indicated that an eclipse had been observed. Of course, for the nights to come, the hours before dawn were devoted to further observations of this star. However, no further variations were recognized, HD 224113 showed a constant brightness all the time.

Back at home I learned (a little disillusioned) that HD 224113 was known to be a single-lined spectroscopic binary with a period of about 2.5 days (Archer and Feast, 1958, *Monthly Notices of the Astronomical Society of Southern Africa* **17**, 9) and that it appeared in my list only because the radial velocity catalogue (Abt and Biggs, 1972) which I used as reference was incorrect: This star was marked only as variable in radial velocity and not as spectroscopic binary. A note in the paper by Archer and Feast that "a faint secondary spectrum is suspected on several of the spectrograms" was the stimulant to let things not rest. Eclipsing binaries showing in their spectra the lines of both components are the only sources for a precise determination of the system parameters in absolute units, including especially the masses. The knowledge of reliable empirical masses is essential for the theory of stellar structure and evolution. At that time system parameters of less

than two dozen B-type main-sequence stars were known with high precision, among them only one B6V star. Since their masses and radii indicated a significant revision of the empirical mass and radius scale for B stars, a closer investigation of HD 224113 seemed to be worthwhile.

During the following years (1979, 1980, 1981) more than 2,700 uvby measurements were collected using the ESO 50 cm telescope. Descending and ascending part of the primary minimum as well as the whole secondary minimum could be covered several times allowing for a precise determination of the period. From the shape of the resulting light curves it is obvious that the interaction between the components is rather weak. The small displacement of the secondary minimum from midphase indicates a slight non-zero eccentricity of the orbit. For illustration the V light curve is presented in Fig. 1. In the course of two observing runs in 1979 and 1980, 36 high-dispersion spectra ranging from the blue to the infrared region could be obtained using the coudé spectrograph of the 1.5 m telescope. A careful inspection revealed that the only detectable lines of the secondary spectrum were those of Ca II-K and Mg II  $\lambda$  4481, both very weak on the baked IIIa-J plates. The hydrogen lines cannot be seen distinctly double; there is only a variable asymmetry in the wings of the Balmer lines. A preliminary analysis (Haefner, 1981, *IBVS* No. 1996), based on radial velocities of the Ca II-K lines and on part of the photometry (Russell-Merrill nomogram method), yielded surprisingly good results for the system parameters when compared with the final solution.

In the meantime I learned that the optical variability had been detected independently by Balona (1977, *Mem. R. A. S.*, **84**, 101) and Burki and Rufener (1980, *Astronomy and Astrophysics* **39**, 121). The roughly 100 photometric measurements of Burki and Rufener which span the orbital period were analysed by Giurcin and Mardirossian (1981, *Astrophys.*

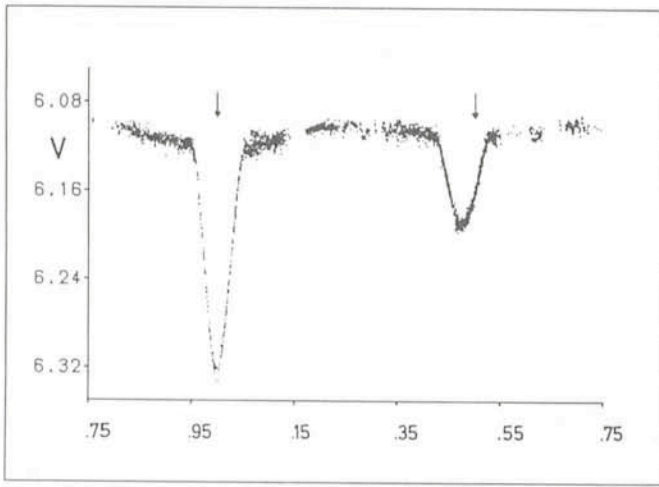


Fig. 1: The V light curve of HD 224113. Included are 21 measurements kindly provided by H. J. Schober and 41 observations obtained by C. Sterken (1982, IBVS No. 2166). The phases 0 and 0.5 are marked by arrows.

Space Sci. 74, 83) using a light curve synthesis programme. Besides this, Dean and Laing (1981, M.N.A.S.S.A. 40, 48) published a Russel-Merrill analysis based on about 120 measurements. However, the results of their analyses are rather discordant, reflecting the paucity of the photometric data as well as the unawareness of the radial velocity curve of the secondary. The latter forced them to rely on quantities which then can only be estimated.

The amount of the available spectroscopic material could considerably be increased by the cooperation of Mart de Groot (Armagh Observatory) who brought in 23 blue spectra which he had obtained on Ila-O plates at the coude spectrograph of the 1.5 m telescope during the years 1970 to 1976. Using the facilities of the St. Andrews Observatory, I. Skillen determined the radial velocities from altogether 47 blue spectra and derived the orbital parameters from the resulting radial velocity curves (Fig. 2). Since the signal-to-noise ratio of the spectra recorded on Ila-O emulsion was inferior to that of the Ila-J plates the velocities derived from the former showed more scatter. This was particularly evident for the secondary lines. It seemed therefore very promising to use the newly

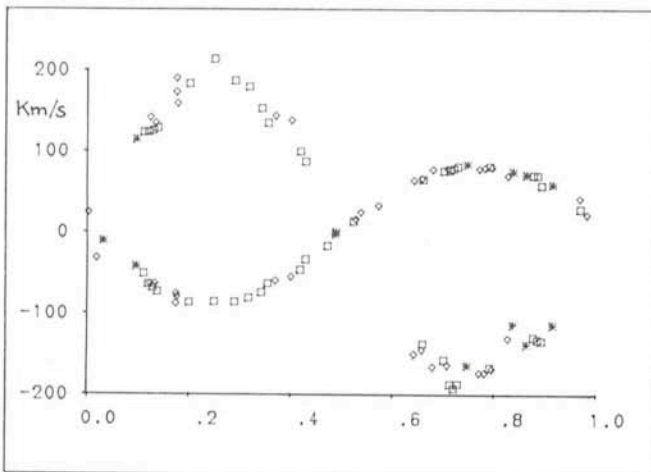


Fig. 2: Radial velocity curves of HD 224113. Included is one Call-K Reticon observation kindly provided by H. Lindgren.  $\diamond$  $\diamond$ : Ila-O plates;  $\square$  $\square$ : Ila-J plates;  $*$  $*$ : Reticon spectra.

available CAT/CES/Reticon combination on La Silla to check or improve the radial velocity curve of the secondary. Among other advantages, the high resolving power makes this combination an ideal system to record very weak lines with high precision. However, due to extremely bad weather conditions prevailing during my observing run at the end of July 1982, the outcome was quite poor with respect to the number of spectra: Only 5 Call-K and 2 H $\alpha$  observations could be obtained. Fig. 3 presents the Call-K line complex showing in particular the very weak and shallow secondary line and the resolved interstellar component for different phases. The radial velocities were determined using the iterative simultaneous least-squares fit for multiple spectral lines of the IHAP system. Despite the fact that these few observations could not substantially improve the radial velocity curve of HD 224113 the combination CAT/CES/Reticon and the IHAP software is highly recommendable for precise investigations of faint secondary lines of spectroscopic binaries.

For the final analysis of the light curves I have used the light curve programme of Wilson and Devinney (1971, *Astrophysical Journal* 166, 605) in a version running at the Bamberg Observatory. This programme generates wavelength-dependent light curves as a function of 15 parameters on the basis of a physically realistic model which allows for rotational and tidal distortion, the reflection effect, limb darkening, and gravity darkening. In principle a least-squares differential correction procedure enables one to fit a calculated light curve to the observations and to determine the best set of these parameters. Since some of them are better determined by the spectroscopic analysis (e.g. mass ratio) or are known to be generally valid for early-type stars (limb-darkening coefficient

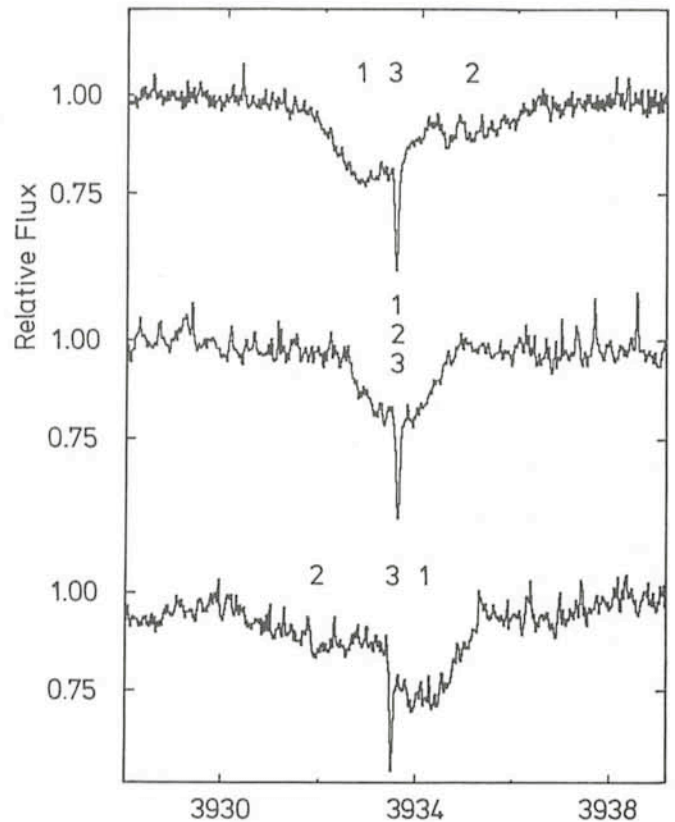


Fig. 3: Reticon observations of the Call-K line complex for different orbital phases. 1: primary component; 2: secondary component; 3: interstellar component. Upper and lower spectrum were obtained half a period apart at phases where primary and secondary lines show about half the maximum separation.

icients, bolometric albedos, etc.) the number of adjustable parameters could be appreciably lowered. The analysis revealed that the system HD 224113 is a detached one with the secondary being an AOV type star. The results for the masses and radii of both components strongly support the trend to values which are about 20–30 % smaller than stan-

dard values commonly used up to now. For detailed results the reader is referred to my article which will soon be published in *Astronomy and Astrophysics*. It is quite funny that an error in a radial velocity catalogue caused this investigation revealing one more early-type binary suitable for a high-precision determination of the absolute system parameters.

## Some Old and New Facts About the Local Group of Galaxies and the Extragalactic Distance Scale

O.-G. Richter, ESO

The number of nearby external galaxies known or believed to lie within about 1.5 Mpc of our own Galaxy (an often used value for the size of the local system) is a rather interesting function of time. In Table 1 I have listed all known such galaxies ordered by absolute magnitude, their date of discovery and some modern data. They form what is called—since nearly 60 years now—the *Local Group* (LG). (The information given in the tables is not claimed to be complete. A reader with a flair for detective work may succeed in adding all the missing data. My primary source for the historical data was the book *The Search for the Nebulae* by Kenneth Glyn Jones [1975, Alpha Academic, The Burlington Press, Foxton, Cambridge].) Before the invention of the telescope only three galaxies were known with certainty, out of which only one appeared in old catalogues, namely the Andromeda nebula. In Fig. 1 the drawing of G.-L. Le Gentil is shown together with a modern photograph. This is in fact the first drawing of a nebula in the history of astronomy. The Persian astronomer Al-Sûfi (903–986), who included the nebula in “the girdle of Andromeda” in his star

catalogue, may also have known the LMC, which—according to R. H. Wilson (1899, *Star Names and their Meanings*, 1963 reprinted as *Star Names, Their Lore and Meaning*, Dover Publ., New York)—he might have meant with an object called the “white ox” (Al-Bakr). Both Magellanic Clouds were certainly known since the earliest voyages to the southern hemisphere and they are mentioned from 1515 on, when the Italian navigator Andraes Corsali (in 1516) drew a (rather crude) map of the southern sky. In the latest edition of his famous catalogue, Charles Messier in 1781 mentioned 3 members of the LG, but not the Magellanic Clouds and—even stranger—not NGC 205. This latter galaxy (proposed by K. Glyn Jones to be named M 110) was found on the 27th of August 1783 by Caroline Herschel. In a later paper C. Messier claimed to have detected it already in 1773; this claim has later been supported by H.-L. D’Arrest. William (Wilhelm Friedrich) Herschel and his son, John Herschel, who detected most of the nebulae listed later by J. L. E. Dreyer in his *New General Catalogue of Nebulae and Clusters of Stars* (1888, abbreviated as NGC),

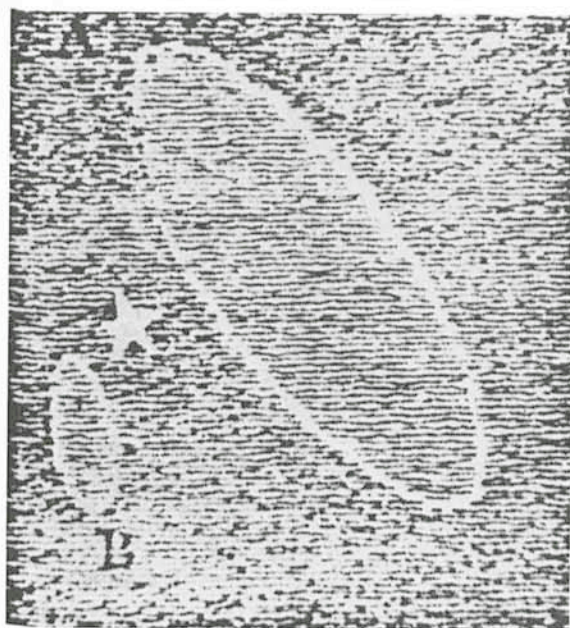
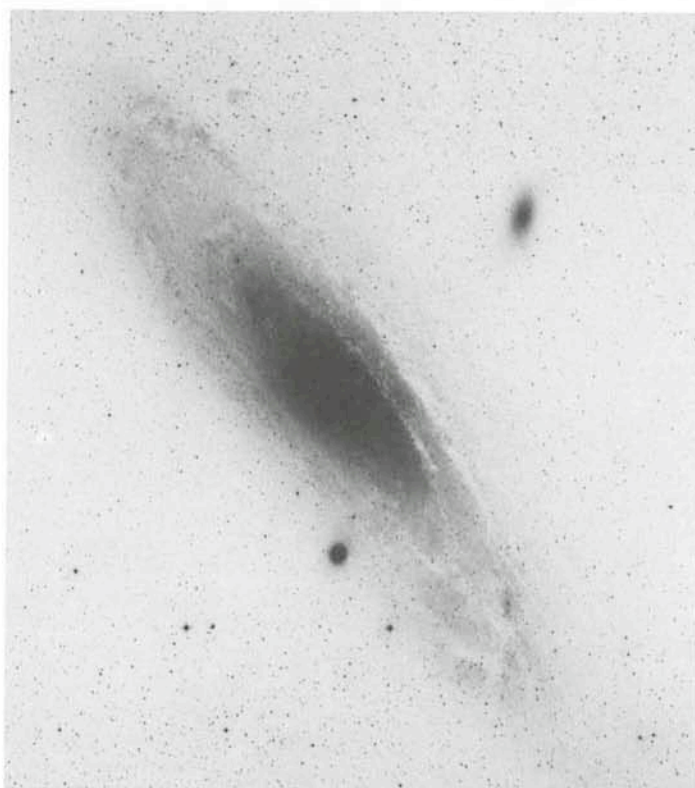


Fig. 1: Le Gentil's drawing from 1749 of the Andromeda nebula and its companion M 32 compared with the Palomar Schmidt photograph (Ila-D+Wr12, courtesy M. Dopita and S. D'Odorico). The identification of the drawn star is not completely obvious (another supernova?). North is up and east to the left.



could add only one (!) galaxy to the LG. This emphasises the difficulties the astronomers still working without photographic techniques had with relatively low surface brightness galaxies. By the time of the completion of the second *Index Catalogue* (IC) in 1908 (also by Dreyer) twelve galaxies in the LG were known. When it finally became clear in 1925 (through the work by E. Hubble) that most of the nebulae were “island universes” (so called by Immanuel Kant already in 1755) outside our own Galaxy it was soon discovered that, apparently, we were member of a small group of these galaxies. This aggregate was then named the “Local Group” by Hubble; he still knew only 13 members including our Galaxy.

After the invention of the Schmidt telescope and later with the advent of the Palomar Observatory Sky Survey a number of dwarf systems were quickly discovered. In a fine review summarizing the knowledge about the LG in 1968 given by S. van den Bergh (*Journ. R. A. S. C.* **62**, 1) already 17 galaxies were listed. Only after the southern hemisphere has been explored by means of the ESO and SRC surveys we can consider our knowledge of members of the LG to be fairly complete. Aside from those mentioned in Table 1 (out of which one, IC 5152, is—according to J. L. Sersic and M. A. Cerruti [1979, *Observatory* **99**, 150]—a very doubtful member only) some other objects have been considered as possible members, most notably the two galaxies Sextans A and Sextans B. Most of the other objects considered at one time or another to be dwarf members of the LG galaxy “club” (see Table 2) are now believed to be very distant globular clusters, sometimes called “intergalactic tramps”. One notable exception is the Phoenix object, discovered by ESO astronomer H.-E. Schuster (see *The Messenger* **4**, 3) and believed to be an extremely distant globular cluster, which was shown by Canterna and Flower (1977, *Astrophysical Journal* **212**, L57) to be a dwarf

galaxy with a (rather uncertain) distance of about 1.8 Mpc. This would place it just outside the boundary of the LG. I am not aware of any further study of this interesting object. The latest addendum to the list of known LG members—the Pisces system LGS 3—dates back to 1978.

In his book *Morphological Astronomy* F. Zwicky estimated the total number of LG galaxies—based on his version of the luminosity function—absolutely brighter than  $-7^m$  to be 92! Where should we search for those not listed in the tables? S. van den Bergh already pointed out that even within the LG strong subclustering occurs. Apparently two dominant galaxies, M 31 and our Galaxy, are surrounded by “clouds” of smaller galaxies. There are only a few exceptions from this “rule”, e.g. IC 1613 or M 33; some astronomers place the latter galaxy even into the M 31 subsystem. We know (at least) nine “satellite” galaxies around our own Galaxy and some more may be hidden behind the disk of the Galaxy (i.e. in the zone of avoidance). If we accept the standard view that M 31 is about 3 times as massive and as luminous as our Galaxy we could perhaps assume that it is surrounded by also 3 times as many dwarf systems as our Galaxy. One could then, in fact, expect up to about 60 satellite galaxies around M 31, whereas only 7 have been found so far. These possible dwarf galaxies near the Andromeda nebula should then have apparent (blue) total magnitudes fainter than  $\sim 14^m$ , but certainly not fainter than about  $18^m$ . As S. van den Bergh (1974, *Astrophysical Journal* **191**, 271) has already performed a search for such galaxies and found only the 3 already mentioned in 1972 (*Astrophysical Journal* **171**, L31), we have to believe that most galaxies belonging to the LG are known by now. Therefore it seems unlikely that many more dwarfs (in the LG) will be discovered in the future. As D. Lynden-Bell (1982, *Observatory* **102**, 202) has suggested, many of the dwarf galaxies around our Galaxy are

TABLE 1: Galaxies belonging to the Local Group

No.	Name	Discoverer and Date of Discovery	Position	Type	$B_T$	D (Mpc)	$M_B^{0.1}$
1	M 31 (NGC 224)	Al-Sûfi?, $\leq 964$	00 <sup>h</sup> 40 <sup>m</sup> +41°	Sb	4 <sup>m</sup> 38	0.67	-21 <sup>m</sup> 61
2	The Galaxy	?, $\leq 550$ B. C.	17 <sup>h</sup> 42 <sup>m</sup> -28°	Sbc		0.01	-20 <sup>m</sup> 6:
3	M 33 (NGC 598)	C. Messier, 25. Aug. 1764	01 <sup>h</sup> 31 <sup>m</sup> +30°	Sc	6 <sup>m</sup> 26	0.76	-19 <sup>m</sup> 07
4	Large Magellanic Cloud	Al-Sûfi??, $\leq 1515$	05 <sup>h</sup> 24 <sup>m</sup> -69°	SBm	0 <sup>m</sup> 63	0.06	-18 <sup>m</sup> 43
5	Small Magellanic Cloud	A. Corsali?, $\leq 1515$	00 <sup>h</sup> 51 <sup>m</sup> -73°	Im	2 <sup>m</sup> 79	0.08	-16 <sup>m</sup> 99
6	IC 10	L. Swift	00 <sup>h</sup> 17 <sup>m</sup> +59°	Im?	11 <sup>m</sup> 70	1.3:	-16 <sup>m</sup> 2:
7	NGC 205 (M 110)	C. Messier, 10. Aug. 1773	00 <sup>h</sup> 37 <sup>m</sup> +41°	S0/E5 pec.	8 <sup>m</sup> 60	0.67	-15 <sup>m</sup> 72
8	M 32 (NGC 221)	G.-J. Le Gentil, 29. Oct. 1749	00 <sup>h</sup> 40 <sup>m</sup> +40°	E2	9 <sup>m</sup> 01	0.67	-15 <sup>m</sup> 53
9	NGC 6822	E. E. Barnard, 1884	19 <sup>h</sup> 42 <sup>m</sup> -14°	Im	9 <sup>m</sup> 35	0.56	-15 <sup>m</sup> 11
10	W.L.M. system	M. Wolf, 1908	23 <sup>h</sup> 59 <sup>m</sup> -15°	IBm	11 <sup>m</sup> 29	1.6	-15 <sup>m</sup> 04
11	IC 5152	D. Steward	21 <sup>h</sup> 59 <sup>m</sup> -51°	Sdm	11 <sup>m</sup> 68	1.6:	-14 <sup>m</sup> 6:
12	NGC 185	W. Herschel	00 <sup>h</sup> 36 <sup>m</sup> +48°	dE3 pec.	10 <sup>m</sup> 13	0.67	-14 <sup>m</sup> 59
13	IC 1613	M. Wolf, 1907	01 <sup>h</sup> 02 <sup>m</sup> +01°	Im	9 <sup>m</sup> 96	0.77	-14 <sup>m</sup> 50
14	NGC 147	H. L. D'Arrest, 1856	00 <sup>h</sup> 30 <sup>m</sup> +48°	dE5	10 <sup>m</sup> 36	0.67	-14 <sup>m</sup> 36
15	Leo A (Leo III)	F. Zwicky, 1940	09 <sup>h</sup> 56 <sup>m</sup> +30°	IBm	12 <sup>m</sup> 70	1.59	-13 <sup>m</sup> 49
16	Pegasus system	A. G. Wilson, $\leq 1959$	23 <sup>h</sup> 26 <sup>m</sup> +14°	Im	12 <sup>m</sup> 41	1.62	-13 <sup>m</sup> 37
17	Fornax system	H. Shapley, 1938	02 <sup>h</sup> 37 <sup>m</sup> -34°	dE0 pec.	9 <sup>m</sup> 04	0.16	-11 <sup>m</sup> 98
18	DDO 155 (GR 8)	G. R. Reaves, $\leq 1955$	12 <sup>h</sup> 56 <sup>m</sup> +14°	Im	14 <sup>m</sup> 59	1.3:	-11 <sup>m</sup> 2:
19	DDO 210 (Aquarius)	S. van den Bergh?, $\leq 1959$	20 <sup>h</sup> 44 <sup>m</sup> -13°	Im	15 <sup>m</sup> 34	1.6:	-11 <sup>m</sup> 0:
20	Sagittarius dIG	H.-E. Schuster, 13 June 1977	19 <sup>h</sup> 27 <sup>m</sup> -17°	Im	15 <sup>m</sup> 6	1.10	-10 <sup>m</sup> 65
21	Sculptor system	H. Shapley, 1937	00 <sup>h</sup> 57 <sup>m</sup> -33°	dE3 pec.	9 <sup>m</sup> 0	0.08	-10 <sup>m</sup> 6
22	Andromeda I	S. van den Bergh, Oct. 1971	00 <sup>h</sup> 43 <sup>m</sup> +37°	dE3	13 <sup>m</sup> 9	0.67	-10 <sup>m</sup> 60
23	Andromeda III	S. van den Bergh, $\leq 1972$	00 <sup>h</sup> 32 <sup>m</sup> +36°	dE	13 <sup>m</sup> 9:	0.67	-10 <sup>m</sup> 6:
24	Andromeda II	S. van den Bergh, $\leq 1972$	01 <sup>h</sup> 13 <sup>m</sup> +33°	dE	13 <sup>m</sup> 9:	0.67	-10 <sup>m</sup> 6:
25	Pisces system (LGS 3)	C. T. Kowal et al., 29. Oct. 1978	01 <sup>h</sup> 01 <sup>m</sup> +21°	Im	15 <sup>m</sup> 5	1.0:	- 9 <sup>m</sup> 7:
26	Leo I (Regulus)	A. G. Wilson, 1950	10 <sup>h</sup> 05 <sup>m</sup> +12°	dE3	11 <sup>m</sup> 81	0.19	- 9 <sup>m</sup> 62
27	Leo B (Leo II)	R. G. Harrington, 1950	11 <sup>h</sup> 10 <sup>m</sup> +22°	dE0 pec.	12 <sup>m</sup> 3	0.19	- 9 <sup>m</sup> 25
28	Ursa Minor system	A. G. Wilson, $\leq 1955$	15 <sup>h</sup> 08 <sup>m</sup> +67°	dE4	11 <sup>m</sup> 6	0.09	- 8 <sup>m</sup> 2
29	Draco system	A. G. Wilson, $\leq 1955$	17 <sup>h</sup> 19 <sup>m</sup> +57°	dE0 pec.	12 <sup>m</sup> 0	0.10	- 8 <sup>m</sup> 0
30	Carina dE	R. D. Cannon et al., 1977	06 <sup>h</sup> 40 <sup>m</sup> -50°	dE4	(> 13)	0.09	- 5 <sup>m</sup> 5::

TABLE: 2: Objects once thought to be Members of the Local Group

Name	Discoverer and Date of Discovery	Position
Phoenix	H.-E. Schuster, March 1976	01 <sup>h</sup> 49 <sup>m</sup> -44°
Sextans B	F. Zwicky, ≤ 1942	09 <sup>h</sup> 57 <sup>m</sup> +05°
Sextans C (Pal 3)	A. G. Wilson, ≤ 1955	10 <sup>h</sup> 03 <sup>m</sup> +00°
Sextans A	F. Zwicky, ≤ 1940	10 <sup>h</sup> 08 <sup>m</sup> -04°
Ursa Major (Pal 4)	F. Zwicky, ≤ 1953	11 <sup>h</sup> 26 <sup>m</sup> +29°
Serpens (Pal 5)	A. G. Wilson, ≤ 1955	15 <sup>h</sup> 13 <sup>m</sup> +00°
Capricorn (Pal 12)	R. G. Harrington & F. Zwicky, ≤ 1953	21 <sup>h</sup> 43 <sup>m</sup> -21°
Pegasus B (Pal 13)	A. G. Wilson, ≤ 1955	23 <sup>h</sup> 04 <sup>m</sup> +12°
UKS 2323-326	A. J. Longmore et al., ≤ 1975	23 <sup>h</sup> 23 <sup>m</sup> +32°

probably tidal debris of the encounter between the—once larger—LMC (called Greater Magellanic Galaxy) and our Galaxy. As there are no obvious candidates—similar to the LMC—for such an encounter with M 31 we then must *not* expect many such dwarf systems around that galaxy (opposite to the statement made earlier). Anyway, I don't think that we can ever reconcile F. Zwicky's estimate of nearly 100 LG members. This implies that the luminosity function of galaxies has a maximum at a yet poorly determined absolute magnitude, and further that this maximum may lie nearer to bright galaxies than believed hitherto.

Now, why should we make every effort to study our neighbours in outer space? As they are the nearest objects of their kind, we can determine their global parameters and study their "ingredients" with the highest possible observational accuracy. Absolute parameters can, of course, only be determined when the distances to these galaxies (or their constituents) are known. This immediately leads us to the question: How can we measure such "astronomically" large distances? Well, we simply assume that the physics of individual objects are the same everywhere in the universe. With some of them in our Galaxy, preferably in the solar neighbourhood, where distances are (a bit) easier to measure, we may solve this problem. Now, which objects are really reliable distance indicators? Or, in other words: Which objects have a very small dispersion in their intrinsic physical properties? It is exactly at this point that "extragalactic" astronomers start to disagree.

Nowadays we have two "schools", one represented by A. Sandage and G. A. Tammann (ST) and the other by G. deVaucouleurs (dV) and to some extent also by S. van den Bergh; they come to results differing by factors of up to two, where the difference is not the data used, but the underlying philosophy. You may take the point of view (dV) that one should use as many distance indicators as possible in order to "share the risk" of eventual unreliability. One may then hope that systematic errors balance out. I could find about 20 or so different indicators in the literature and I found it hard (based on purely physical considerations) to believe in even only half of them. This brings us to the second possible way of thinking (ST): Take only the most reliable indicators, i.e. those of which the physics is (believed to be) understood, and forget all the others. As the results may now be looked at as being more reliable as in the aforementioned case, there is the (everlasting) risk that all distances have to be revised, if only a single indicator becomes revised. This is so because, in general, every distance indicator is applicable only over a certain range in distances (i.e. one builds a distance "ladder"), or is only available from certain distances on. There are only two indicators whose usefulness is agreed upon by everybody, namely the  $\delta$  Cephei stars via their period-luminosity (or

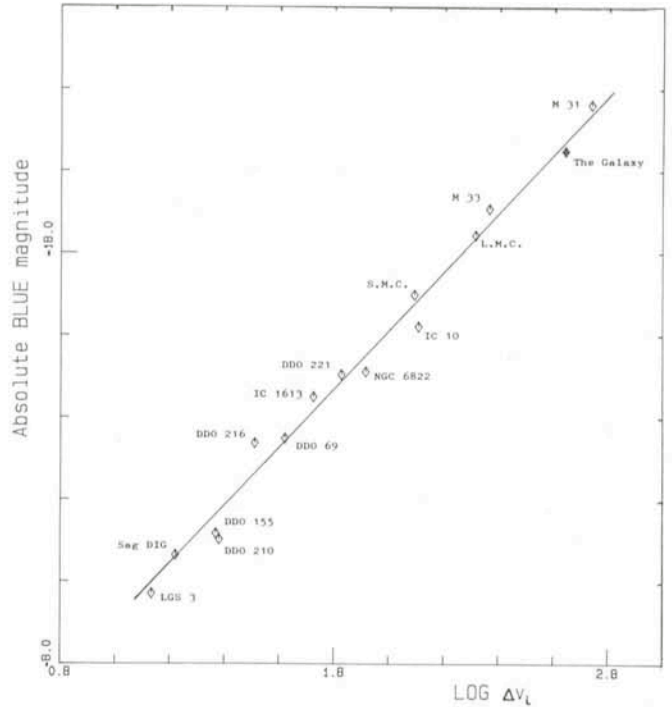


Fig. 2: The Tully-Fisher relation for the spiral and irregular galaxies in the Local Group.

period-luminosity-colour) relation, and the brightest red supergiant M stars via their assumed upper limit in absolute magnitude. One more indicator, namely supernovae of type I, is also commonly used, but the absolute (blue) magnitude during maximum differs considerably between the "schools": dV uses  $-18^m.6$ , ST  $-19^m.7$ , and theoreticians require at least  $-19^m.2$  and some even predict  $-20^m.2$  or so!

Finally, a fourth indicator is in general use since 1977, when R. B. Tully and J. R. Fisher (*Astronomy and Astrophysics* 66, 54) discovered a relation between the absolute total magnitude of a (late-type, rotationally supported) galaxy and its line width in the 21 cm line of neutral hydrogen (HI). This "Tully-Fisher" relation is, again, a rather debatable subject, because (sometimes very) large corrections have to be applied to the observational data. Unfortunately, these corrections are known to vary quite substantially from galaxy to galaxy and, hence, they can be determined and applied only in a statistical manner. Only recently the radioastronomical HI data became complete for the spiral and irregular galaxies in the LG. For a recent calibration of the Tully-Fisher relation I compiled all these data and condensed them into a diagram that is reproduced in Fig. 2. The correlation is evident and looks really convincing. The scatter around the fitted straight line is equal to the combined errors of the magnitudes, distances, inclinations, and 21 cm line widths. This means that there is practically no room for an appreciable intrinsic dispersion for the Tully-Fisher relation. However, in view of the actual uncertainties in the basic data, especially for the galaxies at the faint end, this perfect correlation may well be fortuitous. Anyway, despite the lack of an accepted theory for the underlying physics we may use also this relation for distance estimates. It has been suggested that we see an effect of (nearly) constant surface density in self-gravitating systems, but this has to be worked out in much more detail. The use of all (say, most) other indicators is not at all based on their (known) underlying physical behaviour, but on the *apparently* small dispersion of absolute parameters. In other words, usage of the latter alone

would be just *circular reasoning*, and, further, be subject to prejudice. Therefore, I take the liberty to believe only in the above-mentioned four distance indicators: Cepheids, Supernovae I, brightest M supergiants, and the Tully-Fisher relation.

I should like to add that the upper limit to the absolute luminosity of brightest red supergiants may be *constant* from galaxy to galaxy only if enough such massive stars have been formed in the parent galaxy. If, for instance, a dwarf galaxy failed to produce stars at least as massive as about  $20 M_{\odot}$ , the brightest red stars will be fainter than expected, and, hence, the distance will be overestimated. On the other hand, the existence of an upper limit to the bolometric magnitude of red supergiants requires a special stellar evolution model, namely, the *very* massive (blue) stars ( $\geq 30 M_{\odot}$ ) do not evolve into red supergiants but are directly turned into Wolf-Rayet stars, thus becoming supernovae (type II) progenitors.

The supernovae are unfortunately short-lived, transient phenomena. Normally, galaxies we are studying do not please us with the production of a supernova explosion which would help us to derive the parameters for the system. The Cepheids are certainly the best we have to probe the galaxies within about 10 Mpc, not the least so because corrections to data are only minimum. With the introduction of CCD cameras in astronomy we have a tool to reach the required faint limits of  $B \approx 26^m$  with ground-based telescopes like e.g. the 3.6 m or even the new 2.2 m at La Silla. Such future observations will ultimately prove or disprove the applicability of all other distance indicators. In the meantime we have to rely on a variety of "rods". Here I recommend (because HI 21 cm line

studies are among my prime interests) the Tully-Fisher relation. And this is, at the present state of the art, in favour of the Sandage-Tammann distance scale leading to a Hubble constant of about 50 km/s/Mpc or perhaps a bit higher, but most probably not more than 75 km/s/Mpc.

Now I present the context for the—apparently decoupled—two previous parts of this contribution. If we now apply those four distance indicators to the galaxies in the environment of the Local Group we get the impression that the concept of a local *group* probably can no longer be maintained. Rather we may be embedded in a local *filament* which can be traced at least from the Sculptor group to the "Local Group" and further to the M 81 group, i.e. over more than 5 Mpc. So only a few years after the start of the discussion of filamentary structure in the universe at large we begin to discover this structure in the galactic neighbourhood and in the local supercluster.

Concluding one may say that the routes of reasoning of G. deVaucouleurs and of A. Sandage and G. A. Tammann have both many pros, but perhaps also as many cons. What I wish to say is that one should not blindly trust every statistical application of a *new* distance indicator. This may well imply that the next who writes on the topic of extragalactic distances will show that what I have written here cannot be trusted! As a preventive excuse I may mention that I have written this short contribution while I was observing at La Silla with the ESO 1.5 m telescope where the necessary guiding was interfering.

Detailed references to the data used for Fig. 2 can be obtained from the author.

## Multiple Stars—a Nuisance to the Observers

L. O. Lodén, *Astronomical Observatory, Uppsala*

Already in popular textbooks you can read that double stars are frequent phenomena in the Milky Way. In the first instance this concerns the visual double stars that every one can admire through the telescope. They constitute a considerable fraction of the total stellar content, with a certain statistical frequency dependence upon spectral type and luminosity class that may partly be physically significant but, to an overwhelming extent, is conditioned by selection effects.

If we add the spectroscopic binaries, we increase the number by at least an order of magnitude and if we take into account also the higher multiples, we may find that the number of stars in multiple systems exceeds the number of single stars.

Multiple stars of any type are generally revealed more or less by accident. This means that we have to count upon a considerable number of undetected multiple systems. It is a well-known fact that visual binaries with equal components are much easier to discover than those with a magnitude difference of say  $2^m$  or more. A statistical survey of available double star catalogues will show a significant overrepresentation of components with rather equal temperature, and it is obvious that this effect is predominantly an observational bias. For most studies, however, the visual binaries are harmless objects which do not constitute any real menace to your projects, so we leave them in peace here. Sometimes, of course, you also encounter some sort of semi-visual binaries, i.e. systems which are classified as single objects in the CD and HD catalogues but which can be resolved in the telescope under particularly good seeing conditions. Such objects may

be harassing enough to observe, especially if you try to get a spectrum and cannot be convinced that you have one and the same component on the slit all the time. If the seeing disk is larger than the angular separation of the components, their relative contribution to the resultant spectrum is highly dependent upon the centring on the slit. Personally I suspect that

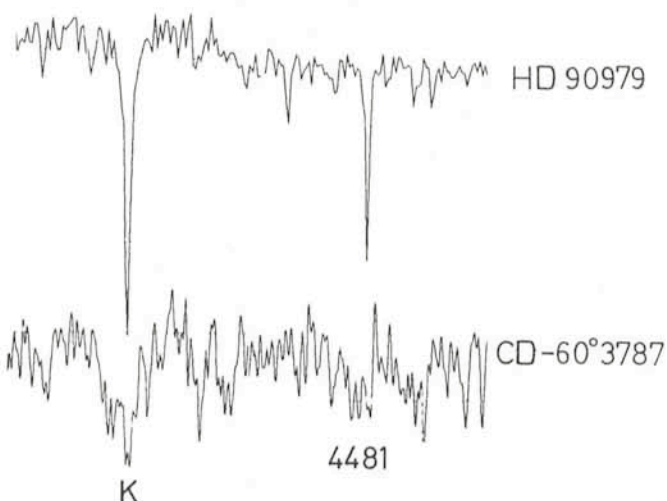


Fig. 1: A comparative study of the Ca II K line and the Mg II line  $\lambda 4481$  for two stars. One of them (HD 90979) has apparently a rather slow rotation and no companions. The other one (CD  $-60^{\circ}$  3787) shows a very complicated spectrum due to multiplicity.

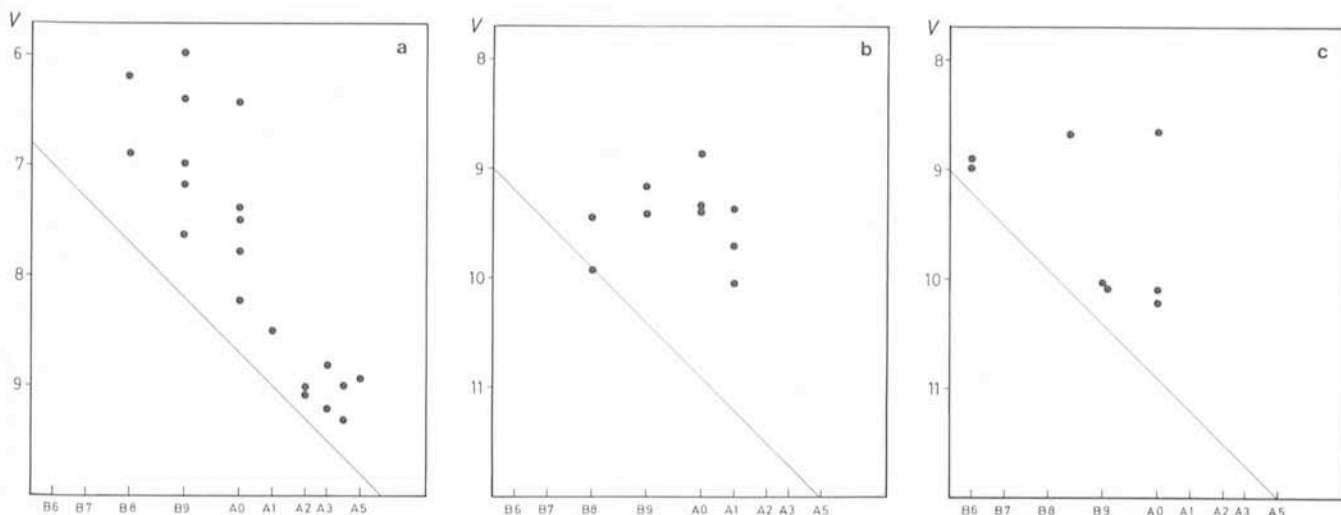


Fig. 2: The relevant part of an HR diagram for three clusterings in the southern Milky Way. (a) NGC 6475; (b) a loose clustering around  $\alpha = 10^{\text{h}} 27^{\text{m}} 3$ ,  $\delta = -56^{\circ} 32'$  (1950); (c) a loose clustering around  $\alpha = 12^{\text{h}} 05^{\text{m}} 1$ ,  $\delta = -60^{\circ} 33'$  (1950). The scale on the spectral type axis is adjusted to give a reasonably linear main sequence in this region (the inclination indicated by the thin line).

individual tendencies on this point might explain some discordant results of spectral classification.

If we then turn to the true spectroscopic binaries, the correlation between on the one hand the similarity in spectral type and on the other hand the probability of detection, is not as strong as in the case of the visual binaries. If the stars are very similar in spectral type you will find no unexpected lines in the spectrum which make it "composite". You can only see if the lines are doubled by Doppler effect but, for spectra of reasonable dispersion, the projected difference in radial velocity has to be rather great and this difference in turn is mainly a function of the inclination of the orbit and the orbital positions of the components. For many binaries it is only during very short time intervals that there is a chance to reveal the duplicity in this way. Furthermore, the displacement of the line components is seldom large enough to be detected by visual inspection of the plates. They have to be photometrically scanned (see Fig. 1). In any case it is advisable to keep in mind that a spectrum with doubled lines will always reveal at least a double star whilst a single-line spectrum gives no direct guarantee of a solitary star.

In cases of more or less pronounced difference between the components we meet another type of difficulties. Difference in spectral type also means a difference in brightness and hence in relative contribution to the composite spectrum. Between, say, a B 8 and an A 8 star the intensity ratio is of the order of 6 to 7 and, in low dispersion, a spectrum formed by such components will look pretty much like a typical B 8 spectrum. In somewhat higher dispersion the superficial appearance may be that of a metallic line A star, etc.

The stars which I have been personally dealing with during the last years are confined to the rather narrow spectral type range B 5 to A 5 with a pronounced concentration around A 0, and the main problem encountered has been connected with plotting of HR diagrams for open clusters. Within the framework of the project in question one has, *inter alia*, to find out if some stars are probable members of a certain cluster or if an apparent clustering of stars really forms a loose but physical open cluster of any kind. The most handy way then is to plot the magnitudes against the spectral type or another suitable temperature parameter. Stars defining reasonably well a main sequence—or at least a common pattern—are the ones to be regarded as good candidates for cluster membership. For some clusters one may get a very nice HR

diagram in that way. In many cases, however, one will find a rather poor grouping around the expected sequence and in those cases it is difficult or even impossible to use the diagram for establishing the physical reality of the suspected cluster and for discrimination of cluster members from field stars. The main reason for such accidents is a predominating occurrence of unresolved multiple stars in the population. The typical member is no more a solitary object with a unique spectral type and absolute magnitude. Fig. 2 shows three examples;

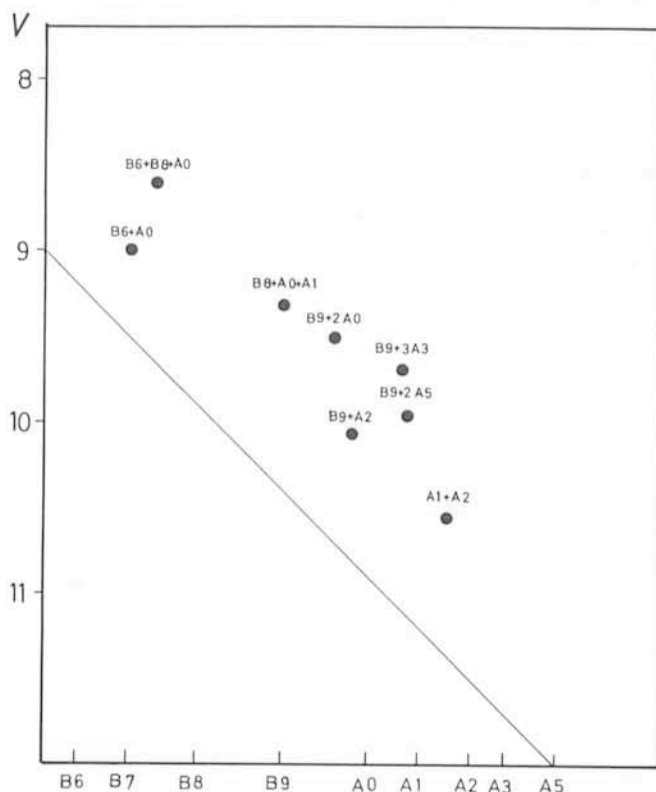


Fig. 3: The thin line indicates the position of the zero-age main sequence for a simulated cluster if there were no multiple stars among the members. The points show the approximate places where you would find them if the objects were composed by combinations of various types of stars.

the well-known cluster M 7 (NGC 6475) and two rather loose clusterings in the Milky Way, the physical reality of which is almost certain although not convincingly confirmed. Attempts have been made to plot the relevant part of the HR diagram on a format where the main sequence should be a straight line. The inclination of this line is indicated in the figures. In no case the connection to the line seems to be particularly nice. Before blaming the multiplicity we have to make a few reservations, of course. Firstly, it is reasonable to expect a few background or foreground stars in the material. Secondly, the main sequence has a finite width.

However, as the multiplicity of a number of stars has been revealed by their spectra, obtained with the coudé spectrograph of the 1.5 m ESO telescope (dispersion 20 Å/mm) and at the Observatoire de Haute-Provence (10 Å/mm), we know that it is there and that it must contribute to the observed scatter. The question then is: Are there no possibilities to correct for the effect of duplicity? Superficially it sounds relatively simple but in practice it is generally not simple at all. In the idealized case, when a system is composed by two identical stars, you

just add 0.75 to the observed V value. The problem is that it is never possible to be sure that there are really two identical stars. In most cases one has only access to the colours and any observed total colour of a system can be synthesized by a multitude of combinations of various stars. Also in cases when spectra are available, there is no unique component composition behind every observed spectrum and, in addition, the result of the classification of a composite spectrum is highly dependent on the actual classification criteria. The most crucial fact is that the revealed number of components is only a lower limit so that the true number, as mentioned above, may be considerably larger. Fig. 3 shows a simulated case of a colour-magnitude diagram on the same format as the diagrams in Fig. 2 in which a number of multiple stars with typical component combinations are illustrated.

The study of double stars, triple stars, quadruple stars or stars of still higher degree of multiplicity is thrilling and interesting indeed, but when they appear with too high a frequency in stellar clusters, they definitely constitute a nuisance to the observer.

## Exciting Stars in the Omega Nebula

*R. Chini, MPI für Radioastronomie, Bonn*

Every astronomer has his favourite object, which he studies sometimes throughout many years. Whenever he gets a few nights for observation he looks at "his" object to see how it is doing. My favourite object is the Omega Nebula, also known as M 17.

M 17 is one of the brightest HII regions in our galaxy. Numerous observations at radio and infrared wavelengths have shown that this complex, associated with a huge molecular cloud, is a site of recent star formation. Due to the large amount of interstellar dust within and around the HII region the exciting stars responsible for the visible nebula could not be identified uniquely. In 1976, I started an investigation of the stellar content of M 17 by photometry of more than 100 stars to be seen within the area marked in Fig. 1. This photometry—which was performed at the Calar Alto Observatory in the wavelength range from 0.3 to 0.9  $\mu\text{m}$ —revealed that a large number of young massive O and B type stars have been born within the region. Some of the objects, however, had energy distributions which could not originate from "normal" stars: according to the spectral type derived from the UBV data, i.e. from 0.3–0.55  $\mu\text{m}$ , the measured brightness at R (0.7  $\mu\text{m}$ ) and I (0.9  $\mu\text{m}$ ) considerably exceeded the expected values. These IR excesses could be produced either by circumstellar dust shells or by gaseous envelopes. To investigate this problem (and some others) I applied—for the first time—for some nights at the ESO 1 m telescope on La Silla with the IR photometer. Fortunately, some time was allocated to my programme, and I had the opportunity to observe M 17 for about 7 hours per night, as it passed through the zenith. For a northern hemisphere observer, who is used to observe the Omega Nebula for only 2 or 3 hours and even then always close to the horizon, this is an unforgettable event. Most of my favourite stars were too faint to be seen in the eyepiece of the IR photometer, but with the help of the experienced night assistant R. Vega, I was able to pick them up at 2.2  $\mu\text{m}$  by scanning the telescope around the expected positions and by watching the equipment to show a signal. Due to excellent weather in August 1981 I could measure all of my interesting

objects from 1.2 to 3.5  $\mu\text{m}$ . Surprisingly, the objects became still brighter with increasing wavelength, i.e. the IR excesses already present at R and I got even larger: The faint optical stars had turned into strong IR sources.

Back in Germany, I tried to understand the new observations and fitted black-body curves to the energy distributions between 1.2 and 3.5  $\mu\text{m}$ . The result was that only extremely

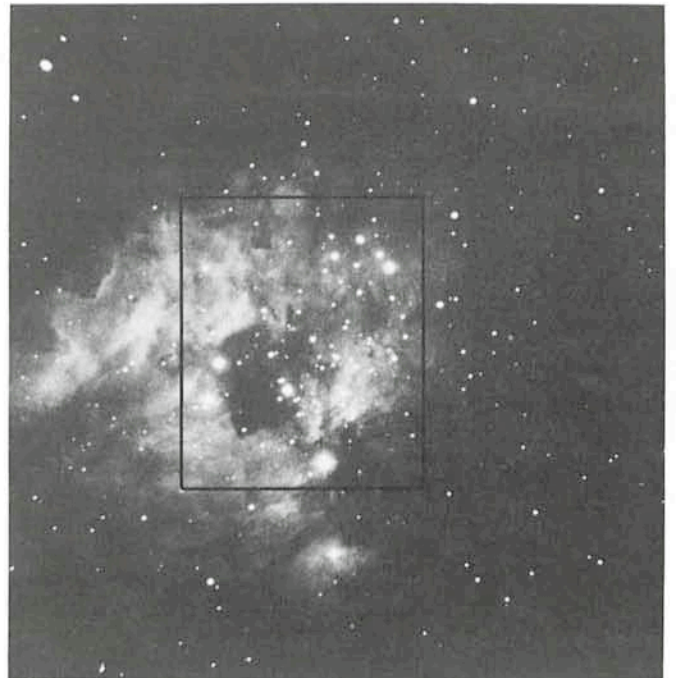


Fig. 1: The Omega Nebula at 0.9  $\mu\text{m}$ . This photograph was taken with an image-tube camera attached to the 1.2 m telescope at Calar Alto. North is at the top, east to the left. Inside the marked area many young stars are embedded in the dust.

hot dust shells with temperatures of 1,800–3,600 K could explain the measurements. Some colleagues argued that also small HII regions around the stars might be responsible for these IR excesses. So I tried another approach towards the solution of the problem a year later. This time I intended to get some spectra of the stars, to learn about their temperature and mass. Furthermore, I wanted to observe the energy distribution out to 20  $\mu\text{m}$ ; this would have answered the question whether the stars are still embedded in dust shells. Therefore I submitted two proposals for spectroscopy and IR photometry, respectively. "Due to heavy demand on the 3.6 m telescope" I got no time for spectroscopy but 7 nights for photometry.

July 1982 was one of the worst observing runs I have ever had: blue skies throughout the day and complete cloud coverage during the night. I could not open the dome for a single hour and left La Silla without any IR observations but with a large number of colour slides of amazing sunsets from these days. I had to wait a whole year before I could "see" my objects again. The application for another IR observing run at the 1 m Telescope was successful and I went to La Silla at the end of August 1983.

Measurements between 5 and 20  $\mu\text{m}$  require excellent weather conditions, a sensitive bolometer and a night assistant familiar with the equipment; a lot of constraints, but I was lucky to find all requirements satisfied. It was possible to observe during 3 nights with a newly developed Ge-bolometer and with the help of R. Vega. After a short time we found that at 10 and 20  $\mu\text{m}$  my objects were so bright that they might well have served as standard stars. This clearly indicated that a lot of hot dust around these stars must give rise to the large IR excesses. Within one night the objects had turned into some of the most heavily reddened visible stars known today. By means of the new infrared equipment on La Silla it was also possible to search for hydrogen recombination lines at 2.2 and 4  $\mu\text{m}$ . They should show up if the stars had formed small HII regions in their environment. No such lines could be found, and that was a further indication that the IR excesses are mainly caused by circumstellar dust.

The observations described so far, i.e. the energy distribution from 0.3 to 20  $\mu\text{m}$ , are shown for a typical object of the sample (C 24) in Fig. 2. For illustration the spectrum of a B2 V star with 6.4 mag of visual extinction (these values have been derived from the UBV photometry) and two black-body curves for temperatures of 1,100 and 170 K have been included. Obviously, these fits do not reproduce the observations very well, but they may help to understand the objects qualitatively: the visible light which is heavily reddened comes from a young luminous star, whose spectral type is uncertain. This star is still embedded in its protostellar dust shell and has not yet formed a detectable HII region. The radiation at IR wavelengths comes from the hot dust shell, whose temperature varies with the distance from the star. The inner regions are comparatively hot (e.g. 1,100 K) whereas the outer regions are "fairly cool" (e.g. 170 K). If this interpretation is correct, we are witnessing a very early short-lived stage of stellar evolution. Additional support for this idea comes from the location of the objects within the M 17 complex. In fact, they are all situated near the interface of the HII region and the molecular cloud, probably indicating that they belong to the youngest generation of newly born stars within that complex. Slightly older stars are found inside the HII region itself and even older stars at larger distances from the complex. In that sense M 17 would be an example of "sequential star formation", where stellar winds of newly formed stars compress the interstellar medium in their surroundings and thus give rise to a subsequent star-forming process.

These far-reaching conclusions need, of course, additional observational support. For that purpose I applied again for

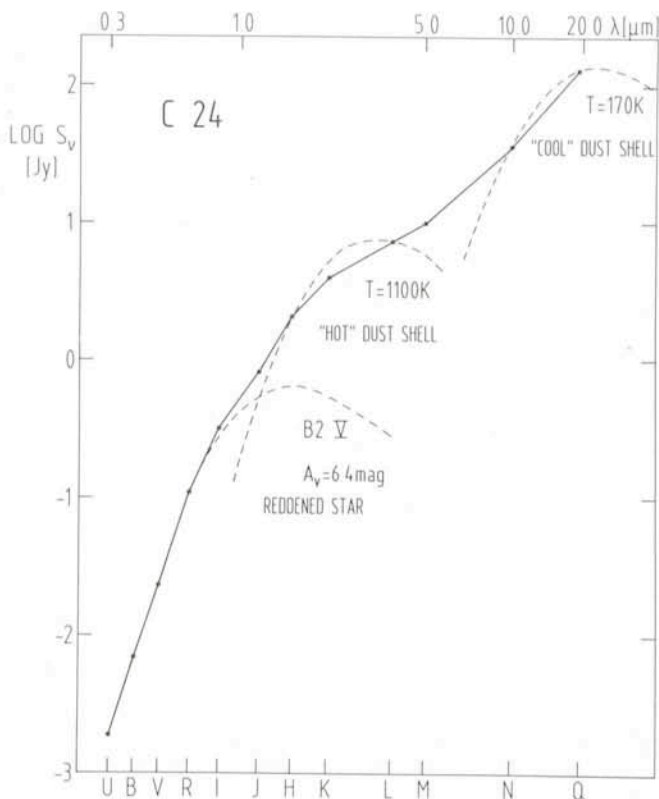


Fig. 2: The observed energy distribution of one of the objects with strong IR excess. Between 0.3 and 0.9  $\mu\text{m}$  the data points can be fitted by a B2V star with 6.4 mag of visual extinction. At longer wavelengths a circumstellar dust shell of various temperatures might explain the observational points. For illustration, two black-body curves of 1,100 and 170 K are shown.

telescope time on La Silla to perform the necessary spectroscopic observations. This time I was successful. Three nights have been allotted to my programme at the new 2.2 m telescope during June 1984. Then I hope to clarify the physical nature of the embedded stars. During five additional nights of IR observations in the same period I want to investigate whether the dust shells are very compact structures or possibly extend to larger distances from the stars. If the objects continue to give me further surprise during future observations I shall still have to spend quite a few hours at the telescope until I may say: "Now I do know my objects."

## Visiting Astronomers

(April 1–October 1, 1984)

Observing time has now been allocated for period 33 (April 1–October 1, 1984). The demand for telescope time was again much greater than the time actually available.

The following list gives the names of the visiting astronomers, by telescope and in chronological order. The complete list, with dates, equipment and programme titles, is available from ESO-Garching.

### 3.6 m Telescope

April: Ulrich / Iye, Zuiderwijk / v. Paradijs, Hunger / Heber / Drilling / Kudritzki, Zuiderwijk / v. Paradijs, D'Odorico / Iye / Bouvier, Zuiderwijk / v. Paradijs, Iye, Zuider-

wijk / v. Paradijs, Kudritzki / Nissen / Gehren / Simon, Zuiderwijk / v. Paradijs, Willems / de Jong, Stanga / Felli / Oliva / Salinari, Shaver, Shaver / Robertson / Cristiani, Danziger / Cristiani / Shaver.

May: Danziger / Cristiani / Shaver, Ilovaisky / Motch / Chevalier / v. Paradijs / Pakull, Larsson / Dravins, Pietsch / Krautter / Sztajno / Trümper, Ilovaisky / Motch / Chevalier / v. Paradijs, Pakull, Oliva / Moorwood, Moorwood / Glass, Fossat / Grec / Gelly, Motch / Pakull / Ilovaisky / Beuermann, Rosa / D'Odorico.

June: Rosa / D'Odorico, Koester / Reimers, Koester / Weidemann, Spite, F. / Spite, M., Zuiderwijk / v. Paradijs, Kudritzki / Méndez / Simon, Zuiderwijk / v. Paradijs, Cristiani / Danziger / D'Odorico, Zuiderwijk / v. Paradijs, Bertola / Zeilinger, Capaccioli.

July: Capaccioli, Ilovaisky / Motch / Chevalier / v. Paradijs / Pakull, Brahic / Sicardy, Ilovaisky / Motch / Chevalier / v. Paradijs / Pakull, Gemünd / Kreysa / Steppe, Steppe / Witzel / Biermann, Schultz, Sieber / Wielebinksi / Kreysa / Gemünd, Caloi / Castellani / Danziger / Gilmozzi, Sadler, Mouchet / Motch / Bonnet-Bidaud, Houziaux / Heck / Manfred.

August: Houziaux / Heck / Manfred, Miley / Lub / de Jong, Gratton / Ortolani / Sneden, D'Odorico / Miley / Heckman / Ciani, Alloin / D'Odorico / Pelat, Bergeron / D'Odorico, Ferlet / Dennefeld / Maurice, Wolf / Appenzeller / Klare / Leitherer / Stahl / Zanella / Zickgraf.

September: Wolf / Appenzeller / Klare / Leitherer / Stahl / Zanella / Zickgraf, Olofsson / Bergvall / Ekman, Danziger / Maraschi / Tanzi / Treves, Perrier / Chelli / Léna / Sibille, Zuiderwijk / de Ruiters, Lequeux / Azzopardi / Breysacher / Westerlund, Barbieri / Cristiani.

## 1.4 m CAT

April: Querci, M. / Querci, F. / Yerle, Noci / Ortolani, Finkenzeller, Gustafsson / Frisk / Edvardsson, Gry / Ferlet / Vidal-Madjar.

May: Gry / Ferlet / Vidal-Madjar, Westerlund / Krefowski, Münch / Gredel, Baade / Danziger, Holweger / Steffen, Weiss / Schneider / Knölker, Felenbok / Roueff / Czarny.

June: Felenbok / Roueff / Czarny, Waelkens / Rufener, Soderblom, Soderblom / Avrett, Soderblom / Hartmann, Soderblom / Kurucz, Vander Linden, Danks / Lambert, Spite, F. / Spite, M., Doazan / Thomas / Bourdonneau.

July: Doazan / Thomas / Bourdonneau, Foing / Bonnet / Crivellari / Beckman, Foing / Bonnet / Fossat / Grec, Foing / Bonnet / Crivellari / Beckman, Foing / Bonnet / Fossat / Grec, Barbuy, Crane / Mandolesi / Hegyi.

August: Crane / Mandolesi / Hegyi, van Dessel, Gratton / Ortolani / Sneden, van Dishoeck / Black, Grewing / Bianchi / Kappelmann.

September: Grewing / Bianchi / Kappelmann, Foing / Bonnet, Gustafsson / Andersen / Nissen.

## 2.2 m Telescope

April: Sadler / Carter, Zickgraf / Leitherer / Stahl / Gail, de Waard / Miley / Schilizzi, Rosa / Richter, Richter / Williams, Ulrich / van Breugel / Miley / Heckman.

May: Ulrich / van Breugel / Miley / Heckman, Ilovaisky / Motch / Chevalier / v. Paradijs / Pakull, Ilovaisky / Motch / Chevalier / Hurley / Pedersen, Pedersen,

Crane / Capaccioli, Chincarini / Manousoyannaki, Motch / Ilovaisky / Pakull / Beuermann, Fusi Pecci / Cacciari / Buonanno.

June: Fusi Pecci / Cacciari / Buonanno, van der Kruit, Chini, Finkenzeller / Mundt, Felli / Stanga / Oliva / Salinari, Bertola / Zeilinger, Kollatschny, Fricke / Witzel, Hoffmann / Geyer, Fricke / Witzel, Kollatschny.

July: Kollatschny, Ilovaisky / Motch / Chevalier, v. Paradijs / Pakull.

August: Sadler, Jensen, Zuiderwijk / de Ruiters, Olofsson / Bergvall / Ekman, Bergvall / Ekman / Johansson, Olofsson / Bergvall / Ekman.

September: Olofsson / Bergvall / Ekman, Bergvall / Ekman / Johansson, Bertola / Danziger, Jensen, Jørgensen / Nørgaard-Nielsen / Hansen, Cayrel R. / Buser, Bergeron / Boissé, Elst / Nelles.

## 1.5 m Spectrographic Telescope

April: Maurice / Louise, Grenon / Trefzger, D'Odorico / Iye / Bouvier, Giovannelli / Persi / Vittone / Bisnovatji / Sheffer / Lamzin, Schulte-Ladbeck, Stenholm / Lundström.

May: Stenholm / Lundström, Friedjung / Bianchini, Bianchini / Sabbadin, Wendker / Heske, Chmielewski / Jousson, Spite, F. / Perrin / Spite, M., Didelon, Gomez / Floquet / Gerbaldi / Grenier, Rufener / Waelkens, Molaro / Franco / Morossi / Ramella.

June: Molaro / Franco / Morossi / Ramella, Schild / Maeder, Didelon, Reimers / Groote, Hänel, de Jager, Vander Linden, Didelon, Chincarini / Kotanyi, Capaccioli, Bica / Alloin.

July: Bica / Alloin, Strupat / Drechsel / Rahe / Wargau, Tanzi / Pakull / Tarengi, Dennefeld / Pottasch, Labhardt.

August: Labhardt, Maciel / Barbuy, Didelon, van Dessel, Dideon / Jaschek, M. / Jaschek, C., Didelon, Testor / Lortet / Heydari-Malayeri / Niemela, Zuiderwijk / v. Paradijs / Bath / Tjemkes, Alloin / D'Odorico / Pelat, Zuiderwijk / v. Paradijs / Bath / Tjemkes.

September: Zuiderwijk / v. Paradijs / Bath / Tjemkes, Danziger / Maraschi / Tanzi / Treves, Zuiderwijk / v. Paradijs / Bath / Tjemkes, Richtler, Zuiderwijk / v. Paradijs / Bath / Tjemkes, Wargau / Drechsel / Rahe / Strupat, Zuiderwijk / v. Paradijs / Bath / Tjemkes.

## 1 m Photometric Telescope

April: Sadler, Liller / Alcaino, Willems / de Jong, Giovannelli / Persi / Vittone / Bisnovatji / Sheffer / Lamzin, Zickgraf / Leitherer / Stahl / Gail, Krautter / Brinkmann / Doll / Kendziorra.

May: Krautter / Brinkmann / Doll / Kendziorra, Wendker / Heske, Oliva / Moorwood, Chalabaev, v.d. Hucht / Thé, Bues / Rupprecht, Koester / Weidemann.

June: Koester / Weidemann, Terzan, Hänel, Chini / Krügel, de Jager, Fricke / Loose, Clementini / Battistini / Focardi / Fusi Pecci.

July: Clementini / Battistini / Focardi / Fusi Pecci, Bertout / Bouvier, Tanzi / Pakull / Tarengi, Houziaux / Heck / Manfred, Heck / Manfred / Didelon, Mouchet / Motch / Bonnet-Bidaud, Sadler.

August: Sadler, Di Martino / Zappala / Farinella / Paolicchi / Cacciatori / De Sanctis / Knezevic / Debehogne / Ferreri, Poulain.

September: Poulain, Olofsson / Bergvall / Ekman, Le Bertre / Epchtein / Nguyen-Q-Rieu, Epchtein / Group of astronomers of São Paulo, Alcaíno / Liller, Wargau / Drechsel / Rahe / Strupat.

### 50 cm ESO Photometric Telescope

April: Scaltriti / Busso / Cellino, Udalski / Geyer, Zickgraf / Leitherer / Stahl / Gail, Gustafsson / Frisk / Edvardsson, Leandersson.

May: Leandersson, Carrasco / Loyola, Lodén, K. / Kennedahl, Mauder.

June: Mauder, Westerlund / Thé.

July: Westerlund / Thé, Carrasco / Loyola, Häfner.

August: Häfner, Di Martino / Zappala / Farinella / Paolicchi / Cacciatori / De Sanctis / Knezevic / Debehogne / Ferreri, Wolf / Appenzeller / Klare / Leitherer / Stahl / Zanella / Zickgraf, Carrasco / Loyola.

September: Carrasco / Loyola, Debehogne / Zappala / De Sanctis.

### GPO 40 cm Astrograph

April: Burnage / Fehrenbach / Duflot, Ferreri / Zappala / Di Martino / De Sanctis / Cacciatori / Debehogne / Lagerkvist.

May: Ferreri / Zappala / Di Martino / De Sanctis / Cacciatori / Debehogne / Lagerkvist, Dommanget / Léonis.

June: Dommanget / Léonis.

September: Debehogne / Machado / Caldeira / Netto / Vieira / Mourao / Tavares / Nunes / Zappala / Di Sanctis / Lagerkvist / Protitch-Benishkek / Bezerra.

### 1.5 m Danish Telescope

April: Veillet / Dourneau / Mignard / Ferraz-Mello, Liller / Alcaíno, Cristiani / Barbieri / Danziger / Romano, Pedersen / v. Paradijs / Lewin, Kunth / Viallefond / Vigroux.

May: Kunth / Viallefond / Vigroux, Pedersen / v. Paradijs / Lewin, Larsson / Dravins.

June: Ardeberg / Lindgren / Maurice / Prévot, Benz / Mayor / Bouvier / Foing / Gondoin, Mayor / Burki, Mayor / Merrilliod, Andersen / Nordström / Olsen.

July: Andersen / Nordström / Olsen, Melnick / Danziger / Terlevich, Castellani / Caloi / Danziger / Gilmozzi, Miley / Lub / de Jong.

August: Miley / Lub / de Jong, Durret / Bergeron, White / Mason / Parmar, Testor / Lortet / Heydari-Melayeri / Niemela, Quintana.

September: Quintana.

### 50 cm Danish Telescope

May: Schneider / Maitzen, Weiss / Schneider / Knölker, Vander Linden.

June: Vander Linden.

### 90 cm Dutch Telescope

April: Grenon / Lub.

May: Grenon / Lub, Pakull / Beuermann / Weißsieker / Klose.

June: de Jager, de Zeeuw / Lub / Blaauw, Foing / Bonnet / Linsky / Walter.

July: Foing / Bonnet / Linsky / Walter, Tanzi / Pakull / Tarengi.

August: v. Paradijs / Tjemkes / Bath / Charles.

September: v. Paradijs / Tjemkes / Bath / Charles, v. Paradijs / Tjemkes / Bath / Zuiderwijk, v. Paradijs / Damen.

### 61 cm Bochum Telescope

May: Lodén, L. O. / Engberg, Wendker / Heske, Vogt.

June: Vogt, Maitzen / Catalano / Gerbaldi / Schneider, Kohoutek / Pauls.

July: Kohoutek / Pauls, Sterken group.

August: Sterken group.

September: Sterken group.

## Magnesium Isotopes in Halo Stars of Various Metallicities

*B. Barbuy, Universidade de São Paulo*

### Introduction

Population II stars are very old objects, and their relative abundances can give clues on the chemical enrichment at early times. The elemental composition of stars depends on the initial mass function of the progenitor stars which enrich the gas from which they form. Some element ratios in the oldest stars are especially sensitive to the mass of the preceding stars, the so-called population III or population O, first generation of zero-metal stars, today disappeared.

Important ratios are, for example, the oxygen-to-iron, nitrogen-to-iron, magnesium isotope ratios, as well as sodium and aluminium-to-magnesium ratios. In halo stars, oxygen-to-iron ratios above solar seem to point to a first generation of massive ( $M > 10 M_{\odot}$ ) stars. Nitrogen-to-iron ratios in these stars indicate the primary nature of nitrogen at early times, and

this can be explained by a first generation of intermediate or high mass stars.

Calculations are available for the production of magnesium isotopes in intermediate mass stars ( $2 < M/M_{\odot} < 8$ ) and in ordinarily massive stars ( $M > 10 M_{\odot}$ ). The main controversy is whether they are formed through explosive or hydrostatic carbon burning. In the explosive case, the isotopic  $^{25}\text{Mg}$  abundance should be proportional to that of  $^{24}\text{Mg}$ , whereas  $^{26}\text{Mg}$  forms from  $^{25}\text{Mg}$ ; in this case, one expects a strong deficiency of  $^{25,26}\text{Mg}$  in metal-deficient stars. On the other hand, if their production occurs in hydrostatic conditions,  $^{24}\text{Mg}$  is formed during hydrostatic carbon burning, whereas during hydrostatic helium burning one has the reaction  $^{22}\text{Ne} (\alpha, n) ^{25}\text{Mg}$  followed by conversion of some  $^{25}\text{Mg}$  into  $^{26}\text{Mg}$  by neutron capture. In this scenario, a small overdeficiency of  $^{25,26}\text{Mg}$  is expected.

## Observations of Magnesium Isotopes

In order to determine the ratios  $^{24}\text{Mg}/^{25}\text{Mg}/^{26}\text{Mg}$ , it is necessary to have very high quality spectra. These can be obtained at the present time using the ESO 1.42 m telescope (CAT) with the Coudé Echelle Spectrometer (CES) and a reticon silicon photodiode array. With a temperature of the reticon maintained at about 150 K, a quantum efficiency around 40 % is achieved, at the wavelengths of 5140 Å, where a spectral resolution  $\Delta\lambda = 0.08 \text{ \AA}$  is obtained at a reciprocal dispersion of  $2 \text{ \AA mm}^{-1}$ . The required signal-to-noise (above 500) and accuracy in the line profile are reached, as illustrated in Fig. 1.

Selection of lines: magnesium isotopic lines are better distinguished through the magnesium hydride. In the system  $A^2\Pi-X^2\Sigma$ , the MgH (0,0) band forms a head at 5211 Å and the band degrades to the violet. The isotopic shifts vary from  $\sim 0.0$  at the band head to  $0.4 \text{ \AA}$  around 5000 Å. Besides having a convenient split of lines, it is important to have no blends and relatively strong lines, in order to still observe them in metal-deficient stars. A compromise between these three requirements is met with lines at  $\lambda\lambda 5134-5137 \text{ \AA}$ , where the isotopic shifts of  $0.06$  to  $0.1 \text{ \AA}$  are seen as red asymmetries in each line.

Selection of stars: the MgH lines present a strong dependence on temperature, on gravity, and also on metallicity. In hot stars, most of the MgH molecules dissociate. Consequently, in order to reach metallicities down to  $[\text{Fe}/\text{H}] \approx -2.0$  (where  $[X] = \log X_{\star}/X_{\odot}$ ), we have selected cold unevolved halo stars from the catalogue by Carney (1980).

### Method for the Determination of Isotopic Abundances

The spectrum synthesis technique is employed to estimate the magnesium isotope abundances. The MgH line profiles are computed, for each star, with the solar isotopic proportions:  $^{24}\text{Mg} : ^{25}\text{Mg} : ^{26}\text{Mg} = 79 : 10 : 11$  and the extreme cases  $100 : 0 : 0$ ,  $60 : 20 : 20$ . The input data required for the synthesis are: molecular data, model stellar atmosphere, elemental abundances and Doppler broadening velocity.

### Results

The results obtained so far show a best fit when solar isotopic ratios are assumed. The most metal-deficient star of the sample studied until now does, however, not show a deficiency greater than  $[\text{Fe}/\text{H}] = -1.2$ . If more metal-deficient

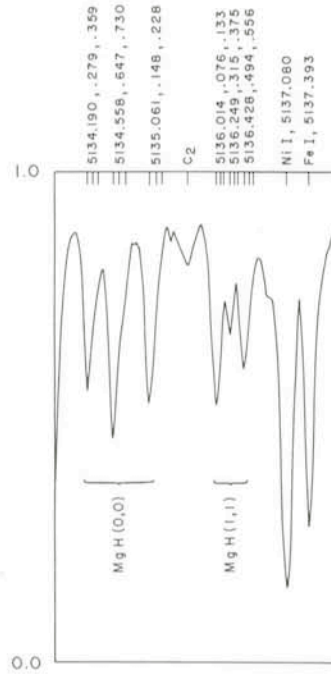


Fig. 1: Spectrum of HD 175329 ( $\omega$  Pav), star of visual magnitude  $V = 5.13$ , obtained in 2.5 hours exposure time in October 1982. The region contains unblended MgH lines: groups of 3 wavelengths indicate each the  $^{24,25}$  and  $^{26}\text{MgH}$  isotopic components.

stars show the same result, then we would have an indication for formation of magnesium by hydrostatic carbon burning. In other words, if the present results extend to all metal-deficient stars, then they are not consistent with production of magnesium isotopes through explosive carbon burning, but indicate rather their production under hydrostatic conditions. Such conditions are found in relatively massive stars, according to Arnett and Wefel (1978), and Truran and Iben (1977). The present results are otherwise in agreement with those by Spite and Spite (1980) regarding sodium and aluminium-to-magnesium ratios in halo stars.

### References

- Arnett, W. D., Wefel, J. P.: 1978, *Astrophysical Journal* **224**, L139.
- Carney, B.: 1980, "A Catalogue of Field Population II Stars", unpublished.
- Spite, M., Spite, F.: 1980, *Astronomy and Astrophysics* **89**, 118.
- Truran, J. W., Iben Jr, I.: 1977, *Astrophysical Journal* **216**, 797.

## The Ultraviolet Absorption Spectrum of NGC 4151

P. Véron, M.-P. Véron-Cetty and M. Tarenghi, ESO

NGC 4151 is one of the first Seyfert galaxies to have been discovered. Indeed it appears in the original list of 12 galaxies published by Seyfert (1) in 1943. It is certainly the most extensively observed of all Seyfert 1 galaxies. As a reminder, Seyfert 1 galaxies are characterized by the presence of an active, non-thermal nucleus, conspicuous both in X-ray and in the optical, and broad permitted emission lines. These nuclei are believed by many to be low luminosity quasars.

NGC 4151 is an Sab galaxy with a galactocentric radial velocity of 978 km/s, corresponding to a distance of about 20 Mpc.

A striking feature of the optical spectrum of NGC 4151 is the presence of non-stellar absorption features (Balmer lines, He I

$\lambda 3889$ ) which are blue-shifted with respect to the emission lines and variable in time. The variations of the equivalent width of these emission lines have been interpreted either as real changes in the amount of absorbing matter, or as due to changes of the nuclear continuum brightness variously diluted by the constant stellar component arising in regions adjacent to the Seyfert nucleus (2).

A number of spectra have been obtained with the International Ultraviolet Explorer (3), a satellite launched on 26 January 1978. They cover the spectral range 1150–3250 Å. A number of absorption features of variable equivalent width have been identified (4). It has been claimed that the equivalent width of at least some of these ultraviolet absorption lines,

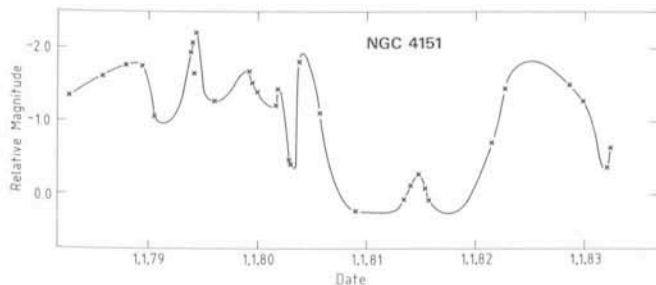


Fig. 1: Light curve of the nucleus of NGC 4151. The plotted magnitudes are defined as  $\sim 2.5 \times \log F$  where  $F$  is the continuum flux measured in the spectral range  $\lambda\lambda$  1720–1850 in units of  $10^{-13} \text{ erg cm}^{-2} \text{ s}^{-1} \text{ \AA}^{-1}$ .

such as for instance NV  $\lambda$  1240, increases with the continuum flux with no time lag, suggesting that the absorption occurs in the outer parts of the very small broad line region (4) (5); the intensity of the broad emission lines is indeed strongly variable with the continuum flux, with a time lag of  $\sim 13$  days, showing that this emitting region has a diameter of about 60 light days (6).

High dispersion IUE spectra of NGC 4151 show the CIV absorption doublet  $\lambda\lambda$  1548.20–1550.77, too deep to be explained solely as absorption of the continuum source. This is also true of the H $\alpha$  absorption line. Some, if not all, of the broad line emission regions must be covered by absorbing Material (4) (7).

We have retrieved from the European Space Agency's Villafranca data base all available low dispersion (resolution  $\sim 8 \text{ \AA}$ ), large aperture ( $10 \times 20$  arcsec), shortwave (1150–1950  $\text{\AA}$ ) spectra, obtained between April 1978 and February 1982. There are 99 such spectra; nine of them could not be used, being affected by microphonic noise. All spectra taken within a few days have been compared and when no significant variation could be seen, averaged together. This resulted in 28 different epochs. The continuum flux has been measured in the spectral range  $\lambda\lambda$  1720–1850, which is free from any strong spectral features. The light curve is displayed in Fig. 1 (extending to March 1983).

Using this material, we have, independently, made again the analysis of the behaviour of the absorption lines.

The strongest absorption lines are shown in Fig. 2.

To determine the strength of each line, we have fitted the spectrum with Gaussian components (Fig. 3). We have

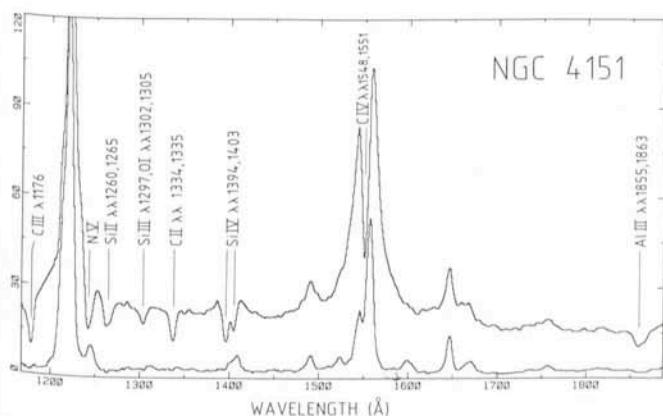


Fig. 2: Spectra of NGC 4151 in the spectral range  $\lambda\lambda$  1150–1950. The upper curve is the average of all spectra obtained when the nucleus was in a bright state; the lower curve is the average of all spectra when the nucleus was faint. The strongest absorption lines are identified.

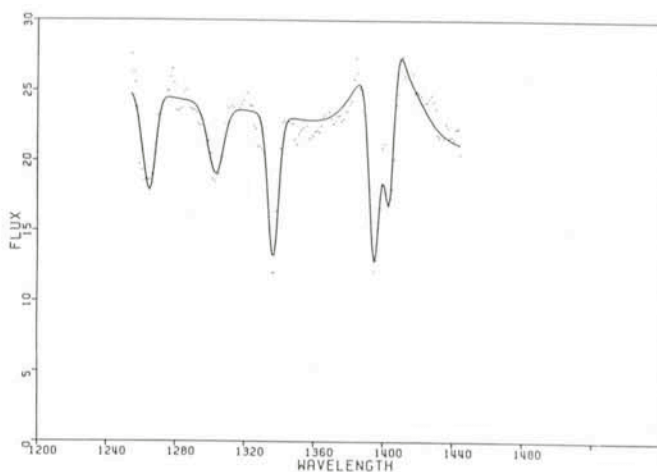


Fig. 3: Example of a fit in the wavelength range  $\lambda\lambda$  1255–1445. Average of two spectra obtained on 23 May 1979, when the nucleus was very bright.

assumed that all absorption lines were unresolved ( $\sigma = 3 \text{ \AA}$ ) and have the same redshift. The relative strengths of the components of each multiplet were fixed.

For many of the absorption lines, there is a problem in determining accurately the strength. The unresolved CIV doublet ( $\lambda\lambda$  1548–1551) is superimposed onto the strong and variable CIV emission; the SiIV doublet ( $\lambda\lambda$  1394–1403) is blended with the variable SiIV  $\lambda$  1397, OIV]  $\lambda$  1402 emission blend; the NV  $\lambda$  1240 and SiII  $\lambda$  1260 absorption lines are blended with the NV emission and with the red wing of Ly $\alpha$ . The absorption feature at  $\lambda$  1300 is most probably a blend of SiIII and OI multiplets, so the total strength of this feature can be measured with a reasonable accuracy, but not the relative contribution of each component. The easiest absorption feature to measure is the CII triplet at 1335  $\text{\AA}$  which appears in a region free of emission lines. Fig. 4 shows a plot of the strength of this absorption feature versus the strength of the continuum. The correlation between these two parameters is strikingly good. The relation is linear, but the absorption line disappears when the continuum still has a finite value

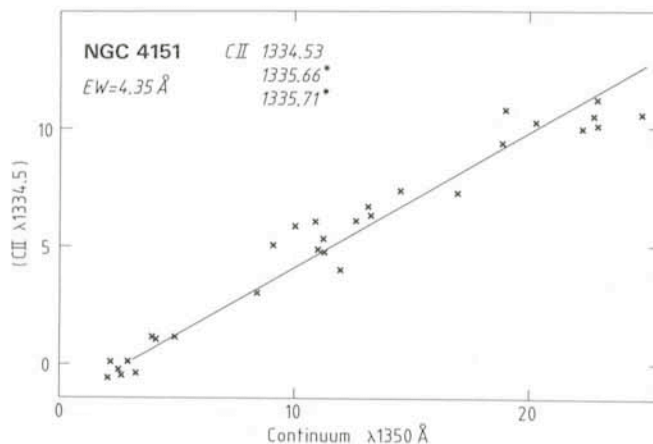


Fig. 4: Plot of the depth of the CII  $\lambda$  1335 absorption line versus the strength of the underlying continuum. There is clearly a good linear correlation between these two parameters, but the absorption line vanishes when the continuum has still a finite value which probably shows that the absorbing cloud covers only a fraction of the continuum source.

( $\sim 3.0 \times 10^{-14}$  erg cm $^{-2}$  s $^{-1}$  Å $^{-1}$ ). This suggests that the continuum flux comes from two spatially distinct components: the first ("A") is variable and covered by the absorbing cloud; the second ("B") is constant and not covered by the absorbing cloud. The equivalent width of the CII feature *with respect to component A alone* is constant and equal to 4.3 Å. It has indeed been previously shown (4) that the ultraviolet continuum is made up of two components with different spectra, one dominating at the long, the other at the short wavelengths.

The X-ray spectrum of NGC 4151 shows a low energy absorption turnover corresponding to a very high hydrogen column density ( $\sim 4 \times 10^{22}$  hydrogen atoms cm $^{-2}$ ) (8); however, the spectral data cannot be reconciled with absorption from a uniform column of cold gas, as the observed spectrum shows a pronounced excess at energies below 2 keV; one suggested possibility is that the low-energy excess is produced farther out from the central source than is the bulk of the X-ray emission (9). It seems possible to identify these two hypothetical X-ray components with the two UV components A and B. In this picture, component B could be a "jet", somewhat similar to the X-ray, optical jet observed in the elliptical galaxy M87 (10) and may be related to the radio jet (11).

As noted earlier (12), several absorption lines in the spectrum of NGC 4151 arise from metastable states. These include the Balmer lines and HeI  $\lambda$  3899 seen in the optical (13), CIII  $\lambda$  1176 and SiIII  $\lambda$  1297. The CIII multiplet is the easiest to measure, being unblended, although it is in a very noisy part of the spectrum. Its equivalent width, with respect to continuum component A, is constant and equal to 2.95 Å. The main populating mechanism for the metastable levels must be collisional, and this probably implies a high density ( $N_e \geq 10^{8.5}$ ) in the absorbing cloud responsible for the CIII  $\lambda$  1176 multiplet (12).

In the optical spectrum of NGC 4151, the CaII K  $\lambda$  3933 line appears relatively strong, the measured equivalent width being  $360 \pm 30$  mÅ (13) of 130 mÅ (14). The radial velocity is  $-41$  km s $^{-1}$ ; this absorption line has been attributed to material lying within our galaxy.

A 21-cm spectrum has been obtained by W. Huchtmeier and O. Richter, on January 4, 1984, with the Effelsberg radio telescope, at the position of NGC 4151 (Fig. 5): the total observed galactic column density in this direction is  $N(\text{HI}) \sim 2 \times 10^{20}$  cm $^{-2}$ . The galactic HI column density in the direction of the quasar 3C 273 is almost the same:  $N(\text{HI}) = 1.8 \times 10^{20}$  cm $^{-2}$ ; the equivalent width of the K line is 220 Å and the IUE spectra show a number of galactic absorption lines including OI  $\lambda$  1302, with an EW in the range 0.5 to 1.1 Å (15). If the OI absorption line observed in the spectrum of NGC 4151 is produced in the dense absorbing cloud associated with the

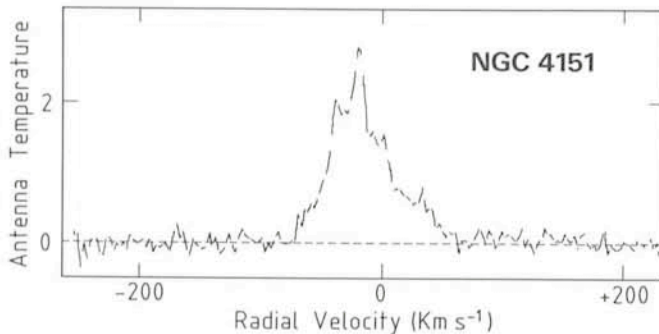


Fig. 5: 21 cm emission profile due to neutral hydrogen in our galaxy in the direction of NGC 4151. The total HI column density is  $\sim 2 \times 10^{20}$  cm $^{-2}$ . The spectrum was obtained by W. Huchtmeier and O. Richter, on 4 January 1984, with the Effelsberg radio telescope.

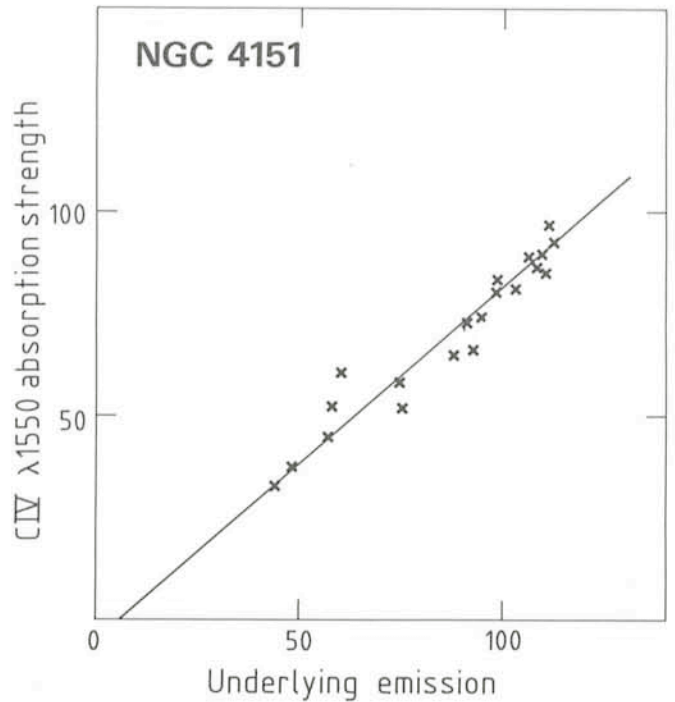


Fig. 6: Plot of the depth of the CIV  $\lambda$  1550 absorption doublet versus the strength of the underlying emission. Again there is a good linear correlation, but in this case, it is not possible to say if the line vanishes before this underlying emission.

nucleus of NGC 4151, the excited fine structure line OI  $\lambda$  1304.87 is expected to appear with a strength equal to 60 % of that of the OI  $\lambda$  1302.17; our fits show that this line is certainly much weaker than this; it is most probably at least three times fainter, suggesting that the observed OI line arises in a low density cloud which could be galactic. Its equivalent width is  $\sim 0.9$  Å, close to the value observed in 3C 273; the measurement errors are rather large, due to the blend with the Si III  $\lambda$  1299 absorption line. The measurements are compatible with a constant EW with respect to the whole continuum intensity, including both components A and B. The observed wavelength of the line is here of no help because the best estimate of the velocity of the absorption lines is  $-820 \pm 100$  km s $^{-1}$  relative to the emission lines (12), and the emission line radial velocity of the nucleus is 978 km s $^{-1}$ ; therefore the radial velocity of the absorption lines is  $\sim 160$  km s $^{-1}$  and the wavelength difference between the two absorption line systems is only 0.5 Å which is too small to be measured with the present resolution which is about 8 Å. Nevertheless, there is some evidence that the OI  $\lambda$  1302 absorption line is mainly of galactic origin.

The CIV doublet ( $\lambda\lambda$  1548, 1551) appears in absorption, unresolved, on top of the broad, variable CIV emission line. To measure the strength of this absorption line, we have to model the emission line. As a guide, we first modelled the CIV emission in another variable Seyfert nucleus, NGC 5548, which has the advantage of not showing any absorption feature, making the fit much easier. We found that we could fit the CIV emission at all epochs with a three Gaussian profile model. The first Gaussian component is unresolved ( $\sigma = 2.8$  Å) and has a constant intensity; this is identified with the extended, narrow line region. Component 2 is resolved ( $\sigma = 11.3$  Å) and strongly variable. A third very broad component ( $\sigma = 25.4$  Å) is also needed; the intensity of this component varies much less than that of component 2. The central wavelengths of these three components are different. We

were able to satisfactorily fit the CIV emission profile at all epochs by varying only two parameters, namely the intensity of the two broad Gaussian components. We found it reasonable to try a similar model in the case of NGC 4151. In this case, the widths of the two resolved components are  $\sigma = 7$  and  $15 \text{ \AA}$  respectively. With this model, we have a good fit for all epochs. Indeed the fit included an unresolved Gaussian component in absorption for which we were able to get the depth at each epoch. We have plotted the depth of the absorption component versus the strength of the underlying component; these two quantities are more or less proportional, but with a rather large scatter; we obtained a much better correlation when plotting the depth of the absorption line versus the total intensity of the emission (continuum plus the two broad emission components) at the wavelength of the absorption line (Fig. 6). The CIV equivalent width is found to be constant and equal to  $7.5 \text{ \AA}$ .

It has been claimed (12) that the equivalent width of NV  $\lambda$  1240 strongly correlates with the continuum flux at  $2500 \text{ \AA}$ . However, this line appears on the blue wing of the NV emission line and on the red wing of the very strong Ly $\alpha$  emission line. Therefore, the measurement of its strength strongly depends on the modelling of the Ly $\alpha$  emission and we have found it impossible to get measurements with a useful accuracy. Therefore we are not able to confirm the result quoted above and we strongly suspect it.

All the available data are compatible with the following conclusions.

- All observed absorption lines in the UV spectrum of NGC 4151 are produced in one or several (as suggested by the splitting of the He I  $\lambda$  3889 absorption line into three components, Anderson 1974); with the probable exception of OI  $\lambda$  1302 which may be mainly of galactic origin;
- these clouds have a high density ( $N_e > 10^{8.5} \text{ cm}^{-3}$ ) as shown by the presence of several absorption lines from metastable levels (C III, Si III, He I);
- the continuum source is double with one constant component and one variable;

- the absorbing clouds cover the variable continuum source and the broad emission line region;
- taking into account the fact that the non-variable continuum source is not covered by the absorbing cloud, the equivalent width of all the absorption lines is constant.

### Acknowledgements

It is a pleasure to thank W. Huchtmeier and O. Richter for obtaining the 21 cm spectrum in the direction of NGC 4151. We are grateful to E. Zuiderwijk for putting at our disposal his line-fitting computer programme.

### References

1. Seyfert, C.K. 1943, *Astrophysical Journal* **97**, 28.
2. Anderson, K.S. 1974, *Astrophysical Journal* **189**, 195.
3. Boggess, A. et al. 1978, *Nature* **275**, 372.
4. Penston, M.V. et al. 1981, *Monthly Notices of the Royal Astronomical Society* **196**, 857.
5. Bromage, G.E. et al. 1982, ESA SP-176, p. 533.
6. Ulrich, M.H. et al. 1984, *Monthly Notices of the Royal Astronomical Society* **206**, 221.
7. Penston, M.V., Clavel, J., Sniijders, M.A.J., Boksenberg, A., and Fosbury, R.A.E. 1979, *Monthly Notices of the Royal Astronomical Society* **189**, 45P.
8. Barr, P., White, N.E., Sandford, P.W., and Ives, J.C. 1977, *Monthly Notices of the Royal Astronomical Society*, **181**, 43P.
9. Holt, S. S., et al. 1980, *Astrophysical Journal* **241**, L 13.
10. Schreier, E.J., Gorenstein, P., and Feigelson, E.D. 1982, *Astrophysical Journal* **261**, 42.
11. Johnston, K.J., Elvis, M., Kjer, D., and Shen, B.S.P. 1982, *Astrophysical Journal* **262**, 61.
12. Bromage, G.E. et al. 1984, preprint.
13. Anderson, K.S., and Kraft, R.P. 1969, *Astrophysical Journal* **158**, 859.
14. Boksenberg, A., and Penston, M.V. 1976, *Monthly Notices of the Royal Astronomical Society* **177**, 127P.
15. Ulrich, M.H. et al. 1980, *Monthly Notices of the Royal Astronomical Society* **192**, 561.

## The Nature of Subdwarf B Stars

U. Heber and K. Hunger, *Institut für Theoretische Physik und Sternwarte der Christian-Albrechts-Universität, Kiel*

### Introduction

Subdwarf B stars from the blue end of the horizontal branch. They occur both in the field and in globular clusters. A large fraction of the field sdB's (as well as sdO stars) has been found accidentally, during a search for faint blue objects (quasars) at high galactic latitudes, whereas the cluster sdB's are the result of a systematic search. The total number of subdwarf B stars presently known is estimated to roughly 70. It is anticipated that the true number is much larger.

Subdwarf B stars have colours and hence temperatures which are typical for B stars, but which, in some cases, even reach up to 40,000 K and beyond. The latter are more precisely defined as sdOB stars. At the temperatures in question, the neutral helium line  $\lambda$  4471 should be prominent in the spectrum of subdwarf B stars. However, in most sdB's this line is barely seen at moderate resolution, or even absent (Fig. 1). The main features are the strong and Stark broadened Balmer absorption lines, besides which hardly any other line can be traced. Most sdOB stars (e.g. Feige 110, Fig. 1) show He II,

$\lambda$  4686  $\text{\AA}$ , but the weakness of helium lines distinguishes subdwarf B and OB stars from the hot subdwarf O stars (Fig. 1). The latter are known to be helium rich (Hunger and Kudritzki, 1981). Do we then have to conclude that subdwarf B (and OB) stars are deficient in helium—a conclusion that obviously would be in conflict with the idea of horizontal branch stars as being evolved stars? Or is the definition of subdwarf B stars as horizontal branch stars to be questioned? For the discussion of the evolutionary status, a necessary prerequisite is the precise knowledge of the fundamental stellar (atmospheric) parameters like effective temperature, gravity and hydrogen-to-helium content.

### Spectral Analysis

Spectral analysis yields the wanted parameters. The best way to determine the effective temperature of a given star is by studying profiles and equivalent widths of an element that is observed in 2 stages of ionization. Only if one has the properly chosen model atmosphere which is defined by  $T_{\text{eff}}$ , besides g

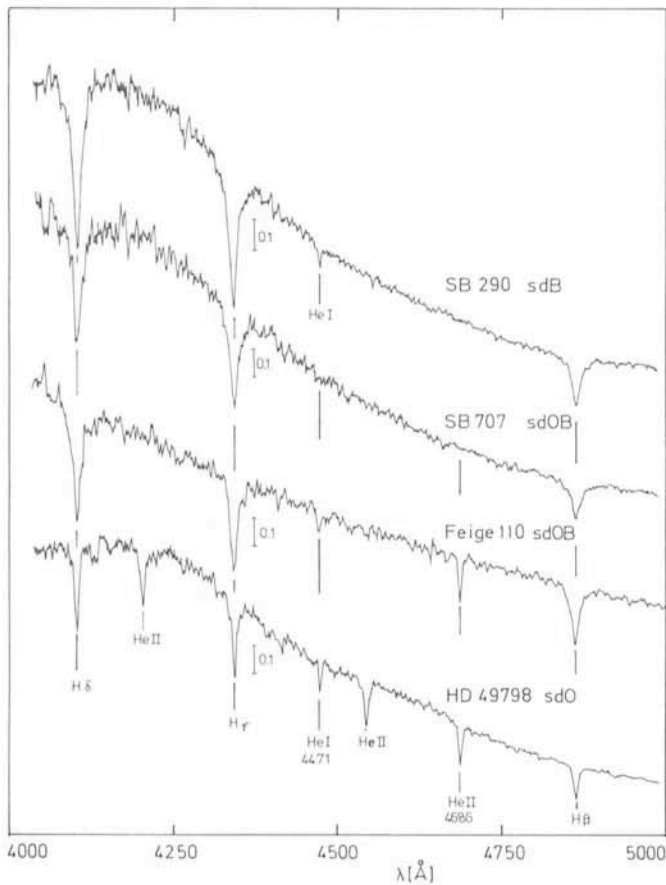


Fig. 1: Medium resolution IDS spectrograms ( $58 \text{ \AA/mm}$ ) of the sdB star SB 290, the sdOB SB 707 and Feige 110, and the sdO HD 49798. 10 % intensity at  $H_\gamma$  is indicated by a vertical bar. (The spectra are flat field corrected, but not calibrated to absolute fluxes.)

and H/He ratio, one is able to reproduce the observed equivalent widths of both stages of ionization with one single abundance of the element considered. In essence, this method is equivalent to the temperature determination from spectral type. The other method makes use of colours. As we have just seen that subdwarf B stars show hardly any metal lines and none in two stages of ionization, one is left with these "colour temperatures". The well-known study of a large sample of subdwarf B stars by Newell (1973) is based on intermediate band colour indices, and in the comprehensive analysis by Greenstein and Sargent (1974), use is made of broadband colours. Similarly, in the early analysis of the two brightest subdwarf B stars spectral scans were compared (see Baschek, 1975).

"Colour temperatures" are reliable whenever the colours are sampled at wavelengths which contribute significantly to the radiated energy. When the temperatures exceed 20,000 K, colours taken in the optical yield decreasingly less reliable temperatures as the bulk of radiation shifts towards the UV. Here is where UV colours become a necessity.

### The Importance of IUE

As for B stars, the main flux is carried in the IUE band; IUE is the ideal instrument for the determination of effective temperatures. Fig. 2 shows the observed spectra of 3 subdwarf B stars: SB 459 (top), LB 1559 (middle) and SB 290 (bottom). They cover the broad wavelength range from 1200 Å to 5500 Å. The IUE spectra are at low resolution, and for SB 459 and LB 1559 in both wavelength ranges. For SB 290, fluxes measured

with the satellite TD 1 (marked by error bars) have been added. At the long wavelengths, Johnson and Strömgren colours are shown. The way the IUE spectra are corrected for interstellar reddening and how, simultaneously, the angular diameter  $\theta$  and the effective temperature  $T_{\text{eff}}$  is determined, is described in detail in the paper by Heber et al. (1984). The principle, however, can be understood from Fig. 2: For SB 459, three theoretical fluxes are reproduced: for  $T_{\text{eff}} = 22,500 \text{ K}$ ,  $25,000 \text{ K}$ , and  $27,500 \text{ K}$ , respectively. The fluxes are from fully line blanketed LTE models (Kurucz, 1979). Even taking into account the internal error of the IUE calibration (which is shown as vertical bar at the left end of Fig. 2), it is clear that the two temperature extremes can be ruled out, and that  $25,000 \text{ K} \pm 1,200 \text{ K}$  can be adopted with confidence.

### The IDS Spectrograms

After having determined  $T_{\text{eff}}$  rather unambiguously (the procedure is largely independent of gravity and He/H ratio) the gravities can be determined straightforwardly from the profiles of  $H_\gamma$  and  $H_\beta$ . In Fig. 3, our three examples, SB 459 (top), LB 1559 (middle) and SB 290 (bottom), are shown for comparison between theory (dashed) and observation (full drawn). The best fits have been obtained for  $\log g = 5.3$  (SB 459),  $5.2$  (LB 1559) and  $5.5$  (SB 290), the error estimate being  $\pm 0.2$ .

In the same manner, the helium content can be obtained from  $\lambda 4471$ , if present. Otherwise upper limits are inferred. As it turns out, all the 19 programme stars are deficient in helium by factors varying from 25 to 100. Before we discuss this remarkable abundance anomaly, let us first turn to the ( $g$ ,  $T_{\text{eff}}$ ) diagram.

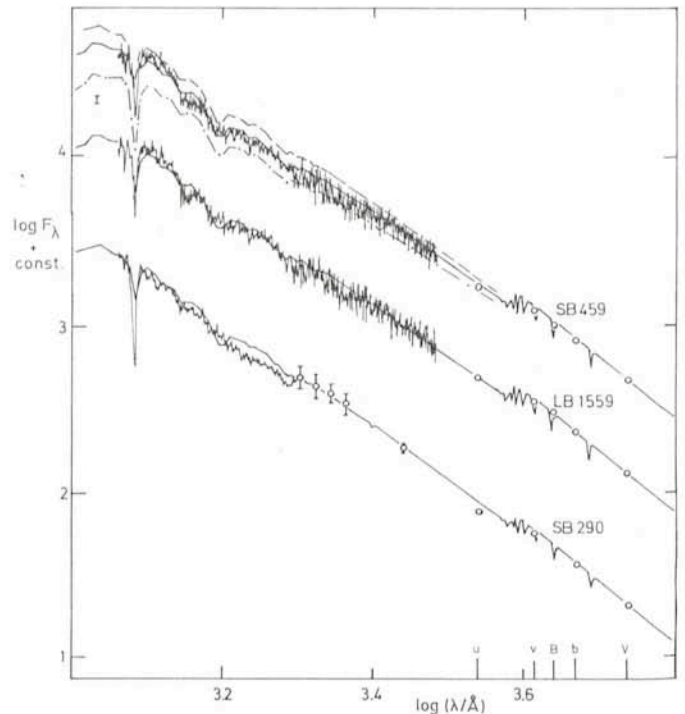


Fig. 2: Comparison of the observed UV spectra with the finally adopted models for SB 459 ( $T_{\text{eff}} = 25,000 \text{ K}$ ), LB 1559 ( $T_{\text{eff}} = 25,200 \text{ K}$ ) and SB 290 ( $T_{\text{eff}} = 28,200 \text{ K}$ ). For SB 459 additional model fluxes with  $T_{\text{eff}} = 27,500 \text{ K}$  (dashed), and  $22,500$  (dashed dotted) are shown. The small error bar indicates the intrinsic accuracy of the IUE calibration (10%). Open circles: Johnson and Strömgren colours. TD1-fluxes are shown with error bar.

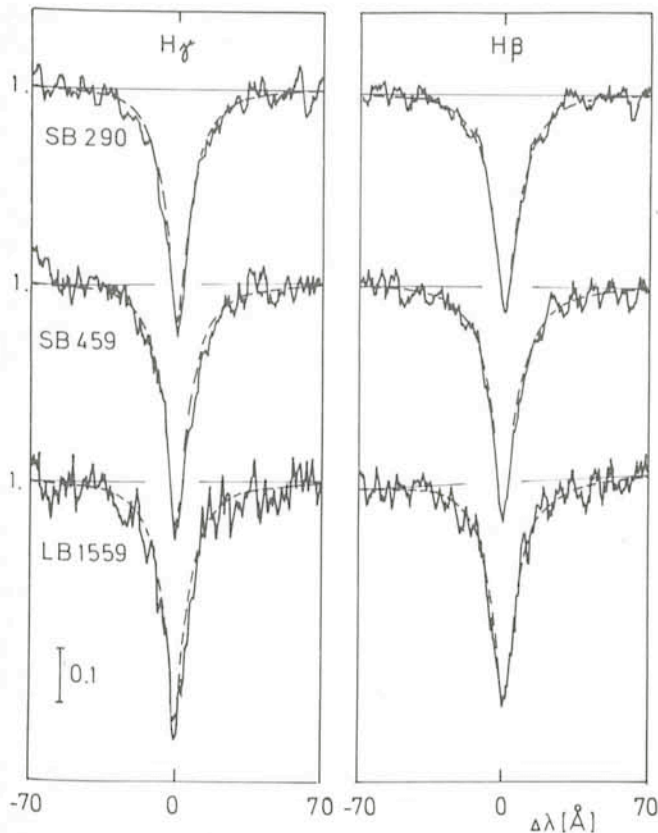


Fig. 3: Comparison of observed profiles of  $H_\gamma$  and  $H_\beta$  with theory for SB 290, SB 459 and LB 1559. The dispersion is  $58 \text{ \AA/mm}$ . 10% intensity is indicated by a vertical bar.

### ( $g$ , $T_{\text{eff}}$ ) Diagram

The ( $g$ ,  $T_{\text{eff}}$ ) diagram, the morphological equivalent to the H. R. diagram, allows the direct comparison between the observations and the results of stellar interior calculations. In Fig. 4, the presently analysed subdwarf B stars (triangles) and their hot counterparts, the subdwarf OB stars (circles) are shown. The accuracy of the observed temperatures and gravities is characterized by crossed error bars (top). The zero-age helium main sequence (He-m.s.) runs at the bottom, while the zero-age horizontal branch (H.B.) extends downwards from the upper right corner. For clarity, the latter is reproduced only for one mass fraction of helium,  $Y = 0.25$ . The H. B. stars are assumed to have core masses of  $M_c = 0.475 M_\odot$ . The envelope masses  $M_e$  are very small, comprising only  $0.06 M_\odot$  at the cool end to  $0.005 M_\odot$  at the hot end. True H. B. stars exist only down to  $M_e = 0.02 M_\odot$  (Gross, 1973), because below this mass, the hydrogen shell burning becomes negligible. The sequence from  $M_e = 0.005 M_\odot$  to  $M_e = 0 M_\odot$  is interpolated (dashed curve). Stars with  $M_e < 0.02 M_\odot$  may be termed generalized helium main-sequence stars in the sense that they have only one single central source of energy left, as the true helium m.s. stars.

The evolution of a helium m.s. star proceeds at a drastically different path than that of an H. B. star. While the former moves horizontally towards hotter temperatures, the latter moves vertically towards lower gravities: the corresponding arrows correspond to an evolutionary time of  $1.4 \cdot 10^8$  years, for both evolutions.

The ( $g$ ,  $T_{\text{eff}}$ ) diagram allows an immediate conclusion as to the evolution of our sample of subdwarf B stars: they have reached their present location along a horizontal vector from the (zero age) extended horizontal branch with  $M_e < 0.02 M_\odot$ ,

i. e. from the generalized helium main sequence. The time that elapsed after they left the sequence until helium core exhaustion is of the order of  $10^8$  years.

Even more dramatically appears the conclusion one has to draw with regard to the subdwarf OB stars: a major fraction—and these are the stars with gravities of the order of  $10^{+6}$ —are true helium main-sequence stars, with  $M_e < 10^{-3} M_\odot$  (e.g. SB 707). These are up to now the only bona fide helium main-sequence stars that are known. However, there is one dilemma: we have seen above that these stars are helium depleted rather than helium rich. The sdOB SB 707 even does not show any helium lines in the visual (see Fig. 1), but, nevertheless, is regarded as a helium main-sequence star. (Those sdOB's with smaller gravities, e.g. Feige 110, have evolved from the generalized helium main sequence [see below]).

### The Helium Main-Sequence Stars (sdOB's) and Their Photospheric Helium Content

It is known that the envelopes of white dwarfs are composed of almost pure helium, even those of the apparently hydrogen-rich white dwarfs of type DA (Dziembowski and Koester, 1981). The very small amount of hydrogen left to these stars floats atop the helium layer due to the enormous gravity present and thus becomes the dominant spectral feature. A similar situation holds for the subdwarf OB stars (Hunger and Kudritzki, 1981). Diffusion in the presence of strong gravity forces the available hydrogen to the surface and hence mimics a hydrogen star, even in those cases where the outer layers are mainly composed of helium. Clearly the same action of diffusion is seen in our subdwarf B stars.

### Metal Abundances

Diffusion not only affects helium, but also the metals. Hence conclusions with regard to evolution (e.g. N enrichment

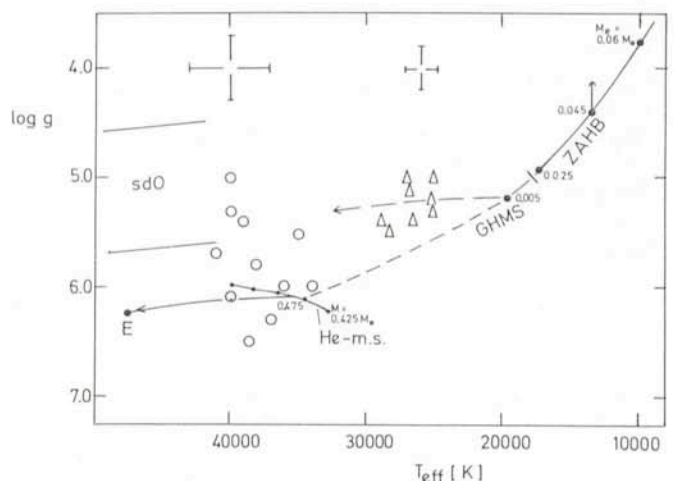


Fig. 4: Position of sdB ( $\Delta$ ) and sdOB stars ( $O$ ) in the ( $\log g$ ,  $T_{\text{eff}}$ ) plane (typical errors are indicated by crossed bars). Also shown are the helium main sequence plus the evolutionary path of a  $0.5 M_\odot$  pure helium star up to core helium exhaustion (point E), and ZAHB models for  $Y = 0.25$  from Gross (1973). The models are labelled with their envelope mass  $M_e$ . The dashed line is an interpolation for very low envelope masses ( $M_e \leq 0.005 M_\odot$ ). The borderline (at  $M_e = 0.02 M_\odot$ ) between canonical ZAHB stars and generalized helium main-sequence stars (GHMS) is indicated by a tick mark. The evolution of (zero age) GHMS stars up to helium core exhaustion proceeds along the (horizontal) dashed vector while the evolution of a canonical ZAHB star proceeds along the vertical vector.

through the CNO cycle, stellar population) cannot simply be drawn from metal abundances.

The optical spectra hardly contain metal lines, whereas in the UV a large number of lines is present. High resolution IUE spectrograms of 3 sdOB stars (HD 149382, Feige 66 and Feige 110) have been analysed with the result that silicon is deficient in all 3 stars, by as much as a factor 40,000 (!) in HD 149382. Carbon likewise is deficient in Feige 110, by a factor 300,000 (!), but only moderately deficient (factor of  $\sim 100$ ) in the 2 other stars, whereas nitrogen appears to be (nearly) solar in all 3 stars. In contrast to the sdOB's, silicon appears (almost) solar in the subdwarf B stars.

Some of these strange abundance anomalies can be understood, for instance the deficiency of silicon: at temperatures occurring near the bottom of the photospheres in subdwarf OB stars, silicon is ionized to  $\text{Si}^{4+}$ . This ion has a noble gas electron configuration with small absorption cross sections. Radiation that otherwise would force the ion upwards can no longer balance gravitation. As a consequence, the ion sinks below the photosphere (Baschek et al., 1982). A complete and quantitative theory, however, is lacking, and one is presently left with a more or less confusing picture of strange abundance patterns. All the information hidden there and being of great potential use in defining the momentary and past state of the photospheres in those subdwarfs, cannot be exploited at present.

## Evolution

From the  $(g, T_{\text{eff}})$  diagram (see above) it was concluded that subdwarf B and OB stars form the blue extension of the horizontal branch towards higher temperatures. After helium core exhaustion they evolve at constant gravity and eventually reach the domain of subdwarf O stars. This means that the  $(g, T_{\text{eff}})$  domain, which is occupied by subdwarf O stars, is also shared by evolved subdwarf B stars. How can these two classes be separated?

It is known that subdwarf O stars are helium rich. They have

temperatures above 40,000 K (Hunger and Kudritzki, 1981). At these temperatures, the He II convection zone extends up to the photosphere and thus inhibits diffusion which would dilute helium. But once helium is depleted as in our sdB sample, He II convection cannot work and hence a subdwarf B star, when crossing the 40,000 K boundary, stays helium poor (Groth and Kudritzki, 1983). For subdwarf O stars, the situation is different: they start from the (canonical) horizontal branch, i.e. with masses between 0.5 and 0.6  $M_{\odot}$ , and hydrogen-rich shell masses in excess of 0.02  $M_{\odot}$ . They move upwards in the  $(g, T_{\text{eff}})$  plane along a "Sweigart" track, attaining gravities which are too small for diffusion, and eventually experience shell flashes. When they reach the sdO domain, they have already mixed helium to the surface and thus convection becomes possible. This means true subdwarf O stars can be distinguished from evolved sdB (and sdOB) stars by their helium content. So far, 3 objects are known whose effective temperatures are in excess of 40,000 K and whose helium contents are subsolar (Heber and Hunger, in preparation). Those are, according to the above described picture, old evolved subdwarf B stars.

## References

- Baschek, B.: 1975, in *Problems in Stellar Atmospheres and Envelopes*, eds. Baschek, B., Kegel, W. H., Traving, G., Springer, Berlin, Heidelberg, New York, p. 101.
- Baschek, B., Kudritzki, R. P., Scholz, M., Simon, K. P.: 1982, *Astronomy and Astrophysics* **108**, 387.
- Dziembowski, W., Koester, D.: 1981, *Astronomy and Astrophysics* **97**, 16.
- Greenstein, J. L., Sargent, A. I.: 1974, *Astrophysical Journal, Suppl.* **28**, 157.
- Gross, P. G.: 1973, *Monthly Notices Roy. Astron. Soc.* **164**, 65.
- Groth, H. G., Kudritzki, R. P.: 1983, *Mitt. d. Astron. Ges.* **60**, 308.
- Heber, U., Hunger, K., Jonas, G., Kudritzki, R. P.: 1984, *Astronomy and Astrophysics* **130**, 119.
- Hunger, K., Kudritzki, R. P.: 1981, *The Messenger* **24**, 7.
- Newell, E. B.: 1973, *Astrophysical Journal, Suppl.* **26**, 37.

# Stellar Metallicity Gradient in the Direction of the South Galactic Pole Determined from Walraven Photometry

Ch. F. Trefzger, *Astronomisches Institut der Universität Basel, Switzerland*

J. W. Pel and A. Blaauw, *Kapteyn Astronomical Institute, Groningen, the Netherlands*

## Introduction

It has been known for a while that the stellar population in our Galaxy changes drastically as a function of distance from the galactic plane—the disk is composed mostly of relatively young stars with solar metal abundances and small velocity dispersions whereas the average metallicity drops and the age increases as we look at stars deeper in the halo. These findings were interpreted by Eggen et al. (1962, *Astrophysical Journal* **136**, 748) in terms of their rapid collapse model of the protogalaxy and the subsequent formation of the disk. However, for a detailed model of the evolution of the Galaxy we need a much broader observational basis, viz. knowledge of the parameters stellar density, metallicity, age and velocity dispersion as a function of distance from the galactic plane. Several attempts have been made to reach this goal.

The Basel halo programme has been described and initiated by Becker (1965, *Zeitschr. f. Astrophys.* **62**, 54). The aim was to study the stellar density function in different halo directions (mostly Selected Areas) in a meridional plane perpendicular to the disk containing the galactic centre and the sun. The programme is based on deep Palomar Schmidt plates taken with the three filters of the RGU system. It is well known that metal-poor stars show UV excesses relative to stars with solar abundances. In the RGU system, this effect is even more pronounced than in the UVV system, and it can be used to separate the metal-poor halo stars from the solar abundance disk stars statistically. The metallicities of the halo stars in the Basel Survey have been estimated on the basis of their colours by Trefzger (1981, *Astronomy and Astrophysics* **95**, 184).

The nearby field star population at the galactic poles has been investigated by Blaauw and Garmany (1975, in Proceed-

ings of the Third European Astronomical Meeting, E. K. Kharadze [ed.], Tbilisi, p. 351) and Blaauw (1978, in *Astronomical Papers* dedicated to B. Strömgren, Reiz and Andersen [eds.], p. 33); the observations were carried out using the Strömgren and Walraven photometric systems. In the latter paper it was shown that Walraven photometry is excellently suited to determine metallicities and luminosities of F and G type stars. However, the measurements did not go fainter than  $V = 12^m$ , reaching distances of at most 700 pc from the plane.

The observations described here—a joint Swiss-Dutch undertaking—aim at determining the relation between stellar metal abundance and distance from the galactic plane in a wider solar neighbourhood. By using the Basel RGU Survey for the selection of the programme stars (of type F and G), we can now extend the earlier photoelectric work to larger distances. On the other hand, the Walraven photometry allows to put the extensive Basel RGU data on a more accurately calibrated photoelectric base. We discuss our first preliminary results, obtained from two observing runs on La Silla in December 1981 and November 1982 with the Walraven photometer at the Dutch 90 cm telescope.

### The Walraven Photometric System

For a description of the Dutch telescope on La Silla and the Walraven VBLUW photometer we refer to an article by Lub (1979, *The Messenger* No. 19, 1). The stellar light is measured simultaneously through five passbands of intermediate width at the following effective wavelengths: V: 5420 Å, B: 4270 Å, L: 3850 Å, U: 3620 Å and W: 3230 Å. Since most of our programme stars are too faint and too cool to give measurable W signals, we are left in this programme with one magnitude (V) and the three independent colour indices (V-B), (B-L) and (L-U).

Assuming negligible or at most small foreground reddening in the directions of the fields investigated (see below), VBLUW photometry enables us to separate the effects of temperature, metallicity and gravity for intermediate-type stars (Lub and Pel, 1977, *Astronomy and Astrophysics* 54, 137, see also Pel, 1982, *The Messenger* No. 29, 1). The colour index (V-B) is a measure of stellar effective temperature, and the indices (B-L) and (L-U) are sensitive to line blanketing (mostly from Fe and other metals) and surface gravity ( $\log g$ ), respectively. This is illustrated in Fig. 1 by the theoretical colours computed from Kurucz model atmospheres (Kurucz, 1979, *Astrophysical Journal Suppl.* 40, 1). By combining the two diagrams of Fig. 1 we can estimate for each programme star the three parameters temperature, gravity and metallicity: The (V-B)-(B-L) diagram provides an almost gravity-independent temperature-metallicity grid, whereas the Balmer jump index (L-U) in the other diagram yields the gravity almost independently of the metallicity.

### Semi-empirical Calibration in Terms of Temperature, Metallicity and Gravity

We do not want to calibrate the diagrams solely on the basis of the computed colours from model atmospheres because it

is known that these still fail to reproduce accurately the colours of cooler stars, especially in the blue and ultraviolet spectral region. We therefore decided to observe nearby F, G and K stars with known physical parameters from detailed spectroscopic analyses and used the data compiled by Cayrel de Strobel and Bentolila (1983, *Astronomy and Astrophysics* 119, 1).

We constructed a semi-empirical calibration of the (V-B)-(B-L) diagram by combining the theoretical Kurucz colours with observations of field stars covering a wide range in

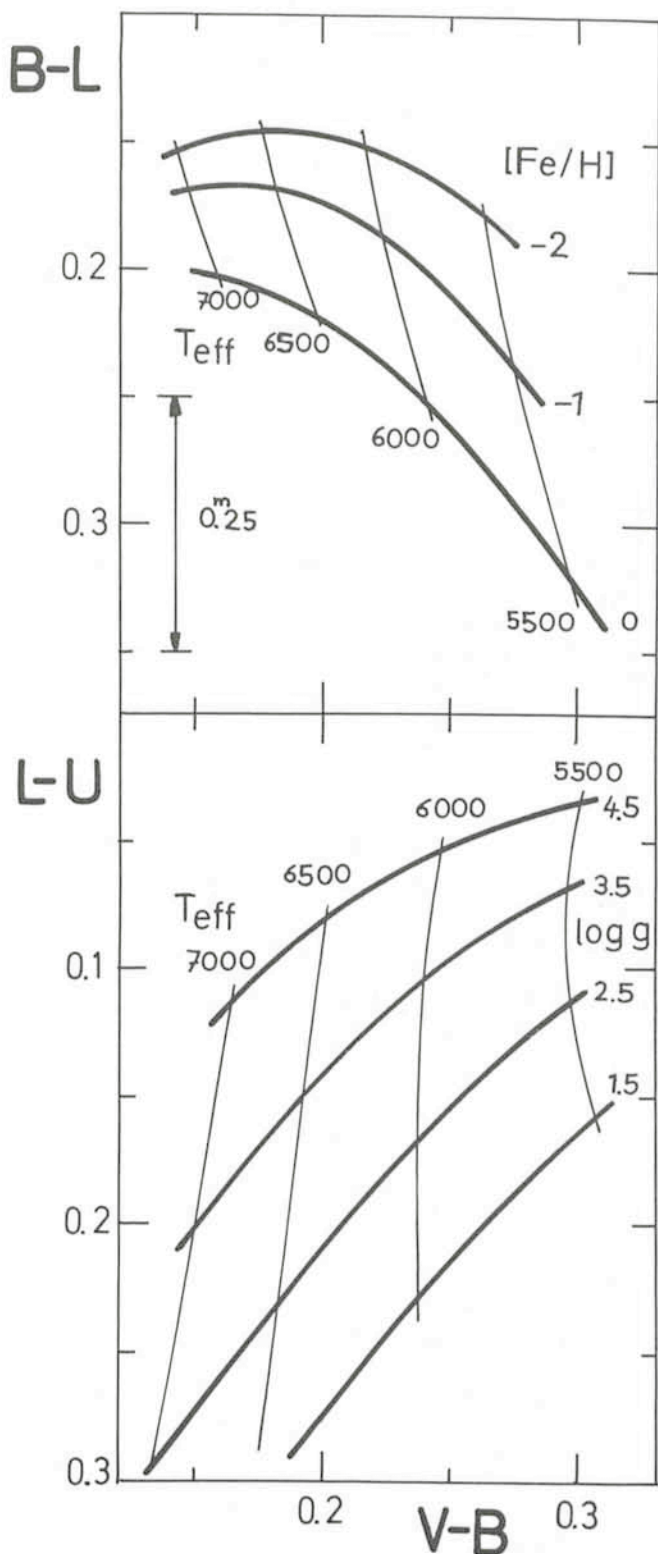


Fig. 1: These two diagrams show how the effects of metallicity and gravity can be separated with VBLUW photometry. The upper (V-B)-(B-L) diagram is almost gravity-independent and gives the stellar metallicity  $[\text{Fe}/\text{H}]$ . The lower (V-B)-(L-U) diagram is almost insensitive to metal line strengths and can therefore be used to determine temperature and gravity independently of  $[\text{Fe}/\text{H}]$ . The drawn lines correspond to theoretical colours calculated from Kurucz models. Note that all VBLUW diagrams are in log (intensity), so multiply by 2.5 to get magnitudes. ▶

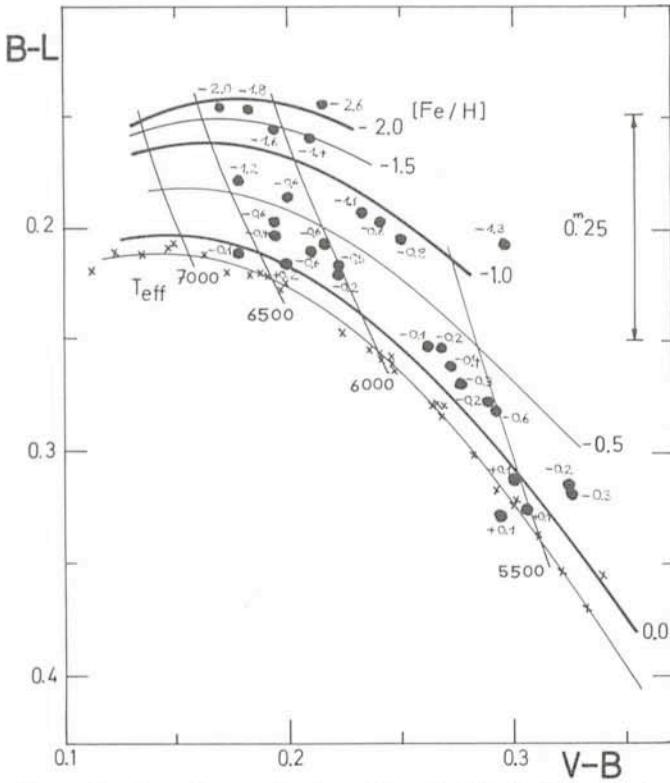


Fig. 2: Semi-empirical calibration of the  $(V-B)-(B-L)$  diagram using stars with spectroscopically known metallicities, temperatures and gravities (full circles with corresponding  $[Fe/H]$  values). Hyades main-sequence stars are indicated by crosses.

metallicity (Fig. 2). The notation  $[Fe/H]$  is a logarithmic measure of the stellar iron abundance relative to the sun: eg.  $[Fe/H] = -1$  means that the iron abundance is 10 % of the solar value. We used the location of the main-sequence stars of the Hyades as our reference line, adopting  $[Fe/H] = +0.15$  for this cluster. The resulting  $T_{\text{eff}} - [Fe/H]$  grid allows us to determine metallicities quite accurately. It is based on data for dwarf stars, but it does not depend strongly on gravity differences.

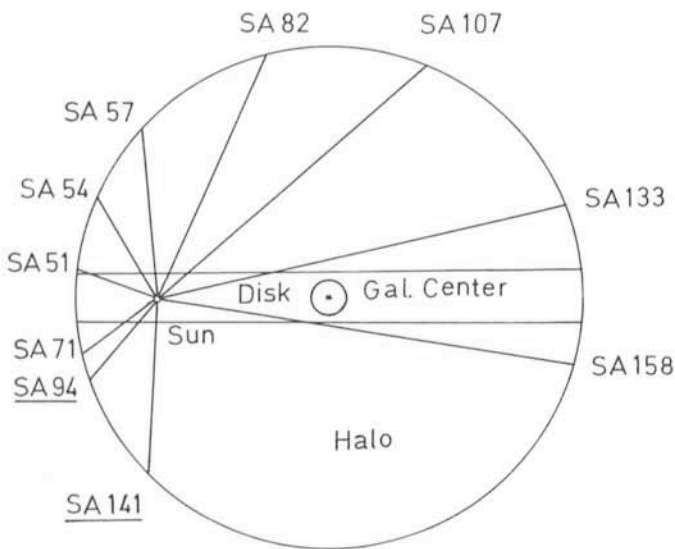


Fig. 3: The Selected Area fields of the Basel halo programme. They are close to a meridional plane perpendicular to the galactic plane containing the galactic centre and the sun. The fields where Walraven photometry has been carried out are SA 141 and SA 94. Their size is about two square degrees.

The location of main-sequence stars ( $\log g \approx 4.5$ ) in the gravity-sensitive  $(V-B)-(L-U)$  diagram agrees reasonably well with the predicted theoretical colours and the same holds for more evolved stars with  $\log g$  in the range between 1.5 and 3.5. Although the calibration of this diagram is still in progress, we are able to separate main-sequence stars from subgiants and giants in this way.

### Metal Abundances of F and G-type Stars in SA141 and SA94

The sample was selected from the existing Basel photographic RGU photometry in the Selected Areas No. 141 and No. 94. The field SA141 points towards the South Galactic Pole and SA94 has a latitude of  $-49^\circ$  in the direction of the anticentre (Fig. 3). The criteria for selecting our programme stars were purely photometric: All stars with  $(G-R) < 1^m.15$  (spectral type earlier than about G7) were measured in each field of  $1^{\circ}.5 \times 1^{\circ}.5$  size. Until now we have analysed 90 stars in SA141 brighter than  $V = 14^m.5$  and about 30 stars in SA94 brighter than  $V = 12^m.7$ . More data in both fields were obtained

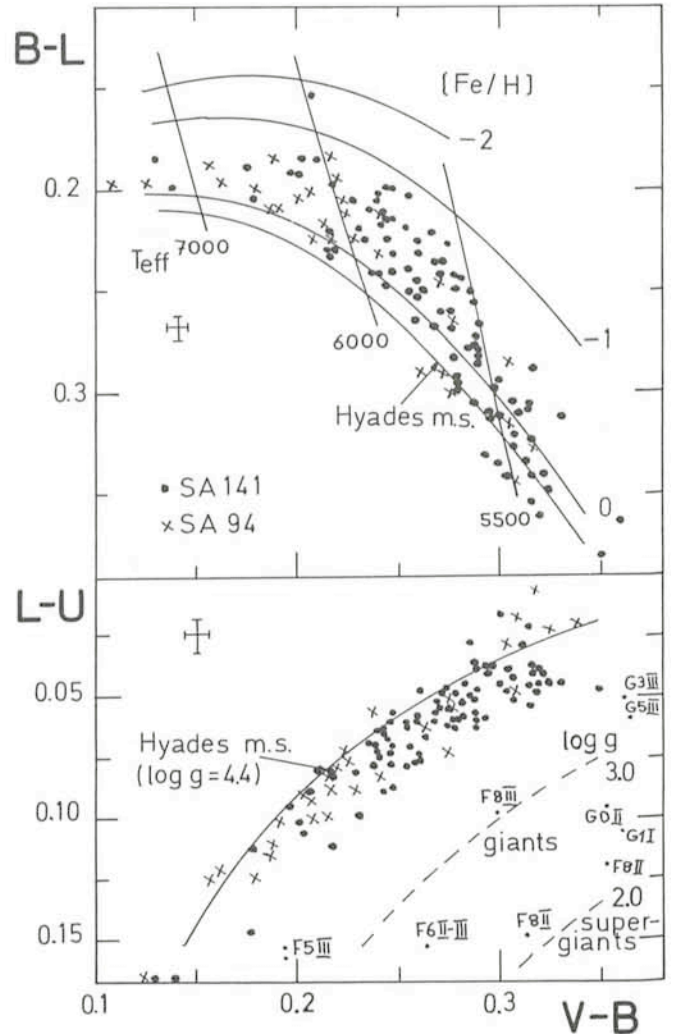


Fig. 4: Walraven photometry of our programme stars. The error bars indicate typical standard deviations. Fig. 4a: The distribution of the stars in the  $(V-B)-(B-L)$  diagram indicates that their metallicities vary between  $[Fe/H] = 0.0$  and  $-1.0$ . Fig. 4b: In the gravity-sensitive  $(V-B)-(L-U)$  diagram the distribution of the stars is quite narrow (around  $\log g = 4.2 \pm 0.3$ ) which suggests that most of them are dwarfs. Indicated is also the location of typical nearby giants and supergiants in this diagram.

in December 1983, but these measurements are not yet fully reduced.

Using the calibrated (V-B)-(B-L) diagram, we determined the parameters  $T_{\text{eff}}$  and  $[\text{Fe}/\text{H}]$  for each programme star (Fig. 4a). For this purpose we assumed that interstellar reddening in the South Galactic Pole field SA141 can be neglected, and we adopted a constant foreground reddening of  $E(B-V)_J = 0^m.05$  for SA94. The distribution of the stars in Fig. 4a indicates that their metallicities are in the range  $-1.0 \leq [\text{Fe}/\text{H}] \leq 0.0$ . In the gravity-sensitive (V-B)-(L-U) diagram (Fig. 4b) the programme stars populate a narrow range suggesting that the gravities are around  $\log g = 4.2 \pm 0.3$ . This means that our stars are probably all dwarfs with only a few possible subgiants.

An empirical absolute magnitude calibration was derived by using the data of Cayrel de Strobel and Bentolila (1983, *Astronomy and Astrophysics* **119**, 1). From their  $[\text{Fe}/\text{H}]$  catalogue we took all stars with known distances, and with the same range in  $T_{\text{eff}}$ ,  $[\text{Fe}/\text{H}]$  and  $\log g$  as our programme stars, to construct an empirical absolute magnitude-temperature relation. With this relation we determined the distances of the programme stars in SA141 and SA94.

In Fig. 5 the metallicities are plotted as a function of vertical distance  $z$  above the plane. The  $z$  values of the programme stars observed until now vary from almost zero up to  $z = 1,000$  pc with a few stars beyond this. The diagram clearly shows a correlation between distance and metallicity in the sense that stars further away from the plane are systematically metal-deficient. For example, stars at  $z = 750$  pc have a mean metallicity of  $[\text{Fe}/\text{H}] = -0.7$  which is five times more metal-weak than the sun.

Our calibrations are in many respects preliminary and improvements are expected for the near future. Measurements of many more nearby metal-deficient stars analysed spectroscopically are now available in the Walraven system so that the calibration of the (V-B)-(B-L) diagram can be put on a broader observational basis. Furthermore, for the determination of the absolute magnitudes we disregarded such effects as metallicity or age differences between the stars and used a mean  $M_V - T_{\text{eff}}$  relation. A more detailed procedure is clearly needed.

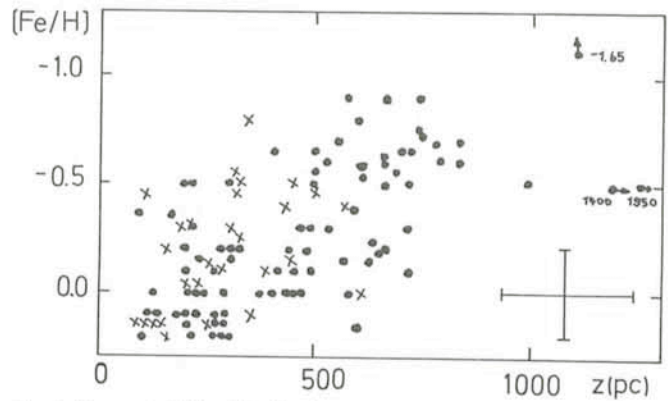


Fig. 5: The metallicities  $[\text{Fe}/\text{H}]$  of our programme stars as a function of vertical distance  $z$  above the galactic plane. The diagram clearly shows that the metal content of the stars decreases rapidly as we go away from the disk into the halo.

Nevertheless, our preliminary results are in reasonable agreement with previous determinations of abundances in the direction of the galactic poles. The earlier work by Blaauw and collaborators indicated that the metallicity drops to about  $[\text{Fe}/\text{H}] = -0.5$  at  $z = 500$  pc which compares well with  $[\text{Fe}/\text{H}] = -0.4$  estimated from our Fig. 5. Our results are also consistent with the metallicities of halo stars derived from the photographic RGU colours (Trefzger, 1981, *Astronomy and Astrophysics* **95**, 184). Our data can be used to check the predicted metallicity distributions at different  $z$  heights derived by Sandage (1981, *Astronomical Journal* **86**, 1643) from the  $W$  velocity components of nearby subdwarfs and several kinematic models.

We hope to get our photometry complete in both fields down to the limiting magnitude of the telescope ( $V = 14^m.7$ ). In SA141 this limit has been reached already, but more observations are needed in SA94. Eventually we will try to extend the observations to other fields as well.

## One-mm Observations of BL Lacertae Objects

H. Steppe, Max-Planck-Institut für Radioastronomie, Bonn

### Introduction

Forty years have elapsed since C.K. Seyfert in 1943 observed galaxies with strong activity in their centres. Twenty years later a new class of extragalactic objects entered the scene: the quasi-stellar objects (QSOs or quasars) representing the most extreme examples of energy output in the Universe. Today there is growing evidence for a continuity of properties among these "active galactic nuclei" (AGN) and it is now generally agreed that what is happening in the centres of these objects is qualitatively the same. This large group of objects also includes other active galaxies, namely radio galaxies with strong emission lines and *BL Lacertae objects*. The latter are named after their prototype lying in the constellation Lacertae (the lizard) and are abbreviated as BL Lac objects. The aim of this article is to describe and interpret some results obtained from 1-mm observations of these BL Lac objects.

Observations in this part of the spectrum are challenging. The Earth's atmosphere is almost opaque to much of the radiation, mainly due to the water vapour content of the atmosphere. To overcome this difficulty observations must be carried out on high, dry mountain sites. In the absence of suitable radio telescopes (surface accuracies of  $\sim 50 \mu\text{m}$  are needed), we had to use large optical telescopes, in particular the ESO 3.6 m telescope on La Silla and the 6 m SAO telescope at Zelenchukskaja in the Caucasus.

### What Are BL Lacs?

The properties of BL Lacs can be summarized as follows:

- Nearly all known BL Lac objects have been discovered because they are radio sources.
- Their radio spectra ( $S_\nu \propto \nu^\alpha$ ) are flat and often inverted, i. a.  $\alpha \geq 0$ .

- The radiation emanates from a compact region ( $\sim 1$  pc) of non-thermal radio emission with an extremely high brightness temperature ( $T \approx 10^{11 \pm 1}$  K).
- BL Lacs show rapid variability at radio, infrared and optical wavelengths.
- They are highly polarized (up to 30%) and the polarization is strongly variable.
- In several cases BL Lac objects appear to reside in giant elliptical galaxies.

The properties of BL Lac objects and radio loud quasars overlap to a certain degree, but the principal *difference* between these two types of objects lies in a deficiency of optical emission lines in BL Lac objects.

BL Lacs lack the broad emission line regions seen in quasars which surround and partially hide the very centre of the AGNs by gas and dust. In BL Lacs we are viewing directly the central mysterious engine which is yielding prodigious amounts of power of the order of  $10^{46}$  erg/sec over the wavelength region from the radio to X-rays. Observations of the spectral energy distribution provide crucial information on the emission mechanism operating in these sources. The continuum has now been measured at all conventionally observable wavelengths such as the radio, infrared, optical and even in some cases in the ultraviolet and X-ray wavelength bands. However, there is an irritating gap of 3 orders of magnitude in frequency between the near infrared and the high frequency radio regime. In this gap information about the spectral behaviour of celestial sources is only gathered at a very slow rate. The extension of the observations to millimetre wavelengths is especially important in order to define the spectral break which must generally occur between the radio and infrared regions. Furthermore, at millimetre wavelengths one is looking deeper into the source and sees the most compact components out of which a major proportion of the energy is emitted.

### The Bolometer as the Detecting Element

For continuum measurements around 1 mm wavelengths ( $\sim 300$  GHz), bolometers are still the most sensitive type of receivers, since they can use very large bandwidths. Our bolometer, cooled with liquid  $^3\text{He}$  down to 0.3 K, consists of a gallium-doped germanium chip as the temperature sensing element. It is—as usual at these wavelengths—of the composite type, in which the energy absorption and temperature measuring layers are separated. The large band-width of approximately 0.5 mm ( $\sim 150$  GHz) is limited by diffraction at the telescope aperture at the long wavelength side (ca. 1.5 mm). The short wavelength limit is set by a filter in combination with absorption by the water vapour in the atmosphere.

A dual-beam chopping system is used. The half-power beam diameter is about  $120''$  at the 3.6 m ESO telescope and the separation of the beams is also  $120''$ . The signal is chopped by means of a sector mirror rotating at 10 Hz.

Flux density calibration and extinction at these wavelengths are usually determined from observations of the planets using their measured brightness temperatures.

However, since the planets cannot be observed around the clock and the conditions of the sky change in a rapid and unpredictable way, we also made "Sky dips" i.e. pointing the telescope at blank sky at different elevations and recording the thermal radiation of the atmosphere as a function of the airmass. The measurements of the transmission of the atmosphere (typically of the order of 70% to 80%) then yield the atmospheric water vapour content, which was combined with absorption line data for atmospheric water vapour and oxygen

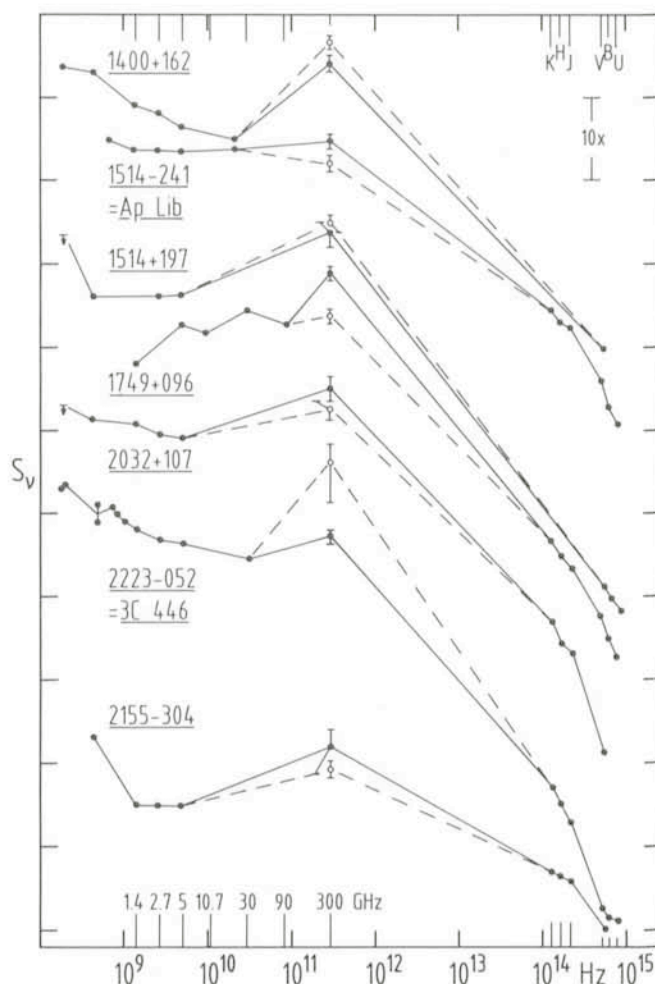


Fig. 1: Overall spectrum (from radio to optical wavelengths) of those BL Lac objects, for which 1 mm observations have been obtained at two observing sessions (● June/July 1982, ○ July 1983). The  $\lambda$  1 mm flux densities are derived assuming a spectral index  $\alpha = 0$ . For reasons of clarity only error bars for 1 mm flux densities are given. The Optical Violent Variable (OVV) 3C446 is included in the sample; it showed an outburst at  $\lambda$  1 mm during July 1983, followed by an optical outburst in August 1983 (IAU circular No. 3856).

to calculate the exact spectral response in the bandpass and the effective observing wavelength.

### The Observations

With the bolometer attached to the prime focus of the ESO 3.6 m telescope on La Silla a source of 1 Jy is detected with a signal-to-noise ratio of 3 in one hour integration time. The observations were performed at two epochs, in July 1982 and in June/July 1983, both times under unfavourable weather conditions.

Our BL Lac objects were selected from the list of Hewitt and Burbidge (1980). About 20 BL Lac objects have an expected flux density at 1 mm wavelength greater than our system sensitivity limit (1 Jy) if the spectrum is extrapolated from optical/infrared and from the radio region towards 15 mm. Out of these objects 15 have been observed. Additionally, six likely BL Lac candidates, not listed in the above-mentioned quasar catalogue were chosen because of their flat radio and steep infrared spectra. The radio data were taken from the available catalogues, and the infrared data have been published by Allen, Ward and Hyland (1981).

## Radio and Infrared Spectrum

Fig. 1 shows the spectral distribution for a few BL Lac objects from the radio to the infrared/optical domain. Data at 1 mm could only be obtained at both observing periods for the few sources presented in the figure. For reasons of clarity only error bars for the flux densities at 1 mm are depicted in the figure. They are estimated to be about 25 per cent, mainly due to uncertainty in calibration.

Most BL Lacs show inverted (65 %) or flat (35 %) radio spectra so that the flux at 1 mm often exceeds the value at lower frequencies. The spectrum of radio quasars on the other hand is flat or decreasing with frequency.

Based on their spectra at high radio frequencies, BL Lac objects will be very numerous in future mm surveys and become the most common type of objects. Extrapolation of the high-frequency radio spectrum towards 1 mm gives a close correlation between the observed and extrapolated fluxes at 1 mm.

The ratio in flux density of the near infrared (NIR) to the mm range  $S_{IR}/S_{mm}$  is a few times  $10^{-3}$ . Fig. 2 shows a graph of the spectral index in the near infrared (J to K,  $\sim 1.2$  to  $2.2 \mu\text{m}$ ) versus the spectral index between the K band and 1 mm. Though there is a wide spread in both spectral indices for a single object, a unique spectral index from 1 mm all the way to the NIR is compatible with the observations (dashed line in Fig. 2). The scatter in the diagram could be attributed partly to the variability of the sources because the observations made in the different wavebands were carried out at different epochs. This could be especially true for AO 0235+164 (e.g. strong outburst at the end of 1977). A scatter could also be caused by a misidentification of an object: 0406+121 is classified as a probable BL Lac object (Aaronson and Boronson, 1980).

## Radiation Processes in BL Lacs

A uniform spectral slope from 1 mm to the NIR can most easily be explained if a single radiation mechanism is the origin of both the radio and infrared emission. The simplest mechanism is the *synchrotron radiation process*. It would also explain variability and strong polarization. The variability increases with frequency so that at millimetre wavelengths variations on a time scale of days are observed. As an example we list in the table our measurement of the source 1749+096:

Source	Date of Observation	$S_{1\text{mm}}$ (Jy) assuming $\alpha = 0$
1749+096	07.07.1982	4.4
	08.07.1982	8.5
	09.07.1982	3.2
	10.07.1982	7.2

Unfortunately we have not yet undertaken polarization measurements, but for the next observing run our instrument will be equipped with a simple polarimeter.

For an explanation of the overall spectrum of the BL Lacs from radio to X-rays the synchrotron-self Compton (SSC) theory seems to be favoured by most astronomers. In the SSC mechanism the synchrotron radiation is scattered by the relativistic electrons to higher energies. This would explain why X-ray emission has been observed for nearly all AGNs which are chosen from radio surveys. The flat or inverted part of the radio spectrum in BL Lac objects could be composed of several distinct, compact components which show synchrotron-self absorption at different wavelengths. The observed turnover frequency due to the synchrotron-self absorption

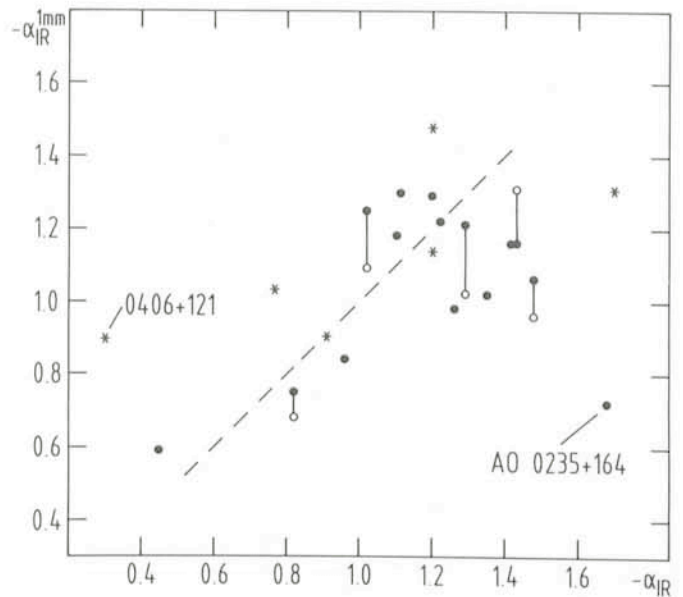


Fig. 2: Correlation between the spectral index in the near infrared ( $\alpha_{IR}$ ) and the spectral index derived from the flux at 1 mm and that in the K-band at  $2.2 \mu\text{m}$  ( $\alpha_{IR}^{1\text{mm}}$ ). Filled circles represent confirmed BL Lac objects while probable BL Lacs are shown by asterisks. Filled circles are from observations in June/July 1982, while open circles belong to July 1983 measurements.

cutoff allows an estimate of the angular diameter which turns out to be a few  $10^{-6}$  arcsec. These most compact regions are the places where the X-ray photons are created by the inverse Compton effect and which make up the highest frequency part of the spectrum in BL Lac objects. At frequencies higher than the turnover frequency the spectrum becomes optically thin and can be represented as a power law  $S_\nu \propto \nu^\alpha$ , with a single spectral index extending into the UV region.

## Future Prospects

Surveys at 1 mm should provide BL Lacs as the most common type of objects. Because the typical variability time scale is of the order of days, it is essential that simultaneous observations at mm and shorter wavelengths are performed, both for measuring the total intensity—to determine the true spectral behaviour—and also the polarization. A systematic monitoring of BL Lac objects in the mm waveband yields opportunities for probing the shortest timescales of these sources. And finally, future millimetre Very Long Baseline Interferometry (VLBI) observations could ultimately reveal the innermost engine on scales of  $\sim 10$  mpc, determine its shape and so provide insight into the origin of activity in BL Lac objects. It is obvious that these problems require a lot of telescope time in long-term programmes. Thus, we are looking forward to using a telescope especially built for mm observations on Pico Veleta, a 2,850 m high mountain near Granada (Spain), hopefully in 1984.

## References

- Aaronson, M., Boronson, R.: 1980, *Nature* **283**, 746.  
 Allen, D. A., Ward, M. J., Hyland, A. R.: 1982, *Monthly Notices of the Royal Astronomical Society* **199**, 969.  
 Hewitt, A., Burbidge, G.: 1980, *Astrophysical Journal Suppl.* **43**, 57. IAU circular No. 3856 (1983).

# Light Curve Variations in Short Period EB Type Contact Binaries

H. Mauder, *Astronomisches Institut Tübingen*

The structure and evolution of contact binaries is still very poorly understood. If two stars are so close together that they are physically touching, then it is to be expected that the normal equilibrium configurations of the single stars are heavily disturbed. Mass and energy transfer between the components can occur which makes the theoretical calculations on stellar structure and evolution extremely difficult.

The well-known and numerous W UMa type subgroup of contact binaries is characterized by the almost equal depth of the primary and secondary minima in their light curves. Consequently, the surface temperatures of both components must be nearly equal as well, regardless of the masses of the two stars. This posed a serious problem to theoretical astrophysics since the stars cannot be far from the main sequence. In 1968 Lucy (1) developed a theoretical model for contact binaries with a common convective envelope which allows a redistribution of the energy output over the whole common photosphere of the system, thus explaining the characteristic W UMa light curves. However, in 1971 Mauder (2) was able to show that this first model was in contradiction with the observations. In the meantime the model has been refined, and it has turned out that contact binaries cannot reach thermal equilibrium. Therefore, W UMa stars must be unstable on a thermal timescale. It was proposed that these systems undergo cyclic variations with alternating phases of true contact and semidetached, but almost contact, phases. During contact phases, the characteristic W UMa light curves should be observed while during the semidetached phases the surface temperatures of the two components should be different, thus producing Beta Lyrae (EB) type light curves. The cycles are also connected with mass exchange between the two components.

Another model for W UMa stars was proposed by Shu, Lubow and Anderson (3), where thermal equilibrium is possible. It is necessary in this case that a so-called discontinuity zone exists below the common convective envelope, which masks the physical properties of the underlying, less massive star. Thus, the structure of the whole photosphere is mainly determined by the more massive component.

Of course, it is interesting for the observing astronomer to look for systems which eventually may be relevant for a decision between the different theories, especially with respect to mass transfer and secular variations of the light curves. For these reasons the author started an observing campaign on several systems which seemed to have unusual properties. From eight systems originally chosen, the two stars FT Lup and V 1010 Oph turned out to be remarkably interesting. In Fig. 1 the V light curve of FT Lup is shown, where observations from 1980–1983 are combined. The light curve

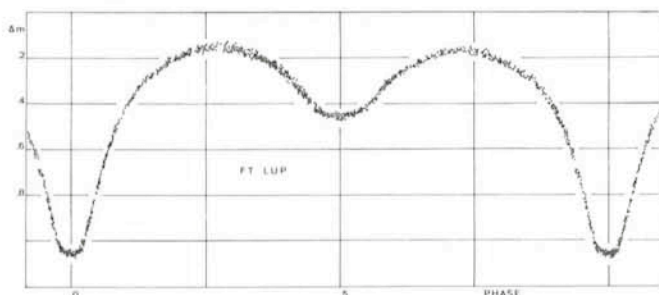


Fig. 1: *V* light curve of FT Lup.

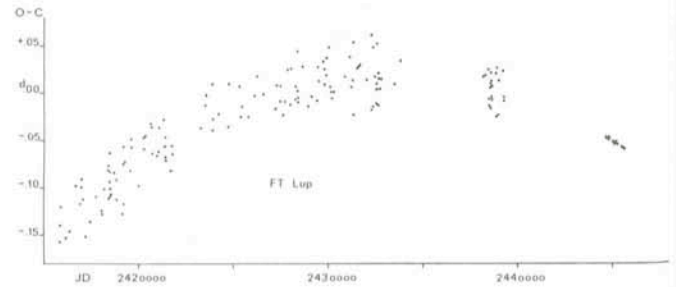


Fig. 2: *Difference between observed and calculated times of minima for FT Lup.*

is well defined and the solution showed that FT Lup is a contact system. However, the two minima are very different in depth, which means that the less massive component has a much lower surface temperature. Therefore, the energy exchange between the two stars in the common convective envelope is far from the expected equilibrium value which characterizes W UMa stars. The solution of the light curve showed that the degree of contact is still shallow. It could be, therefore, that the system is evolving towards a closer contact configuration. In this case, mass transfer should occur, which in turn causes variations of the orbital period. This is clearly seen in FT Lup (see Fig. 2). Here, all times of minima which are known back to 1890 are compared with the expected times of minima, calculated under the assumption that the period is constant. It is obvious that the period has steadily been decreasing since 1890. With the solution parameters of FT Lup, a mass transfer rate of  $3 \cdot 10^{-7}$  solar masses per year is suggested, consistent with the thermal timescale of the stars.

Even more dramatic variations are seen in V 1010 Oph. In Fig. 3 two light curves of this system are combined. The tiny dots show the *V* light curve obtained in 1983 at ESO, the circles are the points of the light curve observed in 1966 by Leung (4). In their light curve solution, Leung and Wilson (5) found V 1010 Oph to be a contact system, and again the degree of contact is rather shallow and the surface temperatures of the two stars are remarkably different. V 1010 Oph shows period variations which are very similar to those found for FT Lup, but even larger. But the most interesting feature is the variability of the light curve. Leung and Wilson (5) have found that their calculated light curve showed systematic differences compared with the observations in the phase interval 0.5 to 0.7: the observed points were all below the calculated values in this phase interval. The new observations of 1983 show that this difference vanished. At the same time the depth of the primary minimum decreased by almost 0.1 mag – the temperature difference between the two stars is therefore smaller now.

It seems to be a natural conclusion that the two systems are in a state of mass exchange during the evolution towards the W UMa stage of contact binaries, thus favouring the theory of cyclic variations. However, the scenario must be much more complicated. In the theory of cyclic variations as described above, the mass transfer during the contact phase is always from the less massive to the more massive component. During the semidetached phase the direction of mass transfer is opposite. V 1010 Oph and FT Lup are contact binaries, but the mass transfer was from the more massive component to the less massive one during the last 100 years. The decrease of the difference in surface temperature of the two stars in V 1010 Oph is evident, but is this really a secular evolution? Doubts

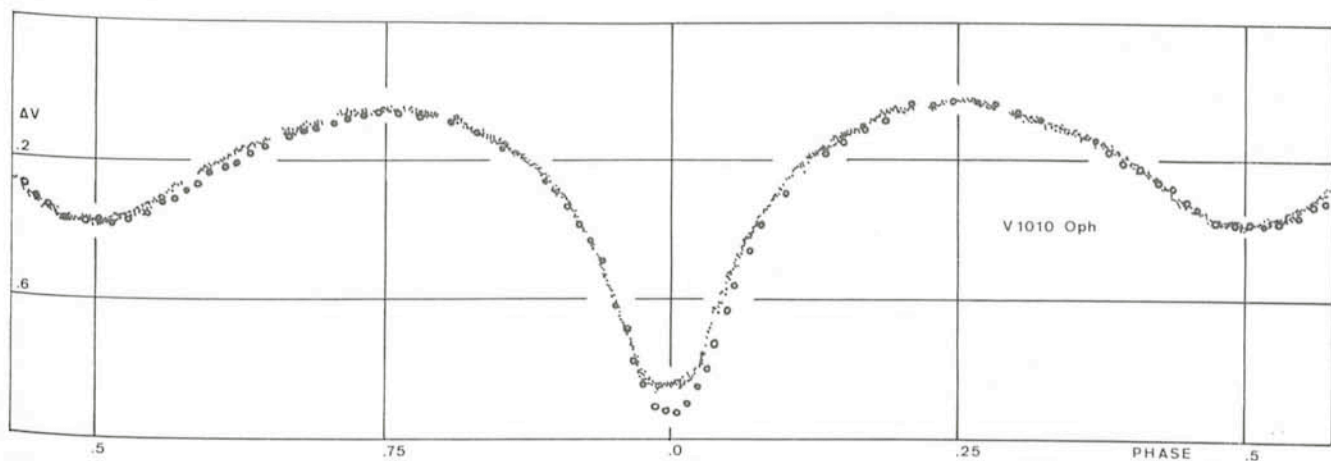


Fig. 3: Two V light curves of V 1010 Oph. The tiny dots are observations from 1983, the circles are normal points of the 1966 observations by Leung.

are appropriate since FT Lup showed an unexpected behaviour at the end of the observing run in 1981. In Fig. 4 the observations during primary minimum are shown. The dots are all observations between 1980 and 1983 as shown in Fig. 1, including observations from June 20, 1981. The circles are observations from June 26 and 27, 1981, only one week later, but unfortunately on the last nights of that run. In the next run, about one year later, the primary minimum was again at its lower value. Thus, the problem is still far from being solved. It is obvious that more extended observations are necessary to find out how these short-period, EB-type contact binaries are connected with the theory of the structure and evolution of W UMa stars.

#### References

1. Lucy, L. B. 1968, *Astrophysical Journal* **151**, 1123, and **153**, 877.
2. Mauder, H. 1972, *Astronomy and Astrophysics* **17**, 1.
3. Shu, F. H., Lubow, S. H., and Anderson, L. 1976, *Astrophysical Journal* **209**, 536.
4. Leung, K. C. 1974, *Astronomical Journal* **79**, 852.
5. Leung, K. C., and Wilson, R. E. 1977, *Astrophysical Journal* **211**, 853.

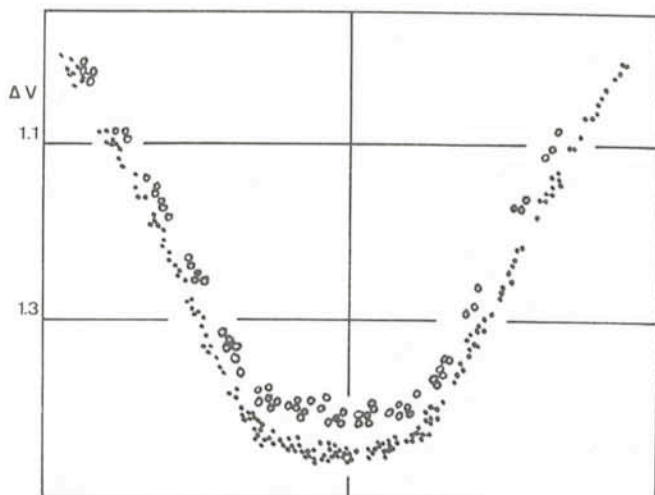


Fig. 4: Primary minimum of FT Lup. The dots are observations between 1980 and 1983, the circles are the observations from June 26 and 27, 1981.

## PERSONNEL MOVEMENTS

### STAFF

#### Arrivals

##### Europe

SJÖBERG, Britt (S), Secretary, 1.3.1984

#### Departures

##### Europe

TANNÉ, Jean-François (F), Project Engineer in Astronomical Instrumentation, 16.3.1984

FLEBUS, Carlo (I), Laboratory Technician, 30.4.1984

##### Chile

MAURICE, Eric (F), Astronomer, 29.2.1984

### FELLOWS

#### Arrivals

##### Europe

MATTEUCCI, Maria Francesca (I), 1.2.1984

BINETTE, Luc (Canadian, Australian), 1.3.1984

BRINKS, Elias (NL), 1.4.1984

GARAY, Guido (RCH), 1.6.1984

#### Departures

##### Europe

PERRIER, Christian (F), 31.1.1984

### COOPERANTS

#### Arrivals

##### Chile

DIDELON, Pierre (F), 21.12.1983

FOUQUE, Pascal (F), 4.1.1984

### ALGUNOS RESUMENES

## Simposio ESO/CERN sobre la Estructura a Gran Escala del Universo, Cosmología y Física Fundamental

En CERN, Ginebra, se realizó el primer simposio ESO/CERN sobre «Estructura a Gran Escala del Universo, Cosmología y Física Fundamental» desde el 21 al 25 de noviembre de 1983. CERN, el Laboratorio Europeo para la Física de Partículas se dedica al estudio de las partículas subnucleares básicas y fuerzas de la materia.

ESO, the European Southern Observatory, was created in 1962 to . . . establish and operate an astronomical observatory in the southern hemisphere, equipped with powerful instruments, with the aim of furthering and organizing collaboration in astronomy . . . It is supported by eight countries: Belgium, Denmark, France, the Federal Republic of Germany, Italy, the Netherlands, Sweden and Switzerland. It operates the La Silla observatory in the Atacama desert, 600 km north of Santiago de Chile, at 2,400 m altitude, where thirteen telescopes with apertures up to 3.6 m are presently in operation. The astronomical observations on La Silla are carried out by visiting astronomers — mainly from the member countries — and, to some extent, by ESO staff astronomers, often in collaboration with the former. The ESO Headquarters in Europe are located in Garching, near Munich. ESO has about 120 international staff members in Europe and Chile and about 120 local staff members in Santiago and on La Silla. In addition, there are a number of fellows and scientific associates.

The ESO MESSENGER is published four times a year: in March, June, September and December. It is distributed free to ESO personnel and others interested in astronomy. The text of any article may be reprinted if credit is given to ESO. Copies of most illustrations are available to editors without charge.

Editor: Philippe Véron  
 Technical editor: Kurt Kjær

EUROPEAN  
 SOUTHERN OBSERVATORY  
 Karl-Schwarzschild-Str. 2  
 D-8046 Garching b. München  
 Fed. Rep. of Germany  
 Tel. (089) 32006-0  
 Telex 5-28282-0 eo d

Printed by Universitätsdruckerei  
 Dr. C. Wolf & Sohn  
 Heidemannstraße 166  
 8000 München 45  
 Fed. Rep. of Germany

ISSN 0722-6691

Al simposio asistieron aproximadamente 200 personas. Las discusiones, que se concentraron en el campo general de la cosmología, ciertamente demostraron que el intercambio entre la física de partículas y la cosmología llevarán finalmente a un mejor entendimiento de las leyes fundamentales que gobiernan nuestro Universo.

## La historia de la estrella binaria eclipsante de líneas dobles HD 224113

Para un astrónomo experimental siempre es muy apasionante poder registrar un evento inesperado, aun cuando éste sea «sólo» el descubrimiento de la variabilidad óptica de una estrella binaria espectroscópica. Fue lo que le sucedió al Dr. R. Häfner del Observatorio de la Universidad de Munich cuando realizaba las observaciones para su programa fotométrico en el telescopio de 50 cm en La Silla en julio de 1978.

Debido a que el período de observación que le fue asignado era algo tarde para observar las estrellas de su programa hasta el final de la noche, había preparado una lista de aproximadamente 20 estrellas de velocidad radial variable para investigar su comportamiento fotométrico en las horas restantes. La primera estrella que seleccionó fue HD 224113. De repente, luego de haberla observado durante algunos minutos, el brillo decayó y palideció en forma continua hasta que la salida del sol le impidió hacer más mediciones. La naturaleza de las observaciones indicaba que se había observado un eclipse. Naturalmente en las noches siguientes se dedicaron las horas antes del amanecer a las

observaciones de esta estrella, sin embargo no fueron notadas más variaciones.

De vuelta en casa supo a través de una publicación de Archer y Feast que HD 224113 era conocida por ser una estrella binaria espectroscópica con un período de aproximadamente 2,5 días y que aparecía en su lista tan sólo porque el catálogo de velocidades radiales que usaba como referencia estaba incorrecto. Esta estrella estaba señalada sólo como variable en velocidad radial y no como binaria espectroscópica. Una anotación en la misma publicación «que se supone un débil espectro secundario en varios de los espectrogramas» fue el estimulante para continuar el estudio. Porque sólo estrellas binarias eclipsantes que muestran en su espectro las líneas de ambas componentes permiten una determinación precisa de los sistemas paramétricos en unidades absolutas, incluyendo especialmente las masas.

Durante los años siguientes (1979–1981) se coleccionaron más de 2700 mediciones en uvby efectuadas en el telescopio de 50 cm de la ESO y 36 espectros de alta dispersión en el espectrógrafo coudé del telescopio de 1.5 m.

Mientras tanto el Dr. Häfner supo que la variabilidad óptica también había sido detectada por algunos otros astrónomos. Sin embargo sus análisis eran algo discordantes, especialmente debido a la escasez de sus datos fotométricos.

La cantidad de material espectroscópico pudo ser aumentada considerablemente por la cooperación entre el Dr. Häfner y el Dr. de Groot (Observatorio de Armagh) quien aportó 23 espectros azules que había obtenido en el espectrógrafo coudé del telescopio de 1.5 m durante los años de 1970 hasta 1976.

Con todo este material el Dr. Häfner pudo determinar con gran precisión tanto el período del sistema como también las masas y radios de los dos componentes. Es interesante notar que esta investigación del sistema binario HD 224113 fue causada por un error en un catálogo de velocidad radial.

## Contents

G. Setti: Report on the First ESO/CERN Symposium on "Large Scale Structure of the Universe, Cosmology and Fundamental Physics" . . . . .	1
Tentative Time-table of Council Sessions and Committee Meetings in 1984 . . . . .	3
Second Announcement of an ESO Workshop on "The Virgo Cluster of Galaxies". . . . .	4
R. Pallavicini: Chromospheric Emission, Rotation and X-ray Coronae of Late-type Stars . . . . .	5
List of Preprints Published at ESO Scientific Group (December 1983—February 1984) . . . . .	10
Y. Chmielewski and M. Jousson: Spectroscopic Study of a Sample of Visual Double Stars . . . . .	11
S. Cristiani: Quasar Surface Densities . . . . .	13
R. Häfner: The Story of the Eclipsing Double-lined Binary HD 224113 . . . . .	15
O.-G. Richter: Some Old and New Facts About the Local Group of Galaxies and the Extragalactic Distance Scale . . . . .	17
L. O. Lodén: Multiple Stars—a Nuisance to the Observers . . . . .	20
R. Chini: Exciting Stars in the Omega Nebula . . . . .	22
Visiting Astronomers (April 1—October 1, 1984) . . . . .	23
B. Barbuy: Magnesium Isotopes in Halo Stars of Various Metallicities . . . . .	25
P. Véron, M.-P. Véron-Cetty and M. Tarenghi: The Ultraviolet Absorption Spectrum of NGC 4151 . . . . .	26
U. Heber and K. Hunger: The Nature of Subdwarf B Stars . . . . .	29
Ch. F. Trefzger, J. W. Pel and A. Blaauw: Stellar Metallicity Gradient in the Direction of the South Galactic Pole Determined from Walraven Photometry . . . . .	32
H. Steppe: One-mm Observations of BL Lacertae Objects . . . . .	35
H. Mauder: Light Curve Variations in Short Period EB Type Contact Binaries . . . . .	38
Personnel Movements . . . . .	39
Algunos Resúmenes . . . . .	39